GEOLOGY AND PETROCHEMISTRY OF OPHIOLITIC ROCKS OF THE BAIE VERTE GROUP EXPOSED AT MING'S BIGHT, NEWFOUNDLAND

RYBURN E. NORMAN

c.1

GEOLOGY AND PETROCHEMISTRY OF OPHIOLITIC ROCKS OF THE BAIE VERTE GROUP EXPOSED AT MING'S BIGHT, NEWFOUNDLAND

by

© Robert E. Norman

A Thesis

Submitted in partial fulfilment of the requirements

for the degree of

MASTER OF SCIENCE

Memorial University of Newfoundland

1973

Frontispiece: Preserved pillow lava in an intensely deformed unit north of Deer Cove in Baie Verte.

CONTENTS

TABLES

ILLUSTRATIONS

FIGURES

ABSTRACT

The Baie Verte Group, as exposed on the peninsula between Baie Verte and Ming's Bight, consists of a disrupted ophiolite sequence. The rock types range from interlayered ultramafics and gabbro to sheeted diabase dikes overlain by pillow lavas and volcanic sediments. The sequence has been disrupted into five structural blocks separated by fault zones containing serpentinized peridotite and/or talc-carbonate; units within each block are separated by less significant faults. This widespread imbrication is similar to 'schuppen zones' in north-east Shetland as described by Flinn (1958). These structures and other deformation features in the Baie Verte Group are interpreted to be related to early Ordovician emplacement with some effects of later Acadian deformation.

The Baie Verte Group is chemically similar to other ophiolite sequences such as in Oman and Papua. A parental magma, interpreted to have been a low-Ti and low-K basaltic magma, crystallized under conditions of low oxygen fugacity in the upper crustal zones beneath a mid-ocean ridge, producing the ultramafics-gabbro-diabase-pillow lava sequence observed.

Mineral occurrences in the area have similar mineralogy (pyrite-chalcopyrite-pyrrhotite-sphalerite) to those of other ophiolite areas such as Betts Cove and Troodos.

CHAPTER 1

GENERAL INTRODUCTION

1.1. Location and Access

The map area, at approximate latitude 50° 00' north and longitude 56° 00' west, lies between the towns of Baie Verte and Ming's Bight on the Burlington Peninsula of north-central Newfoundland (Figure 1). Both communities are serviced by a paved road approximately 65 km. from the Trans-Canada Highway (Route 1). From either of the communities the coastal boundaries of the map area can be reached by boat, easily obtained from many of the local residents. Woods trails near Ming's Bight provide access to the inland regions of the southern part of the area, but overgrowths of alder have obliterated them in many places.

1.2. Physiography

Ridges and valleys of the area trend in a northeasterly direction reflecting the predominant structural trend of the underlying rocks. The higher and more mountainous regions in the northern part of the map area are underlain by the more resistant gabbroic and ultramafic rocks, whereas the southern regions of lower relief are underlain by less resistant volcanic rocks and sediments. Thick growths of spruce, fir and alder cover the areas underlain by volcanic rocks, while vegetation is sparse in areas underlain by gabbroic and ultramafic rocks.

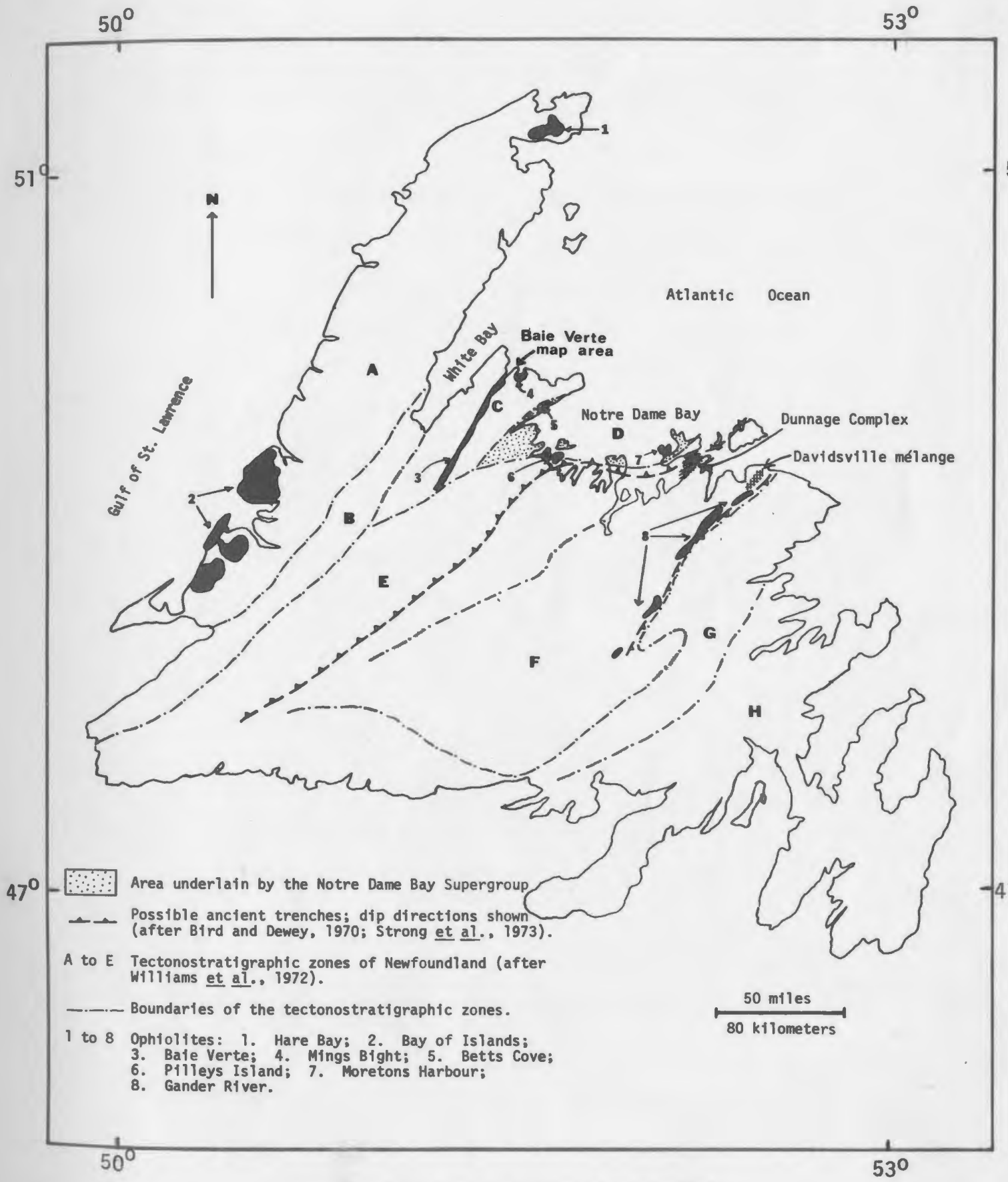

Figure 1: Major tectonic elements of Newfoundland.

Pleistocene glaciers, which moved in a north-easterly direction, left a thin cover of till which is thickest in the lower regions, but also present to a minor extent in the higher regions to the north. Because of this dense vegetation and glacier cover, inland exposure to the south is poor, whereas the gabbroic and ultramafic rocks to the north are superbly exposed.

1.3. General Geology

1.3.1. Tectonostratigraphic Setting

The Appalachian Structural Province extends 2000 miles from its northeastern extremity in Newfoundland southwestwards along the Atlantic seaboard to Alabama. The Newfoundland Appalachians were divided by Williams (1964) into three tectonic belts which formed a two-sided symmetrical system having a central Paleozoic mobile belt bounded to the east and west by Precambrian and Lower Paleozoic rocks. Recently, the Appalachian Structural Province has been divided into nine tectono-stratigraphic zones, designated A to I, with boundaries of each determined by major faults and structural discontinuities (Williams, et al., 1972); only zones A to H are recognized in Newfoundland (Figure 1).

The present study area is included in zone C (Figure 1) which is characterized by the complexly deformed Precambrian Fleur de Lys Supergroup, consisting of psammitic and semi-pelitic schists overlain by mafic and silicic volcanic rocks. A polymictic conglomerate, containing gneissic boulders, forms the base of the Supergroup and overlies a

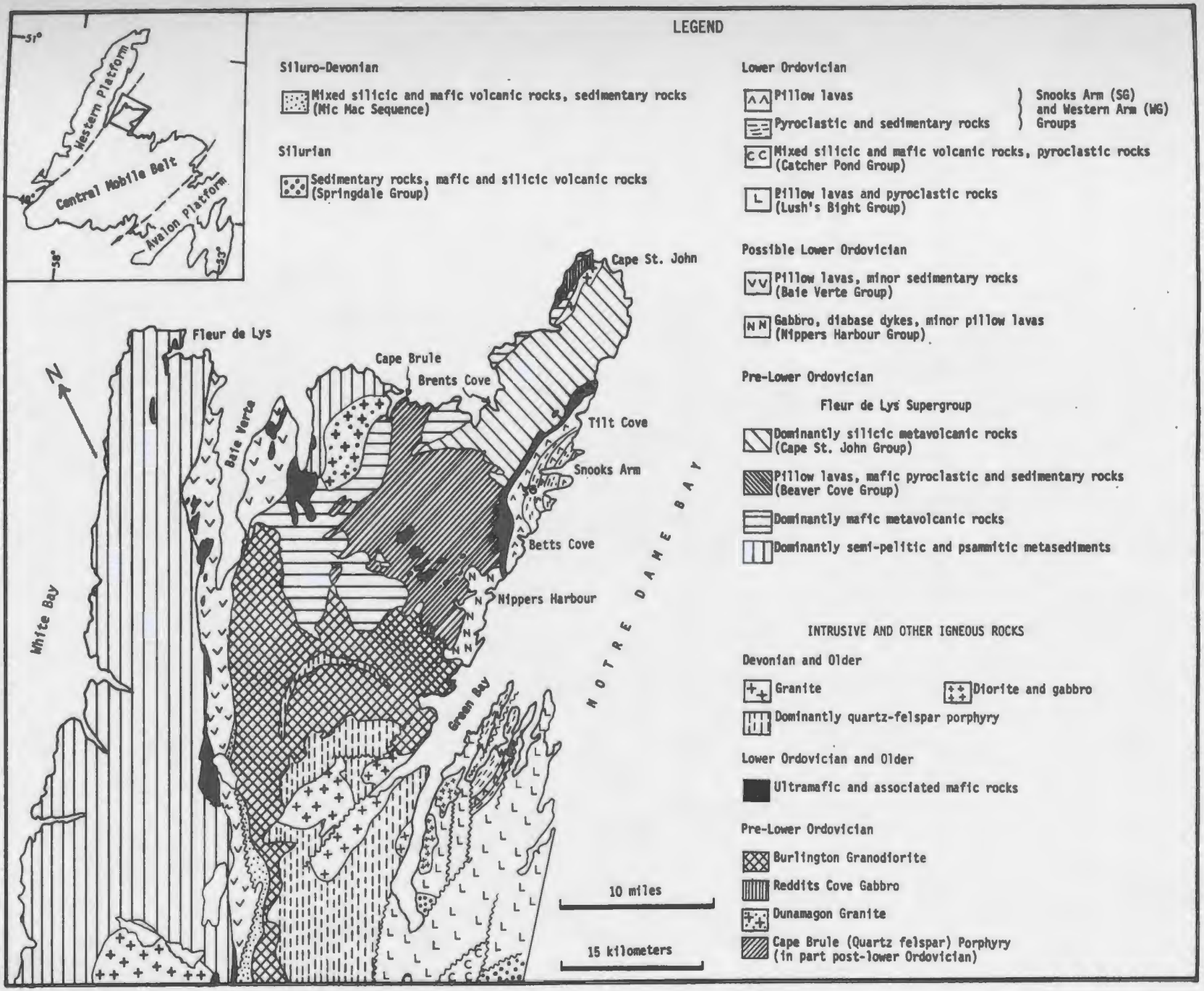

Figure 2: Generalized geological map of the Burlington Peninsula, Newfoundland

metamorphic basement complex (M.F. DeWit, pers. comm.). The Ordovician volcanic rocks of the Baie Verte Group are in fault contact with the Fleur de Lys Supergroup.

1.3.2. Previous Work

Alexander Murray made the first geological observations in the Baie Verte-Ming's Bight area in 1864, during a reconnaissance study of the eastern shores of the Great Northern Peninsula and parts of White Bay and Notre Dame Bay. He referred to the rocks of the present map areas as belonging to the "Quebec Group", overlying "Laurentian gneisses". The earliest geological map of Newfoundland was published by Murray in 1873, on which he showed all of the Burlington Peninsula as underlain by "Laurentian gneiss". Snelgrove (1935) studied several economic prospects in the general area of Ming's Bight, particularly the Goldenville Mine, and on the basis of lithological similarity correlated the volcanic and sedimentary rocks of the area with the Ordovician Snook's Arm group on the west coast of Notre Dame Bay (Figure 2).

The first detailed description of the rock types was given by Watson (1947) during a study of mineral occurrences in the Baie Verte-Ming's Bight area. He named the sequence of volcanic and sedimentary rocks the Baie Verte Formation and considered the gabbroic and ultramafic members to be intrusive. He recognized that the Baie Verte Formation was in fault contact with Precambrian gneisses to the west, which he named the Rattling Brook group, and correlated the Baie Verte Formation with Ordovician

rocks of the Notre Dame Bay region. He named gneisses to the east the Ming's Bight Formation and described them as being part of the Ordovician underlying the Baie Verte formation.

Baird (1951) mapped a large part of the Burlington Peninsula and included a correlation of earlier work. The gneisses and schists west of Baie Verte were named the Fleur de Lys Group which included the Rattling Brook Group of Watson (1947). The Ming's Bight Formation of Watson was renamed the Ming's Bight Group and assigned a Precambrian age. Baird extended the Ming's Bight Group to include similar rocks at Pacquet Harbour (Figure 2) where they were thought to be unconformably overlain by the Ordovician volcanics of the Baie Verte Group, which he had also extended to Pacquet Harbour. He named a sequence of volcanic and sedimentary rocks on the west side of Notre Dame Bay the Nippers Harbour Group and correlated them with the Ordovician Snooks Arm Group. Baird also assigned an Ordovician age to a sequence of silicic volcanics overlying the Snook's Arm Group, which he named the Cape St. John Group.

Neale (1957) recognized a major unconformity between the Cape St. John and the Snooks Arm Groups, and correlated the Cape St. John with the Springdale Group, thought to be of Devonian age. Later, Neale and Nash (1963) suggested a Silurian age for both groups and also correlated them with the MicMac sequence, a series of silicic volcanics and sedimentary rocks to the south. The MicMac sequence was found to unconformably overlie the Burlington Granodiorite, previously taken as a Devonian intrusion, but subsequently interpreted as Ordovician by Neale

and Nash. Church (1966) reported granodiorite pebbles in the base of the Baie Verte Group, and suggested they were derived from the Burlington Granodiorite which he then considered to be Pre-Ordovician in age. Neale and Nash accepted the Baie Verte Group as Ordovician and also interpreted parts of the Fleur de Lys Group as Ordovician. Neale and Kennedy (1967) proposed a possible Silurian age for the Baie Verte Group on the basis that it conformably overlay the Silurian MicMac sequence.

Church (1969) designated all rocks of the main Fleur de Lys belt the "Fleur de Lys Supergroup". He subdivided the metamorphic rocks west of Baie Verte into the Rattling Brook Group (after Watson, 1947) and the White Bay Group (after Betz, 1948). The rocks to the east of Baie Verte he divided into the Ming's Bight Group (after Baird, 1951), the Pacquet Harbour Group and the Grand Cove Group. The Pacquet Harbour Group had been previously mapped by Baird (1951) as part of the Baie Verte Group, whereas the Grand Cove Group was mapped by Baird (1951) as parts of both the Baie Verte and Cape St. John Groups.

1.3.3. Recent Interpretations

The reader is referred here to Table I for a summary of the various interpretations of relative ages and stratigraphy discussed in this section and section 1.3.2.

In recent years the theories of Continental Drift and Plate Tectonics have assumed a dominant role in interpretations of Newfoundland

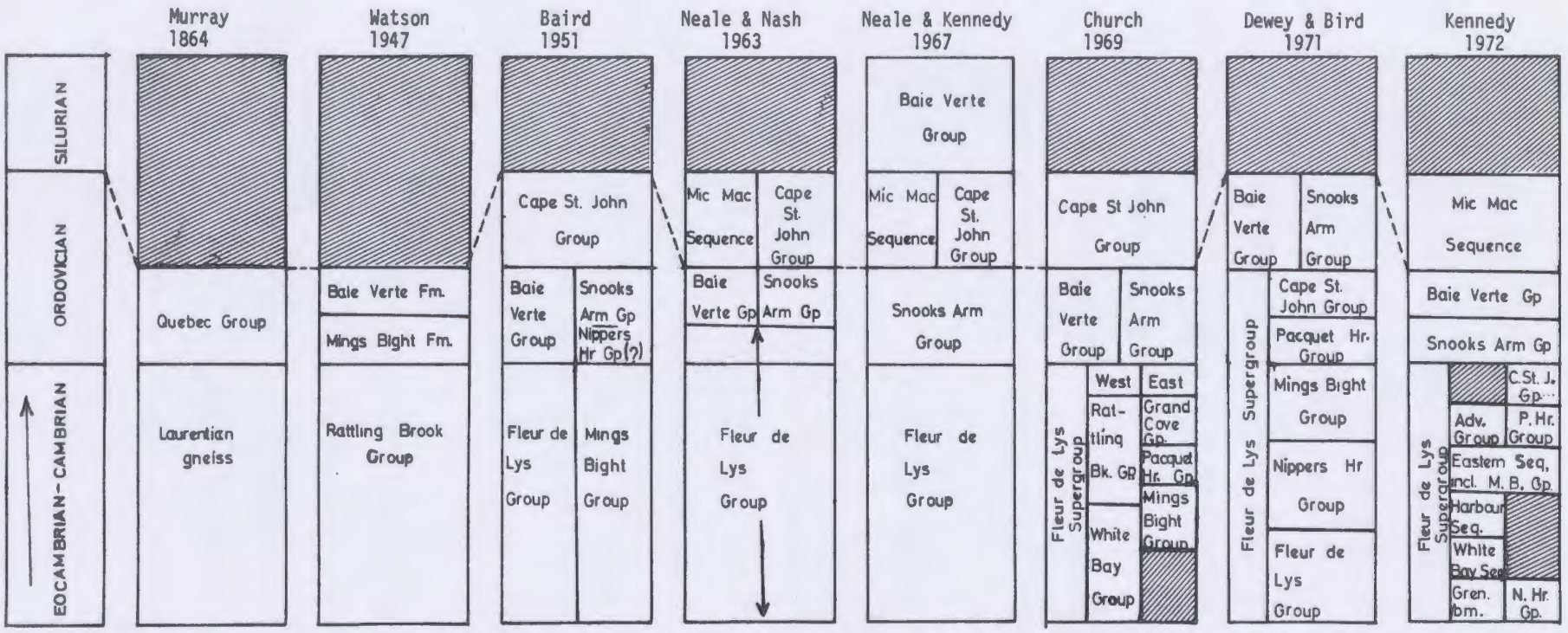

TABLE I: Summary of the various interpretations of relative ages and stratigraphy. C. St. J. (Cape St. John); M.B. (Mings Bight); N. Hr. (Nippers Harbour); Gren. bm. (Grenville basement). Hatched areas represent missing sections. Dashed line represents Ordovician-Silurian boundary.

geology. Kay (1966) outlined stratigraphic and structural similarities between northeastern Newfoundland and the British Isles and southern New England. Church (1965 a, b; 1966) noted similarities between the Fleur de Lys and the Moine-Dalradian of Scotland and Ireland. Later he summarized the geology of the whole Burlington Peninsula correlating it with the Moine-Dalradian (Church, 1969). Phillips, et al. (1967) described similarities in stratigraphic and structural histories of western Ireland and the Burlington Peninsula and they also correlated the Fleur de Lys with the Dalradian.

Church and Stevens (1971) defined the Bett's Cove-Baie Verte mafic-ultramafic sequences and the similar sequences of western Newfoundland as ophiolitic, representing one continuous sheet of oceanic lithosphere before disruption by Acadian (Devonian) folding and faulting. They suggested that these ophiolites were emplaced over a deformed sequence of late Proterozoic-Cambrian clastic sediments (the Fleur de Lys Supergroup) during closing of an ocean basin by underthrusting of a North American continental plate along a south-easterly dipping subduction zone.

Dewey and Bird (1971) described the origin and emplacement of ophiolite suites in some detail. Their proposed models for the evolution of western Newfoundland show continental rifting and generation of proto-Atlantic crust and mantle in Precambrian times. In late Cambrian or early Ordovician, a marginal basin formed west of the Fleur de Lys terrane, in the vicinity of White Bay, with Baie Verte and

Betts Cove ophiolites (i.e. the Baie Verte Group and the lower parts of the Snooks Arm Group) forming in intra-arc basins. The marginal basin began to contract during the early Ordovician with subsequent emplacement of the allochthonous Bay of Islands sequences to the west. The Baie Verte and Bett's Cove ophiolites were tectonically emplaced during a continental collision in Middle Devonian times.

Kennedy (1973) described the ophiolites of the Burlington Peninsula as representing two different ages of ocean crust. Based on the presence of supposed pre-Ordovician structures, the rocks on the west side of Baie Verte (named the "Advocate Group" by Kennedy but mapped as part of the Baie Verte Group by previous workers) and the ultramafics between the Fleur de Lys-Baie Verte contact (Figure 2) were considered by Kennedy to be ophiolites formed in a small ocean basin during pre-Ordovician times. Subduction of oceanic lithosphere to the east of the Burlington Peninsula resulted in island arc volcanism represented by the Pacquet Harbour and Cape St. John Groups which rest upon post-Grenville, pre-Fleur de Lys oceanic lithosphere represented by the Nippers Harbour Group. Continued ocean floor spreading and subsequent obduction of oceanic lithosphere during the early Ordovician emplaced the Bett's Cove complex. The Baie Verte Group was interpreted by Kennedy to be allochthonous, in general agreement with the interpretation of Church and Stevens (1971) that the Baie Verte Group probably originated to the east of Burlington Peninsula.

1.3.4. Definition of "Ophiolite" and Ophiolitic Features of the Baie Verte Group.

The GSA Penrose Conference on ophiolites, held in 1972, defined ophiolite as:

> "a distinctive assemblage of mafic to ultramafic rocks. It should not be used as a rock name or a lithologic unit in mapping. In a completely developed ophiolite the rock types occur in the following sequence, starting from the bottom and working up: ultramafic complex, consisting of variable proportions of harzburgite, lherzolite, and dunite, usually with a metamorphic tectonite fabric (more or less serpentinised); gabbroic complex, ordinarily with cumulus textures, commonly containing cumulus peridotites and pyroxenites and usually less deformed than the ultramafic complex; mafic sheeted dike complex; and mafic volcanic complex, usually pillowed. Associated rock types include (1) an overlying sedimentary section typically including ribbon cherts, thin shale interbeds, and minor limestone; (2) podiform bodies of chromite generally associated with dunite; and (3) sodic felsic intrusive and extrusive rocks. Faulted contacts between mappable units are common. Whole sections may be missing. An ophiolite may be incomplete, dismembered, or metamorphosed, in which case it should be called a partial, dismembered, or metamorphosed ophiolite".

According to the above definition the mafic-ultramafic sequences of the Burlington Peninsula and west coast of Newfoundland are properly described as ophiolites. Church (1972) defined ophiolite on the basis of the rock types found in the Trout River (west coast) and Bett's Cove ophiolites (see Figure 3). The Baie Verte Group is now generally accepted as ophiolite, containing all the characteristic rock types, although the lower parts of the ultramafic complex are not well represented. Ultramafic rocks make up islands in Baie Verte, they are interbanded with gabbro in the map area, and they form a discontinuous belt in the Fleur de Lys - Baie Verte contact to the south of the map area (Figure 2). The latter are considered by most workers (Dewey and Bird, 1971; Church and Stevens, 1971) as forming the base of the Baie Verte ophiolite, and thus of Ordovician age, but Kennedy (1972) considered them part of a pre-Ordovician ophiolite in the Fleur de Lys terrane. Gabbro, massive and banded, occurs in the present map area and in the vicinity of Baie Verte. Sheeted diabase complexes and pillowed lava flows overlain by sediments are present in the map area and also further south at Flatwater Pond, MicMac Pond (W.S.F. Kidd, in Dewey and Bird, 1971) and at Kidney Pond (Kennedy, pers. comm.).

1.4. Present Study

The recognition of ophiolites as representing early oceanic lithosphere has resulted in entirely new interpretations of the geological history of the Appalachians. The origin and emplacement of those ophiolites

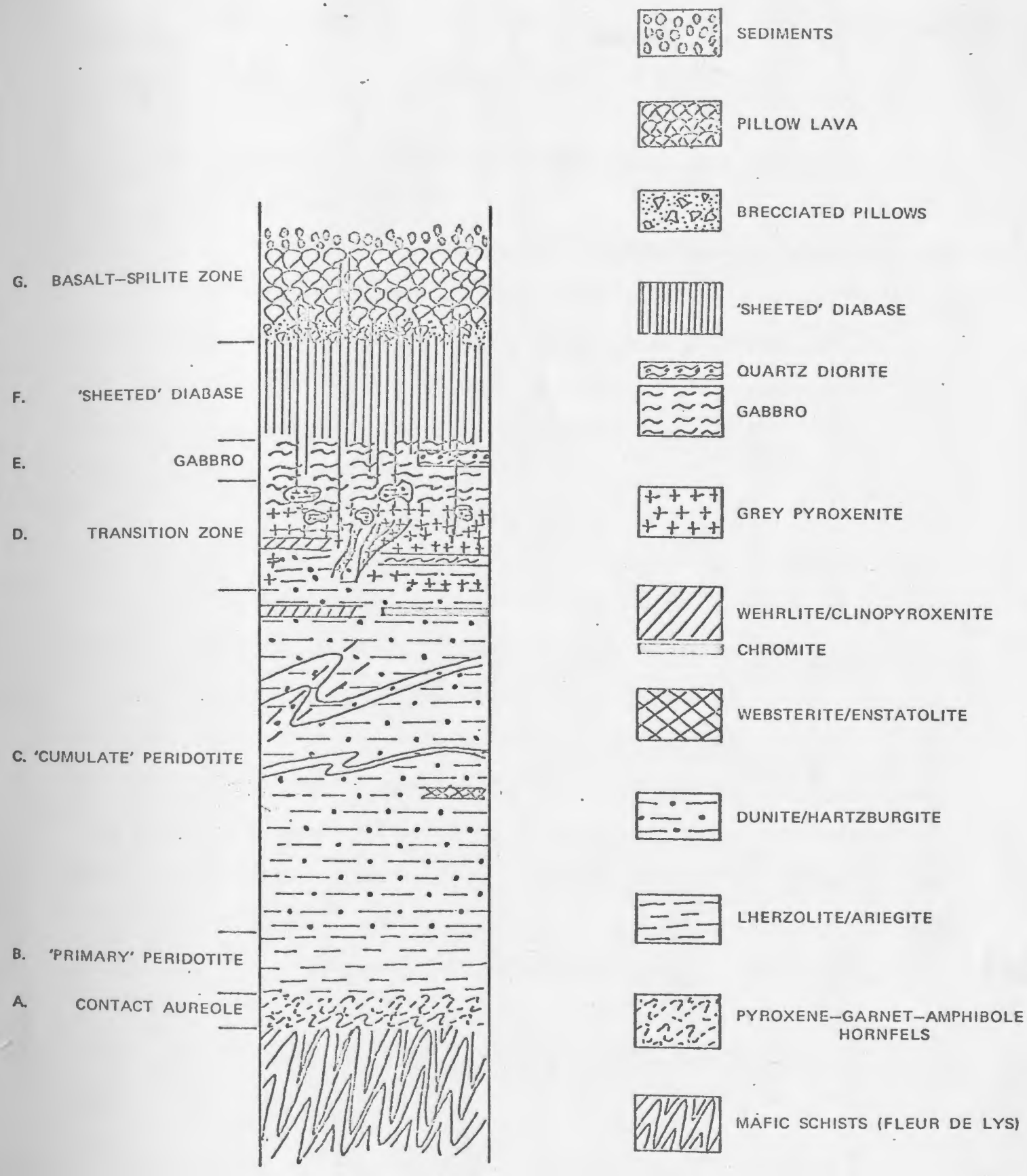

Not to scale

Figure 3: Idealized composite section of an early Ordovician ophiolite based on the Trout River and Betts Cove ophiolites of western Newfoundland and the Burlington Peninsula, respectively (Church and Stevens, 1971, fig. 2). Thickness of the section is about 10 km.

reveals past environments and processes that occurred at continent-oceanic junctions.

The current importance of the ophiolites to understanding the geological history of the Burlington Peninsula has prompted this study. Its objective was to present a detailed geological and petrochemical description of part of the Baie Verte ophiolite where it is well exposed - on the coast between Ming's Bight and Baie Verte.

ACKNOWLEDGEMENTS

A special thank you is extended to Dr. D.F. Strong who suggested the study and whose suggestions and discussions encouraged the writer. The writer is also indebted to the field assistance of Gideon Bowers and Campbell DeLong and to the laboratory assistance of Mrs. G. Andrews and David Press; also to Wilf Marsh, Foster Thornhill, Lloyd Warford and Gerry Ford. Thanks is also extended to Bernice St. Croix for typing the manuscript, and to Dr. H.D. Upadhyay for permission to use figures 1 and 2.

The writer also acknowledges financial assistance from the National Research Council of Canada (Research Grant No. A-5540 to Dr. E.R.W. Neale and No. A7975 to Dr. D.F. Strong) and the Geological Survey of Canada (Research Agreement No. 1135-D13-4-18).

CHAPTER 2

GEOLOGY OF THE MAP AREA

2.1. Field Methods and General Introduction

The area, of approximately 25 square miles, was mapped on a scale of 1 inch = 1/4 mile, using aerial photographs and topographic maps, during the summer months of 1971 (June - August) and 1972 (June - July). The geology of the coastal areas and northern inland areas was emphasized because of the excellent exposure; poor exposure contributes to the questionable relationships between various rock types and units in the regions to the south.

A consanguinous ophiolite sequence, from ultramafics and gabbro to sheeted dikes overlain by pillow lavas and sediments has been disrupted into five distinct structural blocks within the map area. The blocks are separated from each other by fault zones, represented by either serpentinised peridotite or talc-carbonate, and show abrupt discontinuity by (1) the number of units present, (2) by different relationships between corresponding units, (3) physical or chemical differences of certain corresponding units, and (4) by having different orientations of primary structures. These blocks are herein named as the:

1. Western Block.
2. Eastern Block.
3. Ming's Block.
4. Point Rousse Block.
5. Deer Cove Block

as outlined on Figure 4.

2.2. Ultramafic Rocks

2.2.1. Introduction

Like other ultramafic complexes of the Alpine type, the ultramafic bodies of the Baie Verte area occur in an orogenic belt in tectonic contact with the country rock and are found along major thrust faults. As mentioned above the ultramafic belt of serpentinite and serpentinized peridotite running southwestwards from Baie Verte, lies in the Baie Verte-Fleur de Lys thrust contact. Bodies of serpentinized peridotite with unfoliated banded centres and schistose talc-bearing margins (as described by Kennedy, 1971) lie near the town of Baie Verte west of the map area. Ultramafic layers, interbanded with gabbro, were observed near the mouth of Rattling Brook at the head of Baie Verte, south of the map area. Serpentinized peridotite and serpentinite, bordered by talc-carbonate, and associated with a large body of gabbro, separates the eastern boundary of the Baie Verte Group from the Ming's Bight Group, at the head of Ming's Bight. Gabbro and ultramafic rocks observed along the road to Ming's Bight exhibit a gradational contact between the two types. Within the map area ultramafics are represented by serpentinized peridotites, serpentinites and talc-carbonate rocks. These three varieties are the result of different stages of alteration, from serpentinization to steatitisation of a single ultramafic body.

2.2.2. Serpentinized Peridotite and Serpentinite

Serpentinized peridotite and serpentinite form a belt, averaging 100 metres in width, running approximately 5 kilometres south-

westwards from Devil's Cove (Fig. 4). The rocks weather a reddish-brown and contain disseminated, minute, euhedral chromite and locally magnetite grains; greyish-green altered pyroxene crystals in a black serpentinite matrix are exposed on fresh surfaces. Networks of chrysotile with fibrous crystals up to 5 millimetres occur throughout the belt.

For the most part the belt consists of subrounded blocks, up to 1.5 metres in diameter, of serpentinized peridotite in a sheared serpentinite matrix (Plate I, Fig. a). At Devil's Cove, blocks contained in shear zones are gradational into more massive forms. Larger zones of the massive variety are located further south along the western shore of Norman's Pond. The more intensely sheared zones occur between Devil's Cove and Devil's Cove Pond where the rocks have been intensely sheared and polished into dark to bright green serpentinite. At Norman's Pond and Deer Cove the peridotite has been altered to pale green "virginite", a local term for a rock, consisting of carbonate, quartz and fuchsite.

The direction of shearing in the serpentinized peridotite and serpentinite, as well as in the talc-carbonate varieties, is variable and follows the contact with the nearest structural block; the shearing is probably related to the emplacement of the blocks, as discussed below.

Serpentinized harzburgite and lherzolite make up the peridotite masses exposed on Grassy Island (Fig. 4) and are indistinctly layered with variable proportions of pyroxene and olivine (Plate 1, Fig. b). Magnetite and chromite are disseminated throughout; chromite also forms irregular patches and lenses up to 24 cm. in length (Plate 2, Fig. a). Similar layered masses underlie the Tin Pot Islands at the mouth of Coachman's Cove on the

west side of Baie Verte. Serpentinized harzburgite and dunite forms reefs (The Sisters) lying approximately 1 kilometer northwest of Point Rousse.

2.2.3. Talc-Carbonate and Carbonate-Talc

Talc-carbonate and carbonate-talc (depending on the predominant mineral) forms a discontinuous belt from Deer Cove to Red Point (Fig. 4). The carbonate was determined by X-ray Diffraction to be predominantly magnesite, but other carbonates such as calcite and dolomite are also present. Talc is generally predominant in highly sheared zones and is the most abundant mineral in the talc-carbonate zone between Deer Cove and Deer Cove Pond. The weathered surface of talc-carbonate varies from pale brown (due to the presence of magnesite) to dark grey with increasing talc content. Fibrous white to bluish-green tremolite is common along shear surfaces. The talc-carbonate is gradational into serpentinite near the northwest end of Deer Cove Pond. Talc and carbonate veins cut serpentinite near talc-carbonate rocks, and several blocks of serpentinized peridotite were observed in a talc-carbonate matrix.

In a zone stretching from the eastern end of Deer Cove Pond to Red Point, carbonate is the predominant mineral and locally forms 80% of the rock. Thin section studies of this zone revealed talc replacing serpentine. Anastomosing quartz veins and veinlets are common throughout the carbonate-talc zones. In the hills east of Devil's Cove Pond, alteration has produced a carbonate-quartz rock with disseminated magnetite

grains. Carbonate and quartz are present in equal amounts and on the yellowish-brown weathered surface networks of quartz stand out in relief.

Layering, 2 millimetres to 3 centimetres in thickness, is quite common throughout the talc-carbonate at Deer Cove Pond and in the carbonate-talc body at Red Point (Plate 2, fig. b). The layers, varying from a light grey to blackish grey, are due to varying ratios of magnesite-talc-magnetite and locally quartz. Magnetite is present in four forms (Plates 3 and 4) - (1) as lenses and layers, probably a primary, cumulate feature, interlayered with carbonate and talc, (2) as secondary, dust particles concentrated in the centres of carbonate grains, (3) as grains of possibly secondary material forming rings around talc pseudomorphs of olivine, and (4) as disseminated grains throughout talc and carbonate, either primary or secondary. Several layers vary from light grey to brown depending on the quantity of iron-rich magnesite.

The layering is interpreted to be relics of former, primary banding in an ultramafic body that, after undergoing serpentinization, was subjected to steatitisation and carbonatisation. Serpentinization of olivine can be achieved by simply adding water, as illustrated by the following equation (after Turner and Verhoogen, 1960):

$$5\ Mg_2SiO_4 + 4H_2O \rightleftharpoons 2H_4Mg_3Si_2O_9 + 4\ MgO + SiO_2$$

Olivine — serpentine — removed in solution

Further alteration of serpentine, by a silica-rich solution would form talc as in the equation:

$$Mg_3SiO_5(OH)_4 + 2\ SiO_2 \rightleftharpoons Mg_3Si_4O_{10}(OH)_2 + H_2O$$

In the presence of CO_2, under high pressures, magnesite and quartz could be derived from talc as:

$$H_2Mg_3Si_4O_{12} + 3CO_2 \rightleftharpoons 3MgCO_3 + 2.51SiO_2 + H_2O + 1.49\ SiO_2$$

talc — magnesite — quartz

Replacement of talc by magnesite is a common feature of the carbonate-talc rocks. Formation of magnesite and quartz directly from serpentine could take place as follows:

$$H_4Mg_3Si_2O_6 + 3CO_2 \rightleftharpoons 3MgCO_3 + 1.17SiO_2 + H_2O + .83\ SiO_2$$

removed in soln.

Such processes may have been responsible for the carbonate-quartz rocks frequently encountered in the area.

Subrounded blocks, up to .75 meters in diameter, of talc-carbonate and carbonate-talc (commonly of the layered variety) are intermingled with blocks of basic rock at Hammer Cove (Fig. 4), where the carbonate-talc body is overthrust by a unit consisting of sheeted diabase dikes belonging to the Point Rousse Block. Layering occurs in a unit approximately .6 meters thick overlying the blocks. Similar layering occurs on the north side of Red Point and near the contact with interlayered ultramafic and gabbro of the Eastern Block to the south. Kennedy and Phillips (1971) interpreted the layering as serpentinite sediment representing an unconformity between ultramafic and mafic rocks; the writer did not find any evidence for this.

2.3. Western Block

2.3.1. General Description

The Western Block is an overturned, south-facing conformable sequence exposed between Deer Cove and Pine Cove and in fault contact with the serpentinized peridotite belt to the east (Fig. 4). It comprises a layered ultramafic-gabbro unit passing southwards, with a gradual increase in dikes, into sheeted coarse diabase dikes overlain by pillow lavas and sediments. The trend of the layered unit is approximately 85 degrees east of north, dipping 50 to 60 degrees north. The dikes are near perpendicular to the layers, deviating little from a north-south trend.

2.3.2. The Layered Unit

The layered unit, cut by numerous basic dikes, is approximately 1300 metres thick. The layers vary from a few millimeters to one metre in thickness, and individually can be traced along strike for distances of 20 metres or more before lensing out or terminated by faulting. The unit can be divided into two zones; a lower zone forming the base, characterized by interlayered peridotite and gabbro, grading transitionally into an upper zone of normal layered gabbro with rare pyroxenite bands.

The lower zone, exposed along the coast between Deer Cove and Fox Gulch (Fig. 4) has a thickness, possibly exaggerated by fault repetition, of approximately 100 metres. At several places (e.g. Western Cove) gradational contacts exist in sequences from peridotite to gabbro. A typical section exhibits, over a thickness of 5 or 6 metres, transitional

layering, due to varying proportions of olivine-orthopyroxene-clinopyroxene, from serpentinized dunite, harzburgite and lherzolite to websterite overlain by layered gabbro (Plate 5, Fig. a).

Elongate patches of lherzolite, up to 50 centimetres in diameter, occur in one layer of harzburgite (Plate 5, Fig. b). They contain pale green pyroxene crystals, up to 2 millimetres in diameter, in a black serpentinized olivine matrix. They have irregular contacts with the harzburgite and appear as "pockets" within the original magma. Large poikolitic actinolite crystals, originally pyroxene, containing round, steatitised olivine grains in a talc matrix (probably olivine cumulate) were observed in one of the peridotite layers (Plate 6, Figs. a and b). This feature is texturally similar to the poikilitic harzburgite (olivine-orthopyroxene cumulate) of the ultramafic zone of the Stillwater Complex (Wager and Brown, 1966) and the postcumulus plagioclase and poikilitic orthopyroxene in the olivine cumulate of the 'Granular Gabbro' member of the Papuan Complex (Davies, 1971). Such textures develop during crystallization of intercumulus liquid trapped between and surrounding cumulate crystals.

At two localities between Deer Cove and Western Point, the peridotite layers have been faulted into large blocks up to 4 metres in diameter. The blocks, as appears to be a general feature of deformed ultramafic bodies, both on a large and small scale, have schistose talc peripheries and massive, serpentinite centres.

Transitionally between the lower and upper zone persistent layering from a few millimetres to 50 centimetres in thickness occurs.

It is best exposed immediately west of Deer Cove. Varying ratios of orthopyroxene-clinopyroxene-plagioclase form layers ranging from pyroxenite to gabbro; olivine was only observed locally. Slump features (Plate 7, Fig. a) were observed in one sharp contact between gabbro and pyroxenite. Several zones of pegmatitic pyroxenite, containing crystals up to 18 centimetres long, occur grading into the normal layers (Plate 7, Fig. b).

The upper zone, mainly layered gabbro of undetermined thickness, is best exposed between Fox Gulch and Green Point (Fig. 4). Layering is less persistent than in the lower zone and more massive gabbro is present. The mineralogy is approximately the same as the gabbro in the lower zone, except iron-rich actinolite and green hornblende is much more common as alteration products of the pyroxenes, probably a reflection of more iron-rich later differentiates. Dikes are also much more abundant than in the lower zone and become increasingly more abundant as the overlying sheeted unit is approached.

2.3.3. Sheeted Diabase Unit

Sheeted coarse diabase dikes are exposed between Lower Green Cove and Green Cove (Fig. 4) forming a thickness of approximately 900 metres. They differ from the sheeted dikes in other blocks in being much wider and coarser grained. They have an average width of approximately 2.5 metres and range from .5 metre to 5 metres. They are intruded by numerous smaller diabase dikes. Chilled contacts are quite distinct and in many cases appear only on one side. Gabbro inclusions and screens were observed in a few instances (Plate 8, Fig. a).

The chilled contacts and the finer grained dikes are generally composed of saussuritized plagioclase and clinopyroxene (usually altered to actinolite-tremolite). The coarse dikes contain approximately the same mineralogy as the underlying gabbro. Pyroxenes (diopsidic augite and hypersthene) are partially altered to green hornblende and actinolite; plagioclase is completely replaced by epidote and quartz. Carbonatization has also been effective, producing zones that appear as reddish brown layers in the dikes.

The sheeted dikes cut and probably feed the pillow lavas at Green Cove.

2.3.4. Pillow Lavas

Pillow lavas crop out between Green Cove and just south of Pumbly Point (Fig. 4). The top of the unit, lying somewhere south of Pumbly Point, has not been defined because of poor exposure. The upper part of the unit is overturned, as determined from pillow lava relationships at Pumbly Point, dipping north and facing south.

Some of the features described by Carlisle (1963) in the pillow lavas and isolated pillow lavas on Quadra Island, British Columba, were recognized in this unit. The pillow lava (Plate 8, Fig. b) is similar to that which Carlisle named "ordinary pillow lava" and defined as "the typical close-packed or fairly close-packed accumulations of unbroken pillows - a rock with less than 10% matrix". In many cases the pillow lavas are overlain by 'isolated pillow breccia' which Carlisle defined as "irregularly shaped but unbroken pillows widely separated from each other by a tuffaceous matrix".

The pillows are ellipsoidal in shape and commonly flattened. They vary in size up to maximum dimensions of approximately 2 metres by 1.5 metres by .65 metres. Chloritized chilled margins up to 4 centimetres thick are invariably present. The pillows are medium green to grey and are composed of epidote, plagioclase, sphene, chlorite, actinolite and quartz. Pale green amygdules up to 4 millimetres in diameter are usually present around the margins. The matrix is of a tuffaceous nature, containing similar minerals as the pillows, but is usually represented by chlorite schist molded around the pillows. In several cases, the matrix has been affected by metamorphic differentiation which has produced, to some extent, alternating bands of chlorite and quartz (Plate 9, Fig. a).

Isolated pillow breccias display discrete and intriguing patterns on weathered surfaces (Plate 9, Fig. b). They vary in shape from irregular, assymetrical to globular forms up to 20 centimetres in diameter to elongated bodies up to 30 centimetres in length. Generally the pillow breccias are composed of fine grained, fibrous actinolite in a groundmass of quartz, feldspar, epidote and chlorite. They weather brown to greenish grey and are widely separated by a greenish brown, coarse grained tuffaceous matrix. The latter contains fragments made up of predominantly epidote in an originally glassy groundmass. Chilled margins, 2 to 3 millimetres in thickness, are always present, composed of fine grained, turbid epidote and sphene. The rims of some pillows are comparable to those described by Carlisle (1963) in which chilling has produced an outer rim of devitrified "sideromelane" (a pale, translucent zone containing epidote, minor tremolite and chlorite) and an inner zone of "tachylyte" consisting mostly of turbid epidote.

The coastline south from Pumbly Point to the head of Baie Verte was not mapped in detail, but it consists of a monotonous sequence of sediments (including reworked tuff) and minor pillow lavas. The better exposures of sediments in the Eastern Block are regarded as typical and thus a detailed description is given in that section.

The small block of intensely deformed sediments and pillow lavas at Green Point (Fig. 4) is in fault contact with the sheeted dike unit of the Western Block. Its features are similar to that described below for identical rocks in the Deer Cove Block and will not be described further in this section.

2.4. Eastern Block

2.4.1. General Description

Like the Western Block, the Eastern Block has layered ultramafic-gabbro sequences, sheeted dikes, pillow lavas and sediments. Generally it differs as follows:

1) the layered sequence generally trends north-south.

2) the diabase dikes are fine grained and average 70 centimetres in thickness, considerably less than the average thickness of the coarse diabase dikes of the Western Block.

3) the pillow lavas overlying the sheeted dikes are chemically similar to the dikes, but are more mafic than the pillows of the Western Block.

The Block is bounded to the west, and separated from the Western Block, by the serpentinised peridotite belt. The eastern boundary

has not been clearly defined but is represented by a fault, 2 kilometres south of Big Head that separates sediments of the Eastern Block from pillow lavas of the Ming's Block to the south.

2.4.2. The Layered Unit

Interlayered peridotite-pyroxenite-gabbro is very persistent throughout the unit which has an outcrop width of several metres at its northeastern extremity, but reaches a maximum width of over 2.5 kilometres to the south. The true thickness of the unit has been eradicated by complex faulting, mostly by east-west block faulting, and thus the continuity of the layering is probably a misconception. The trend of the layering is generally north-south but swings sharply (up to 60^{o}) towards the east near the contact with the serpentinized peridotite belt. Interlayered peridotite-pyroxenite-gabbro sequences occur all along the contact from where it is exposed at the coastline in Ming's Bight south-westwards to at least as far as Norman's Pond. That the serpentinized peridotite and talc-carbonate belt is the base of the layered unit is not known with certainty. It was noted from thin section studies that serpentine in the serpentinized peridotite layers of the layered unit was replaced by up to 50% talc (Plate 10, Fig. a) near talc-carbonate or carbonate-talc zones, but decreases gradationally to nil away from the zones. The layers also occur in close proximity to altered peridotite (virginite) of the sheared belt in the vicinity of Norman's Pond and to layers in the talc-carbonate south of Red Point.

East-west block faulting within the layered unit is most obvious in the coastal exposures. Several of the small scale faults have displaced dikes up to 2 metres, but the larger faults have brought massive serpentinized peridotite and carbonate-quartz (similar to that in the carbonate-talc belt approximately 400 metres to the west) in proximity to interlayered peridotite-pyroxenite-gabbro sequences. The massive peridotite (approximately 20 metres in length and an indeterminable width) occurs at two localities. The fault contacts are marked by large subrounded ultramafic blocks up to 3 metres in diameter, consisting of serpentinized peridotite centres and schistose talc rims. Gabbro near the faults is broken up into large blocks, and in the more intense zones is represented by crenulated actinolite-chlorite schists.

The layering (Plate 10, Fig. b) is similar to that of the western block, consisting of varying proportions of olivine-pyroxene-plagioclase, forming peridotite, pyroxenite and gabbro, gabbro being predominant throughout. For the most part the layered unit is comparable to the lower zone of the Western Block, but in a fault block near the southern contact with sheeted diabases, layered gabbro, lacking peridotite bands and cut by numerous dikes, is comparable to the upper zone.

Pegmatitic zones, containing varying proportions of uralitized pyroxenes and saussuritized plagioclases producing all gradations from pure pyroxenite to gabbro, occur throughout the gabbro. These zones (Plate 11, Fig. a) range from less than 1 centimetre by 20 centimetres to maximum dimensions of 2 metres by 7 metres. The contacts with normal gabbro are not generally defined but were observed in a few cases to be gradational.

2.4.3. Sheeted Diabase Unit

Sheeted diabase dikes, averaging between 50 and 75 centimetres in thickness, form a unit approximately 500 metres thick, exposed at Big Head (Fig. 4). They strike between 85° to 110° azimuth, generally perpendicular to the layered unit, and dip 65° north. The unit is in fault contact with the layered gabbro, but this fault is interpreted to be of minor displacement and the dikes gradational from the layered gabbro. The fault is sub-parallel to the strike of the dikes and cuts the gabbro. Several large dikes averaging 1-1/2 metres thick cut the layered gabbro near the contact with the sheeted dikes, and approximately 2 kilometres west of Big Head a gabbro dike, approximately 5 metres in thickness, is parallel to and chilled against the diabase dikes.

Chilled contacts are excellently exposed, commonly occurring on one side only, a feature common to ophiolites (Vine & Moores, 1970; Upadhyay, et al., 1971). The diabases are fine grained, highly epidotized and dark to medium grey in colour. Anastomosing epidote and quartz veinlets are common in places.

2.4.4. Pillow Lavas

The pillow lavas form a unit approximately 300 metres thick, overlying the sheeted diabases. They are cut by several diabase dikes up to 1.5 metres in thickness; a large gabbroic dike, 7 metres in thickness, was observed chilled against the pillows. The contact between the sheeted diabases and the pillow lavas is somewhat sheared, but it is probably gradational. The shearing has destroyed most primary features in the

pillows near the base of the unit, but zones of pale-green amygdules delineate pillows upon close examination. Further up the sequence, the pillows become more distinct with chilled rims and marginal ellipsoidal to spherical amygdules up to 5 millimetres in diameter. The pillows average approximately 15 centimetres in length, but a few up to 1.5 metres were observed. In some places, especially near the top of the unit, pillows are set in a brecciated matrix (Plate 11, Fig. b). The matrix consists of angular, dark greenish grey, epidotized fragments in a groundmass containing quartz, carbonate, and fragments of actinolite.

The pillows are separated from the overlying pyroclastics and sediments by non-persistent beds (interlayered with tuff) of ferruginous chert averaging 75 centimetres in thickness. The chert is dark red to wine in color, containing magnetite, specular hematite and quartz. In thin section, hematite was observed disseminated throughout the quartz grains. Thin layers in the chert beds are due to the variation in the amounts of hematite.

2.4.5. Pyroclastic and Sedimentary Rocks

Pyroclastic and sedimentary rocks form a unit approximately 800 metres in thickness, consisting of interbedded agglomerate, crystal and crystal-lithic tuffs, thinly laminated green to red beds of reworked tuff, and tuffaceous breccia (comprising large angular cherty blocks in a tuffaceous groundmass). It separates the underlying pillow

lavas from pillow lavas in the overlying Ming's Block, and represents the top of the Eastern Block.

The agglomerates are composed of large subangular to subrounded pale greenish-grey clasts up to 20 centimetres in diameter, containing euhedral pyroxene fragments (altered to actinolite) up to 1 centimetre in length. The clasts are in a greenish-grey tuffaceous groundmass consisting of pyroxene crystal fragments up to 1 millimetre in length.

The crystal and crystal-lithic tuffs contain fragments of euhedral crystals of pyroxene and angular to sub-angular lithic fragments of andesitic and basaltic texture in a greyish-green groundmass. Layering from 1 millimetre to 40 millimetres in thickness, due to variation in grain size and proportion of groundmass to fragmental crystals, is common and most distinct on weathered surfaces.

Reworked tuff (the greywacke of previous workers) is made up of very fine grained, laminated layers from less than a millimetre to 12 millimetres in thickness, ranging in colour from yellowish-green to light and dark green; red layers are also common in some sections. These are usually interlayered with "tuffaceous breccia" characterized by large greenish, cherty, angular fragments up to 30 centimetres in length, in a greenish-grey tuffaceous groundmass. These fragments are laminated and similar to the reworked tuff and are typical, pre-consolidation rip-up slabs.

Graded bedding, observed both in the field and in thin section, and sporadic slump features (Plate 12, Fig. a) both indicate that tops face south and that the sequence is overturned.

2.5. The Ming's Block

2.5.1. General Description

The Ming's Block differs from the others in that it is an upright, north-facing sequence, as evidenced by the pillow lava relationships. The base is marked by sheared serpentinized peridotite, 100 metres south of the community wharf in Ming's Bight, which is overlain by layered gabbro of unknown thickness. The gabbro is in fault contact with overlying pillow lavas, isolated pillow breccia, and minor sediments, which are abruptly terminated by a fault contact with the pyroclastic unit belonging to the Eastern Block.

The serpentinized peridotite is similar to that occupying the serpentinized peridotite zone to the northwest, and the layered gabbro is typical of that already described above. The relationship between these rocks and the nearby peridotites and gabbro at the head of Ming's Bight and along the Ming's Bight road, were not studied, but their close proximity suggest they are part of the same ultramafic-gabbro sequence that is thrust over (or at least in fault contact with) the Ming's Bight and Pacquet Harbour Groups (of the Fleur de Lys Supergroup) to the south and east. Alternatively the sheared peridotite at the base of the Ming's Block may represent a thrust zone indicating thrusting of the block over the ultramafic-gabbro sequence which, consequently, would in turn be a separate slice thrust against the Fleur de Lys Supergroup.

2.5.2. The Pillow Lava Unit

This unit comprises a monotonous sequence of pillow lavas, isolated pillow breccia and minor greywacke and tuff. In the fault contact

with the layered gabbro, the rocks have been deformed into crinkled, chloritic schist, and nearby pillow lavas have been almost entirely replaced by epidote and cut by epidote and quartz veins. Much of this southern part of the unit has been intensely sheared and for a length of 850 metres, the coastline trends diagonally through a porphyritic diabase dike, about 100 metres thick, that trends southwestwards and forms the cliffs to the west of the community wharf. The dike is bordered on both sides by pillow lavas that it has intruded. To the north of the dike, although local shearing is common, the pillows are quite distinct, up to 1.5 metres in length, and in several cases are overlain by isolated pillow breccia similar to that described in the Western Block. The matrix consists, in many cases, of chloritic schist molded around the pillows. Numerous dikes, trending north-south, cut the pillow lavas perpendicular to the general trend. In the vicinity of Barry and Cunningham adit (Fig. 4) the rocks are intensely sheared for 30-40 metres along the coast. In the fault contact with the pyroclastic unit of the Eastern Block, a short distance north of the adit, pillows are intensely sheared and pale green cherty boudins in chloritic schist were observed. Reworked tuffs of the Eastern Block are also deformed in the fault contact.

2.6. Deer Cove Block

2.6.1. General Description

The Deer Cove Block is exposed between Devil's Cove and Deer Cove (Fig. 4). It comprises a layered unit, approximately 900 metres thick, in fault contact with an intensely sheared sequence of dikes, pillow lavas

and sediments approximately 700 metres thick. It is bordered to the east by the serpentinized peridotite and separated from the Western Block by talc-carbonate at Deer Cove.

2.6.2. The Layered Unit

This unit is most comparable to the upper zone of the Western Block. Its layering is generally striking 80^{0}, but varies from 40^{0} to 100^{0}, dipping 50^{0} to 60^{0} north. It is broken by numerous shear zones trending northeasterly and movements of at least 4 metres have taken place along normal and reverse faults trending 80^{0} to 120^{0}.

Layered gabbro (Plate 12, Fig. b) is the predominant rock type with only one occurrence of serpentinite in a small zone near Devil's Cove Head. The latter consists for the most part of small subrounded blocks of serpentinite, up to 14 centimetres in diameter, in a comminuted serpentinite matrix, faulted against the gabbro. The layers in the gabbro vary from less than a centimetre to 50 centimetres in thickness. Pyroxenite layers, gradational from the gabbro, are common, especially in the southern part of the unit. Pegmatitic zones (described for the Eastern Block) are also well exposed, with plagioclase and pyroxene crystals up to 5 centimetres in length. Diabase dikes are abundant, varying from .5 to 2 metres in thickness, trending perpendicular to the layers.

2.6.3. Dikes, Pillow Lavas and Sediments

Because of the intense deformation (Plate 13, Fig. a) it is difficult to divide the dikes, pillow lavas, and sediments of this block into

separate units, but generally a sequence from dikes and pillow lavas in the north to minor sediments in the south can be discerned. Near the fault contact with the layered unit, the rocks have been deformed into crenulated chloritic schist, but 100 metres away dikes are preserved trending north-south, and overlain by pillow lavas. Coarse grained gabbroic blocks, up to 50 centimetres in length, occurring in nearby schist are probably remnants of large dikes. Despite the deformation pillow lavas, up to 2 metres in length, are in places clearly recognizable with amygdules still preserved near the margins (See Frontispiece). These amygdules serve to indicate the presence of pillow lavas in shear zones where otherwise pillows would not be recognized. Towards the south, red chert (jasper) occurs as lenses and pods (up to 2 metres in diameter) containing abundant magnetite, specular hematite, pyrite and traces of chalcopyrite. Throughout the unit oxidized, yellowish-brown zones up to 4 metres wide contain nodules of massive pyrite. Close examination reveals layers of pyrite and epidote interbanded with quartz (Plate 13, Fig. b). Pale to dark green layers of chlorite-sericite-quartz schist are also present interlayered with the pillows. These layers are probably deformed reworked tuff. A few bright green zones within the schist are due to the presence of fuchsite.

2.7. Point Rousse Block

2.7.1. General Description

The Point Rousse Block, at the northern extremity of the map area, comprises a layered unit cut by large, coarse diabase dikes, in

fault contact with an overlying diabase unit. Pillow lavas and sediments are absent. The diabase unit is in thrust contact, as described above, with the carbonate-talc body at Hammer Cove. The Block is separated from the Deer Cove Block by the serpentinized peridotite belt at Devil's Cove. Regional features suggest that the Block is overturned, as there is a rapid increase of dikes from north to south, a feature quite common from bottom to top in conformable ophiolite sequences.

2.7.2. The Layered Unit

The layered unit is almost entirely gabbro, comparable to the upper zone of the Western Block. Only a few layers of pyroxenite were noted, the largest (15 metres thick) of which occur at the tip of Point Rousse; indistinct layering occurs within the latter, but was not mapped in detail. Orientation of the layers varies sharply from 0^{o} to 120^{o} azimuth, over short distances, due to abundant faults, especially in the northern part of the unit; southwards the orientation is more constant, generally 80^{o}. Both normal and reverse faults, and transcurrent faults were observed, displacing dikes up to distances of 4 metres.

Towards the south gabbro tends to be more massive and frequently occurs as screens in sheeted coarse diabase dikes that form up to 70% of the unit between the lower layered gabbro and the overlying sheeted diabase unit. The sheeted, coarse diabase dikes, trending 160^{o} to 180^{o} azimuth, perpendicular to the layering, averages 2 metres in thickness but decreases to .5 metres near the contact with the overlying diabase unit. Dikes up to 10 metres in thickness are rarely observed.

Pegmatitic zones, as described for the Eastern Block, are common in the layered unit. Intrusive breccia (Plate 14, Fig. a) resulting from intrusion of trondhjemitic material (80% albite feldspar) into dikes and gabbro is fairly extensive. Large angular blocks of dikes and gabbro up to 60 centimetres square, set in the white trondhjemitic matrix, is characteristic. Trondhjemite is also common in the gabbro outside these brecciated zones, as small veins and veinlets.

2.7.3. The Sheeted Diabase Unit

The sheeted diabase unit, in fault contact with the coarser diabases and gabbro, consists of 100% dikes, averaging 65 centimetres in thickness, and is similar to the diabase unit of the Western Block to the south. The trend of the dikes is generally north-south but deviates to 40° east of north near the thrust zone at Hammer Cove, where they have been thoroughly brecciated by faulting. Transcurrent faulting is common throughout, mostly in an east-west direction, and displacements up to 5 metres were observed.

2.8. Summary and Discussion

Peridotites and pyroxenites interlayered with gabbro is characteristic of the critical zone, or 'transition zone' described by Church (1972), which occurs between underlying ultramafic and overlying gabbro in a complete ophiolite suite (Figure 3). The Baie Verte Group is an incomplete ophiolite sequence containing interlayered peridotite

and gabbro representative of the critical zone, overlain by sheeted diabases, pillow lavas and sediments. In the map area this sequence is disrupted into five structural blocks separated by thrust zones containing serpentinized peridotite, serpentinite, and/or talc-carbonate. The various units within each block are separated by shear or fault zones.

The widespread imbrication of the Baie Verte Group is similar to that in 'schuppen zones' described by Flinn (1958) in ophiolites of north-east Shetland. These schuppen zones separate two allochthonous thrust sheets or nappes derived from a layered ultramafic-mafic sequence; a schuppen zone also separates the lower nappe from a gneissic basement. These zones consist of large blocks, or slices, including serpentine and greenschist (metagabbro) that themselves are separated into smaller slices by shears, thrust and dislocations and the author suggests that the map area can be similarly termed a schuppen zone. However, further comparison of the Baie Verte Group with that of north-east Scotland requires a discussion of the regional geology of the Baie Verte Peninsula, which is beyond the scope of this thesis.

CHAPTER 3

STRUCTURE

3.1. Introduction

The rocks of the map area are characterized by a single regional penetrative cleavage (S_1). In numerous local areas this cleavage is folded by later crenulations, kink bands and small scale folds (F_2); F_1 folds are displayed in folded veins and veinlets.

Distinct thrust faults separate the structural blocks, as described in Chapter 2, from the serpentinized peridotite belt in the middle; thrust faults also separate units within the structural blocks. Numerous transcurrent and both normal and reverse faults occur throughout.

3.2. Fabric

All the structural blocks exhibit a penetrative cleavage, S_1, with a strike of 30° to 70° and a dip of 50° north-west. The cleavage, defined mainly by chlorite, is strongly developed in the pillow lavas, diabase dikes and sedimentary rocks, but weakly developed in the gabbro. The varying orientation of the cleavage due to folding and faulting, makes it generally difficult to determine the significance of any variations from block to block, but the orientation of 90° to 110° in the Deer Cove Block is distinctly different from that of the others. This can be explained as due to the thrust faulting with the S_1 cleavage developed prior to disruption of the ophiolite sequence. Flattened pillow lavas (Frontispiece) and lineated amygdules indicate that S_1 can be described as

an L-S (S>L) fabric (Flinn, 1965). Boudinaged diabase dikes, formed in the plane of the S_1 schistosity (Plate 14, Fig. b) were recognized in a few places. The deformation related to S_1 appears to have been inhomogeneous as highly deformed zones lie in close proximity to lesser deformed zones (Plate 15, Fig. a) a feature especially prominent in the tuffaceous units.

3.3. Folds

The present investigation was not concerned with a sufficiently large area to reveal regional folding such as the anticline and syncline described in the area by Watson (1947). Nevertheless, two phases of folding on a smaller scale were recognized. Ptygmatic folds, F_1, related to the S_1 cleavage and having axial planes parallel to it, were observed in large veins (Plate 12, Fig. a) and smaller veinlets. Later, small open folds, F_2, with wavelengths up to 2 metres fold the S_1 cleavage and have axial planes that trend east-west and dip 30^0 to 45^0 north, similar to the faults of the area. Their common orientation suggest that these folds are probably related to the thrusting and faulting associated with the formation of the structural blocks.

3.4. Kink Bands

Two sets of sinistral kink bands locally fold and kink the S_1 cleavage. The younger set, striking east-west, is sub-horizontal and folds the older set that trends 60^0 to 80^0 and plunges approximately 50^0 north-westwards. This can be best observed in sediments just north of Deer Cove and south of Big Head.

3.5. Faults

Transcurrent, normal and reverse faults, with displacements up to at least 5 metres, were observed throughout. Most of the faults trend between 85° to 120° and have an average dip of approximately 50° N. The trend of the faults is consistent with the thrust faults throughout and is probably related to the thrusting. Larger thrust faults have been described in Chapter 2. These are found between the structural blocks and the serpentinised peridotite belt, and between the different units within the blocks.

3.6. Age of Deformation and Discussion

It is agreed by previous workers that the Baie Verte ophiolite sheet was folded into a tight syncline during the Acadian Orogeny of Middle Devonian age (Church and Stevens, 1971; Kennedy, 1973). It is also agreed by these workers that the Baie Verte ophiolite was emplaced during the Early Ordovician. This emplacement caused deformation which is most intense near the planes of movement and decreases away from them. Further Acadian deformation result in complex, polyphase structures near the planes of movement and simpler structures in much less deformed rocks away from these planes. It follows that the more deformed rocks of an allochthonous sheet would be found near the contact with the country rock. Accordingly, the more intensely deformed rocks of the Baie Verte Ophiolite suite are found near the east and west contact with the Fleur de Lys rocks.

The complexly deformed rocks occurring immediately west of the present map area (on the western shores of Baie Verte) have been described by

Kennedy (1973) as the Advocate Group belonging to ophiolites of pre-Baie Verte age. The writer interprets these rocks to be part of the Baie Verte ophiolites deformed near the thrust contact with the Fleur de Lys rocks. This interpretation is based solely on the similar lithologies, including ultramafics, gabbro and greenschist, in close proximity to each other, occupying the east and west shores of Baie Verte. Islands within Baie Verte, between the Baie Verte Group and the Advocate Group, are underlain by ultramafic and gabbro further suggesting a correlation between the rocks on the east and west sides of Baie Verte; i.e. a correlation between the Baie Verte Group and the Advocate Group, respectively. This is in agreement with Church and Stevens (1971) and Dewey and Bird (1971) that the ultramafic belt between the Baie Verte-Fleur de Lys contact forms the base of the Baie Verte ophiolite suite. The composite fabrics (Kennedy and Phillips, 1971) on the margins of these ultramafics is taken as related to early Ordovician emplacement and later Acadian deformation. The eastern contact of the Baie Verte Group with the Fleur de Lys rocks is characterized by intensely deformed gabbro and diabase dikes exposed along the Ming's Bight road and a similar interpretation holds there.

The rocks underlying the map-area are considered to have been far enough away from the major zones of movement to have escaped most of the deformation during the Early Ordovician. The faulting, thrusting, and related cleavages, which disrupted the Baie Verte Group into structural blocks, is probably similar to processes that formed the schuppen zones described by Flinn (1958) in northeastern Scotland (see discussion in Chapter 2).

CHAPTER 4

PETROLOGY

4.1. Petrography

4.1.1. Serpentinized Peridotites and Talc-Carbonate

In the serpentinized peridotite belt olivine crystals have been completely serpentinized and the only evidence of their former presence is the outlining of the crystal boundaries by minute grains of magnetite. Pyroxenes were recognized by remnants in serpentinized crystals and by relics of their characteristic cleavage. Textures vary from cross-hatched minute fibers of serpentine to radiating sheaves (Plate 16, Figs. a and b). Veinlets of chrysotile are common throughout.

Near the talc-carbonate and carbonate-talc bodies, the serpentine in the peridotites have been replaced by calcite and magnesite. In the talc-carbonate bodies, talc-pseudomorphs of olivine are outlined by magnetite, and only rare minute patches of serpentine remain (Plate 4, Fig. a). In the carbonate-talc assemblages, grey magnesite with relic pyroxene cleavage was noted. Magnesite, the predominant carbonate, occurs in euhedral to subhedral crystals.

Dunite underlying the reefs northwest of Point Rousse is composed of olivine cores surrounded by a mesh network of serpentine (Plate 17, Fig. a).

4.1.2. The Layered Units

Serpentinization of the ultramafic layers in the layered units is similar to, but less intense than, that described above. In the

Western Block, the fresher pyroxenes occur in the websterite and gabbro layers where serpentine is rare. The websterite, gradational from lherzolite, is composed of euhedral to subhedral cumulus enstatite and diopsidic augite. Exsolution lamellae of orthopyroxene in the clinopyroxene is common (Plate 17, Fig. b) and reaction rims of clinopyroxene around orthopyroxene are also characteristic.

In the gabbro layers, plagioclase is usually replaced by turbid epidote, but compositions between An_{10}-An_{15} were determined in several metamorphic plagioclases. In gabbroic layers near peridotite, enstatite is present as well as diopside. The diopside crystals are commonly zoned and have turbid cores (probably orthopyroxene exsolution), rimmed by clear tremolite. Margins of the pyroxenes are commonly embayed, reflecting replacement by the intercumulus plagioclase matrix, now consisting of turbid epidote (Plate 18, Fig. a). In the pyroxene-rich layers overlying the lower zone of the Western Block, the pyroxenes are rimmed by tremolite and have calcite cores.

In the layers of the upper zone, actinolite replaces the clinopyroxenes and the rare orthopyroxenes. It is very pleochroic, from pale green to dark green, probably reflecting iron-rich crystals in more differentiated layers. Plagioclase is invariably replaced by turbid epidote. Calcite cores in subhedral crystals of diopside rimmed by actinolite, are very common, especially in the upper layers of the Point Rousse Block; magnetite commonly rims such cores (Plate 18, Fig. b).

In the peridotite layers of the Eastern Block, near the contact with the carbonate-talc at Red Point, distinct textures are developed

consisting of irregular patches of minute, cross-hatched serpentine in the coarser sheave variety (Plate 19, Fig. a). The pyroxene crystals exhibit a "rib" texture (Plate 19, Fig. b) consisting of fresh remnants of pyroxene alternating with zones of serpentine. Pale green layers, interlayered with the black serpentinite, consist of fibrous tremolite being replaced by serpentine. Carbonate is also common replacing the serpentine in some layers; magnetite outlines much of the completely serpentinized olivines (Plate 20, Fig. a).

4.1.3. Sheeted Diabase Dikes

The coarse diabase dikes of the Western Block and the Point Rousse Block are composed of actinolite, replacing pyroxenes, in a groundmass of fine grained epidote and sericite with secondary quartz present locally. The actinolite crystals are subhedral to anhedral and commonly twinned. The chilled contacts of these dikes consist of minute fibrous grains of actinolite in a groundmass of turbid epidote and minor quartz.

The fine grained diabase dikes of the Eastern Block, Deer Cove Block and Point Rousse Block consist generally of 40% plagioclase (An_{10}-An_{15}), 40% actinolite-tremolite and 20% epidote, chlorite, calcite, sphene, zoisite and quartz; the chlorite commonly replaces actinolite. Secondary quartz is common locally, especially in the dikes of the Eastern Block. Relict igneous textures vary from granular to intergranular, with plagioclase laths averaging .5 millimetre in length.

4.1.4. Pillow Lavas

The pillow lavas and pillow breccia of the Western Block are composed of variable proportions of chlorite, epidote, sericite, quartz, plagioclase, actinolite-tremolite, and opaques, minerals characteristic of the greenschist metamorphic facies. Several of the petrographic features are described in Chapter 2. The margins of some of the pillow lavas are strongly foliated with parallel plagioclase laths and epidote crystals augened by chloritic schist. Towards the core the pillows consist of coarser grained, in some cases foliated, assemblages of approximately 50% plagioclase (An_{10}-An_{15}), 30% chlorite, 10% epidote and 10% opaques. The margins of the plagioclase laths, up to .5 millimetres in length, are corroded and replaced by chlorite.

The more mafic pillow lavas of the Eastern Block differ from those of the Western Block in containing greater percentages of actinolite-tremolite. The actinolite-tremolite, up to 60%, is a reflection of the dominance of mafic constituents in the original mineralogy. Typically, the pillows are composed of 40% actinolite-tremolite, 20% calcite, and 40% epidote, chlorite, sericite, quartz, zoisite and clinozoisite. Amygdules, commonly present in the pillows, consist of similar mineralogy as the groundmass. Some of the amygdules are concentrically formed, consisting of epidote, zoisite and clinozoisite at the margins with increasing amounts of calcite and sericite towards the centres; others contain radiating, accicular crystals of actinolite in a groundmass of epidote (Plate 20, Fig. b).

4.1.5. Pyroclastic and Sedimentary Rocks

The large clasts forming the agglomerates of the Eastern Block consist of euhedral plagioclase crystals (An_{10}-An_{15}) up to 2 millimetres in length, and pyroxene crystals entirely or partially replaced by actinolite, up to 1 centimetre in length. Epidote, zoisite, clinozoisite, chlorite and calcite make up the remainder of the clasts. Similar mineralogy is present in the crystals and crystal-lithic tuffs.

The fine grained reworked tuffs are generally made up of epidote, sphene, anhedral plagioclase crystals, calcite and quartz. The pale green to dark green layers are due to variations in grain size and concentrations of these minerals. Similar mineralogy make up the fragments of the tuffaceous breccia. The groundmass of the tuffaceous breccia contains angular fragments of plagioclase (An_{12}) up to 3 millimetres, and fine grained andesitic lithic fragments, containing sericite and calcite, up to 4 millimetres in length.

4.2. Petrochemistry

4.2.1. Introduction

Chemical analyses for both major element oxides and trace elements were carried out on 135 samples. The major element oxides, excluding P_2O_5, were analyzed using a Perkin Elmer 303 Atomic Absorption Spectrometer after they were crushed to 1/2 inch chips with a jaw-crusher and pulverized in a tungsten-carbide TEMA swing mill to -200 mesh. 0.2000 grams of sample were dissolved in 55 cc of HF. This was further diluted with 50 cc of saturated boric acid and made up to 200 cc with distilled

water. Further dilutions (5 in 50) were made for comparison with standard blends, both artificial and United States Geological Survey rock standards.

For CaO and MgO, 10 cc of La_2O_3 and 5 cc of HCl were added per 55 cc solutions to act as a releasing agent to suppress the interference of aluminum and phosphorus with these determinations.

Trace element determinations were carried out by X-ray Fluorescence using a Phillips PW 1220C computerized spectrometer. A standard program to analyze only eight trace elements was used. The samples which were ground to -200 mesh were pressed at 15 tons for 1 minute into Borax based discs of powder, with 10% sugar solution as a binding agent. A tungsten X-ray tube and LiF analyzer crystal were used. Excitation was 80 kV and 20 mA. Accuracy and precision of both Atomic Absorption Spectrometer and X-ray Fluorescence are given in Tables 2 to 4. The results, along with C.I.P.W. norms, are tabulated in Tables 5 to 8. All rock types are represented except the pyroclastic and sedimentary rocks, and rocks from the Ming's Block. An effort was made to select the fresher portions of the samples as far as hand specimen determination would allow; i.e. those samples that were sheared, amygdaloidal or contained veinlets of secondary mineral were discarded.

TABLE 2

Accuracy of Atomic Absorption

BCR-1

Wt. %	A	B
SiO_2	54.36	54.38
TiO_2	2.24	2.28
Al_2O_3	13.56	13.45
Fe_2O_3	13.40	13.36
CaO	6.94	6.82
MgO	3.46	3.48
Na_2O	3.26	3.22
K_2O	1.67	1.65
MnO	0.19	0.19

A = Abbey's proposed values. (1968)

B = Values obtained in this study.

TABLE 3

Precision of Atomic Absorption Analysis

BCR-1

Wt. %	$\bar{X}$	R	S	N	C%
SiO_2	55.38	54.93-55.78	0.37	4	0.01
TiO_2	2.35	2.21- 2.60	0.18	4	0.08
Al_2O_3	13.50	13.10-13.76	0.27	5	0.02
Fe_2O_3	13.00	12.64-13.41	0.28	5	0.02
CaO	6.63	6.59- 6.74	0.07	4	0.01
MgO	3.57	3.50- 3.65	0.06	5	0.02
Na_2O	3.23	3.16- 3.31	0.05	5	0.02
K_2O	1.73	1.68- 1.79	0.05	4	0.03
MnO	0.18	0.18- 0.19	0.01	5	0.02

$\bar{X}$ = Mean

R = Range (max.-min.)

S = Standard deviation from mean

N = No. of determinations

C = Coefficient of variation

TABLE 4

Precision of X-Ray Fluorescence

Element	No. of Determinations	Mean	Standard Deviation
Zr	23	438	4
Sr	31	197	5
Rb	31	94	2
Zn	30	59	1
Cu	30	109	4
Ni	29	210	3
Co	32	176	1
Cr	31	362	2
V	32	63	1
Ba	31	1783	13

TABLE 5

Major and Trace Element Analyses

Western Block

	Ph-5	Ph-6	BV-87D	BV-87E	BV-81A	BV-95A
SiO_2	39.30	39.00	38.20	39.10	39.10	41.10
TiO_2	-	-	-	-	-	0.05
Al_2O_3	1.10	3.47	2.29	0.98	1.42	2.11
Fe_2O_3	12.10	10.25	12.85	12.18	12.88	11.07
MnO	0.17	0.16	0.16	0.15	0.10	0.10
MgO	35.56	32.96	34.62	36.63	34.33	32.86
CaO	0.84	1.83	0.23	0.33	0.15	0.49
Na_2O	-	-	0.05	-	0.05	-
K_2O	-	-	-	-	-	-
P_2O_5	-	-	-	0.02	-	-
L.I.	11.36	11.51	10.87	11.01	10.80	10.46
Total	100.43	99.18	99.27	100.40	98.83	98.24
Q	-	-	-	-	-	-
Or	-	-	-	-	-	-
Ab	-	-	.49	-	.49	-
An	3.42	10.48	1.31	1.71	.86	2.81
Ne	-	-	-	-	-	-
Aug	1.01	-	-	-	-	-
Hy	25.90	26.53	27.06	25.79	32.45	45.87
Ol	69.64	62.83	69.09	71.96	64.98	49.81
Ilm	-	-	-	-	-	.11
Ap	-	-	-	.05	-	-
C	-	.17	2.05	.49	1.23	1.41
Rb	12	9	9	10	14	12
Sr	-	-	-	-	-	-
Ba	46	36	32	33	40	27
Zr	3	-	8	4	6	7
Cu	2	36	28	6	-	1
Zn	68	67	67	67	55	55
Cr	867	1106	1030	439	447	2007
Ni	1162	1685	1816	1659	2378	1934

PH-5 Serpentinized harzburgite
PH-6 Serpentinized lherzolite
BV-870 Serpentinized peridotite
BV-87E Serpentinized peridotite
BV-81A Serpentinized peridotite
BV-95A Serpentinized harzburgite

TABLE 5 (Cont'd.)

	BV-87C	BV-87A	BV-87F	BV-87	BV-80A	BV-80B
SiO_2	45.40	45.80	46.60	46.90	43.00	51.40
TiO_2	0.03	0.05	0.05	0.08	0.07	0.07
Al_2O_3	2.57	8.56	15.26	15.55	5.18	2.81
Fe_2O_3	6.58	6.91	3.71	3.47	6.50	5.60
MnO	0.15	0.12	0.08	0.08	0.11	0.11
MgO	20.88	21.09	11.76	11.25	23.62	24.01
CaO	17.50	13.50	18.16	18.14	12.12	11.36
Na_2O	0.09	0.13	0.78	1.08	0.05	-
K_2O	-	-	-	-	-	-
P_2O_5	0.01	0.01	-	-	-	0.01
L.I.	6.55	3.86	2.09	0.08	7.40	5.20
Total	99.76	100.03	98.49	98.62	98.05	100.57
Q	-	-	-	-	-	-
Or	-	-	-	-	-	-
Ab	-	1.15	3.65	4.31	.47	-
An	7.14	23.85	39.72	39.07	15.46	8.09
Ne	0.45	-	1.74	2.81	-	-
Aug	62.10	36.74	42.97	43.24	40.69	40.54
Hy	-	9.37	-	-	6.40	44.86
Ol	27.62	28.77	11.82	10.41	36.83	6.35
Ilm	0.06	0.10	0.10	0.16	0.15	0.14
Ap	0.03	0.02	-	-	-	0.02
C	-	-	-	-	-	-
La	2.60	-	-	-	-	-
Rb	12	13	9	100	10	12
Sr	6	11	62	1090	1	0
Ba	10	3	4	120	16	13
Zr	13	4	5	80	5	5
Cu	21	18	26	230	157	102
Zn	59	56	40	400	53	54
Cr	2364	1303	1107	991	2358	2581
Ni	634	513	321	293	987	801

BV-87C Clinopyroxenite.
BV-87A Clinopyroxenite.
BV-87F Gabbro-near peridotite.
BV-87 Gabbro near pyroxenite
BV-80A Pyroxenite.
BV-80B Websterite.

TABLE 5 (Cont'd.)

	BV-80C	BV-86A	BV-86	BV-83A	BV-91	BV-93
SiO_2	45.20	48.10	46.50	46.20	46.10	44.30
TiO_2	0.03	0.58	-	0.03	0.05	-
Al_2O_3	2.10	15.20	16.54	15.13	22.70	24.36
Fe_2O_3	8.69	10.85	4.02	3.54	2.21	3.06
MnO	0.10	0.16	0.09	0.08	0.03	0.07
MgO	30.00	8.78	11.66	11.33	7.37	7.12
CaO	1.21	9.50	19.10	19.03	16.29	15.86
Na_2O	0.05	2.92	0.69	0.53	1.56	1.43
K_2O	-	-	-	-	-	-
P_2O_3	-	0.04	0.07	-	-	-
L.I.	9.65	2.32	2.69	2.45	2.51	3.09
Total	97.03	98.45	101.36	98.32	98.82	99.29
Q	-	-	-	-	-	-
Or	-	-	-	-	-	-
Ab	0.49	25.99	-	1.34	10.54	6.97
An	6.34	29.85	42.78	40.73	57.18	62.63
Ne	-	-	3.22	1.82	1.73	3.06
Aug	0.46	15.98	41.69	46.15	21.36	15.53
Hy	67.18	9.41	-	-	-	-
Ol	25.45	17.51	11.91	9.90	9.09	11.82
Ilm	0.07	1.16	-	.06	.10	-
Ap	-	.10	.17	-	-	-
C	-	-	-	-	-	-
La	-	-	.24	-	-	-
Rb	10	13	9	10	8	10
Sr	-	51	87	85	135	113
Ba	29	61	2	0	170	0
Zr	-	31	6	4	33	5
Cu	116	83	12	13	7	7
Zn	56	80	46	41	33	39
Cr	2625	101	777	907	832	215
Ni	1652	71	464	369	170	137

BV-80C Serpentinized harzburgite.
BV-86A to BV-93 Gabbro.

TABLE 5 (Cont'd.)

	BV-1D	BV-1E	BV-1L	BV-95B	BV-96	BV-84
SiO_2	46.20	46.50	47.80	44.90	43.50	48.50
TiO_2	0.15	0.15	0.15	0.28	-	0.57
Al_2O_3	14.30	12.00	5.04	7.57	18.33	15.67
Fe_2O_3	5.19	6.60	8.06	9.46	3.92	9.58
MnO	0.10	0.12	0.13	0.14	0.08	0.14
MgO	13.30	14.24	20.85	23.11	10.84	9.23
CaO	14.10	13.66	11.61	9.83	15.98	10.63
Na_2O	1.61	0.61	0.17	0.23	0.73	2.74
K_2O	0.21	-	-	-	-	-
P_2O_5	-	-	.06	0.02	-	0.03
L.I.	4.81	4.12	4.83	6.12	4.64	2.34
Total	99.99	98.00	98.70	100.66	98.02	99.43
Q	-	-	-	-	-	-
Or	1.31	-	-	-	-	-
Ab	10.13	5.54	1.54	2.08	4.15	24.12
An	32.93	32.18	13.97	20.97	50.27	31.69
Ne	2.30	-	-	-	1.35	-
Aug	32.64	32.41	37.89	20.50	27.86	18.75
Hy	-	17.72	31.31	24.67	-	7.40
Ol	20.38	11.85	14.83	31.17	16.37	16.83
Ilm	.31	.31	0.31	.57	-	1.13
Ap	-	-	0.14	.05	-	.07
Rb	14	14	12	13	9	13
Sr	105	776	3	1	94	68
Ba	54	29	23	22	3	50
Zr	12	15	11	19	6	30
Cu	69	158	43	2	31	31
Zn	46	55	59	55	41	51
Cr	525	967	1386	1214	1036	70
Ni	325	522	448	775	284	63

BV-1D Gabbro
BV-1E Gabbro
BV-1L Pyroxenite
BV-95B Gabbro near ultramafic
BV-96 Gabbro
BV-84 Diabase dike - lower zone.

TABLE 5 (Cont'd.)

	BV-100	BV-100A	BV-103	BV-125	BV-127	BV-122
SiO_2	45.00	48.80	49.00	49.70	50.30	50.30
TiO_2	0.13	0.13	0.13	0.28	0.30	0.21
Al_2O_3	7.50	13.27	16.31	15.40	15.31	15.25
Fe_2O_3	8.21	3.82	5.81	7.22	7.94	6.31
MnO	0.12	0.10	0.12	0.12	0.14	0.12
MgO	5.84	11.59	9.86	9.23	8.58	9.23
CaO	7.61	17.34	14.68	13.85	12.96	13.07
Na_2O	0.08	1.28	1.00	1.23	1.68	1.50
K_2O	-	0.18	-	-	0.19	1.20
P_2O_5	0.08	-	0.03	-	-	0.06
L.I.	5.84	1.66	2.18	2.22	2.42	2.25
Total	99.15	98.17	99.12	99.25	99.82	99.50
Q	-	-	-	.77	-	-
Or	-	1.11	-	-	1.16	7.35
Ab	0.73	10.12	8.78	10.81	14.71	13.14
An	21.74	31.14	41.53	37.90	34.86	32.43
Ne	-	0.62	-	-	-	-
Aug	14.72	46.36	27.23	27.09	25.81	27.67
Hy	33.60	-	21.55	22.88	22.83	13.04
Ol	28.75	10.39	0.58	-	.04	5.82
Ilm	0.27	0.26	0.26	.55	.59	.41
Ap	0.20	-	0.07	-	-	.14
Rb	14	12	11	8	11	18
Sr	-	135	117	67	111	69
Ba	13	23	9	38	31	55
Zr	8	13	14	16	19	19
Cu	-	24	17	6	4	21
Zn	59	42	55	48	43	52
Cr	2799	987	279	252	185	416
Ni	1972	203	154	151	106	102

BV-100 Gabbro intermediate level.
BV-100A Gabbro pyroxene-rich
BV-103 Gabbro - intermediate level.
BV-125 Gabbro - high level.
BV-127 Gabbro, high level.
BV-122 Gabbro high level.

TABLE 5 (Cont'd.)

	BV-129	BV-98	BV-94A	BV-90	BV-102A	BV-105
SiO_2	49.70	50.60	48.40	48.50	50.00	51.70
TiO_2	0.30	0.69	0.30	1.00	0.43	0.48
Al_2O_3	15.50	14.81	14.73	12.88	15.28	15.44
Fe_2O_3	8.13	11.36	8.04	7.36	9.60	9.34
MnO	0.12	0.14	0.11	0.11	0.14	0.12
MgO	8.92	7.96	9.46	11.05	8.60	8.73
CaO	12.43	7.61	13.43	10.50	9.22	9.12
Na_2O	1.96	3.88	1.82	3.12	3.03	3.38
K_2O	0.18	-	-	0.18	-	-
P_2O_5	0.11	0.03	0.16	0.84	0.02	0.04
L.I.	2.30	2.13	1.84	2.59	2.81	2.55
Total	99.65	99.21	98.29	98.13	99.13	100.90
Q	-	-	-	-	-	-
Or	1.10	-	-	1.12	-	-
Ab	17.18	34.23	16.10	27.84	26.88	29.36
An	34.15	23.97	33.48	21.74	29.46	27.68
Ne	-	-	-	-	-	-
Aug	23.58	12.51	28.49	22.05	15.04	15.12
Hy	17.71	13.27	11.84	6.31	18.10	17.73
Ol	5.42	14.60	9.10	16.88	9.61	9.09
Ilm	0.59	1.37	0.60	2.00	0.86	.94
Ap	0.26	0.07	0.39	2.06	0.05	.10
Rb	10	15	12	10	14	-
Sr	141	160	63	521	146	-
Ba	-	53	29	499	38	-
Zr	23	44	17	230	32	-
Cu	16	5	45	76	11	-
Zn	50	54	48	83	61	-
Cr	120	44	314	341	126	-
Ni	124	36	155	499	104	-

BV-129 Gabbro high level.
BV-98 to BV-90 Diabase dikes from lower zones.
BV-102A Diabase dikes from intermediate levels.
BV-105 Coarse diabase dikes from sheeted unit.

TABLE 5 (Cont'd.)

	BV-105A	BV-110	BV-111A	BV-115	BV-116B	BV-116A
SiO_2	51.80	46.60	43.40	47.40	51.40	51.10
TiO_2	0.44	0.99	3.28	1.20	0.60	0.60
Al_2O_3	14.69	17.31	14.62	15.63	14.87	16.06
Fe_2O_3	10.58	9.16	14.21	11.04	10.18	9.81
MnO	0.16	0.15	0.22	0.16	0.14	0.13
MgO	8.48	7.99	6.66	7.87	6.95	6.71
CaO	8.81	11.86	9.00	11.59	9.67	7.75
Na_2O	2.75	1.69	2.70	1.99	3.42	4.00
K_2O	-	0.28	-	0.18	-	-
P_2O_5	-	0.05	0.82	0.28	0.05	0.03
L.I.	2.54	3.07	3.34	2.80	2.60	2.61
Total		99.15	98.25	100.14	99.88	98.80
Q	-	-	-	-	-	-
Or	-	1.74	-	1.11	-	-
Ab	24.07	15.03	24.44	17.50	30.06	35.55
An	28.70	40.79	29.71	34.48	26.21	27.17
Ne	-	-	-	-	-	-
Aug	13.57	16.92	10.22	19.22	19.23	10.73
Hy	32.70	13.46	11.46	15.14	17.68	16.37
Ol	0.09	9.97	15.48	9.51	5.53	8.91
Ilm	0.87	1.98	6.66	2.37	1.18	1.20
Ap	-	0.12	2.04	0.68	0.12	.07
Rb	11	14	13	13	11	11
Sr	155	241	320	212	173	187
Ba	50	84	228	91	60	72
Zr	35	79	244	85	34	45
Cu	6	74	28	52	85	-
Zn	69	76	113	80	54	46
Cr	131	208	106	224	33	40
Ni	81	145	87	117	32	45

BV-105A to BV-116A Coarse diabase dikes from sheeted unit.

TABLE 5 (Cont'd.)

	BV-125A	BV-126B	BV-128	BV-129A	BV-133	BV-133D
SiO_2	49.30	49.90	51.10	51.50	51.00	50.30
TiO_2	0.37	0.44	0.27	0.39	-	0.48
Al_2O_3	14.87	14.87	14.64	16.04	15.50	14.64
Fe_2O_3	9.13	9.95	11.08	8.14	8.28	9.47
MnO	0.14	0.13	0.13	0.08	0.09	0.11
MgO	8.40	8.63	7.32	8.98	8.50	8.66
CaO	11.76	11.66	10.65	9.25	12.00	11.59
Na_2O	1.89	2.13	1.79	3.05	1.39	1.78
K_2O	-	0.28	-	0.38	-	0.38
P_2O_5	0.03	0.02	0.03	-	-	0.02
L.I.	2.25	2.50	2.47	2.86	3.26	2.55
Total	98.14	100.51	99.48	100.67	100.02	99.98
Q	-	-	3.41	-	3.44	-
Or	-	1.71	-	2.32	-	2.33
Ab	16.84	18.58	15.79	26.61	12.26	15.61
An	33.79	31.12	33.28	29.85	37.59	31.96
Ne	-	-	-	-	-	-
Aug	22.44	23.25	17.88	14.20	19.97	22.49
Hy	24.95	16.94	29.03	17.63	26.75	25.71
Ol	1.18	7.50	-	8.63	-	.91
Ilm	0.74	0.87	0.54	0.76	-	.95
Ap	0.07	0.05	.07	-	-	.05
Rb	13	14	13	9	10	13
Sr	82	100	102	94	101	97
Ba	48	57	56	-	-	12
Zr	24	29	33	17	16	22
Cu	20	7	7	10	10	11
Zn	52	48	47	40	44	49
Cr	91	224	35	120	193	197
Ni	91	123	23	130	129	117

BV-125A to BV-133D Coarse diabase dikes from sheeted unit.

TABLE 5 (Cont'd.)

	BV-135	BV-135A	BV-135B	BV-136B	BV-138	BV-140
SiO_2	52.80	52.20	51.10	53.00	52.00	51.20
TiO_2	0.53	0.51	0.60	0.60	0.48	0.53
Al_2O_3	14.46	14.18	15.00	14.73	14.80	14.58
Fe_2O_3	8.59	9.37	10.14	9.80	9.53	11.37
MnO	0.13	0.14	0.14	0.23	0.18	0.19
MgO	7.12	6.89	7.14	6.62	6.86	6.52
Na_2O	2.31	3.26	2.46	3.00	3.40	3.03
K_2O	1.17	0.38	0.53	0.52	0.15	0.05
P_2O_5	0.04	0.05	0.05	0.05	0.06	0.04
L.I.	1.84	2.01	2.52	2.71	2.28	2.31
Total	99.38	99.06	99.78	99.21	98.57	98.80
Q	1.53	-	-	2.81	-	.17
Or	7.16	2.34	3.26	3.22	0.93	0.31
Ab	20.22	28.70	21.63	26.57	30.17	26.89
An	26.51	23.87	29.43	26.37	25.89	27.31
Ne	-	-	-	-	-	-
Aug	21.76	22.87	18.38	12.04	16.20	15.90
Hy	21.68	18.39	25.87	27.67	25.00	28.28
Ol	-	2.71	0.13	-	0.71	-
Ilm	1.04	1.01	1.18	1.19	0.96	1.06
Ap	.10	.12	0.12	.12	0.15	.10
Rb	15	9	14	16	8	6
Sr	91	102	116	105	148	90
Ba	49	4	28	38	16	-
Zr	24	31	30	37	32	37
Cu	6	23	24	47	29	96
Zn	55	52	59	69	71	96
Cr	45	76	77	70	48	53
Ni	53	60	56	45	55	41

BV-135 to 140 Coarse diabase dikes from sheeted unit.

TABLE 5 (Cont'd.)

	BV-140A	BV-141E	BV-142	BV-144B	BV-141	BV-141A	BV-146
SiO_2	49.90	59.60	52.20	52.60	55.70	62.70	52.70
TiO_2	0.44	0.65	0.70	0.60	0.63	0.44	0.21
Al_2O_3	15.21	15.73	14.80	15.07	16.00	14.02	11.20
Fe_2O_3	8.85	10.25	9.30	10.50	13.07	8.50	5.82
MnO	0.18	0.12	0.11	0.15	0.16	0.11	0.08
MgO	8.59	1.59	3.66	6.00	2.96	1.55	6.10
CaO	9.98	2.59	9.95	11.91	2.38	2.88	7.38
Na_2O	2.16	6.97	2.70	0.41	5.82	5.95	1.82
K_2O	1.70	0.85	0.62	-	1.63	0.71	0.21
P_2O_5	0.06	0.06	0.09	0.12	0.05	0.05	0.02
L.I.	2.58	1.09	0.11	3.03	1.74	1.09	13.64
Total	99.65	99.50	100.14	100.39	100.14	98.12	99.15
Q	-	1.49	6.29	13.10	-	12.49	18.18
Or	10.45	5.16	3.94	-	9.93	4.37	1.25
Ab	19.00	60.56	24.51	3.60	50.72	52.34	18.13
An	27.85	9.37	28.36	40.79	11.82	9.83	25.74
Ne	-	-	-	-	-	-	-
Aug	18.96	2.95	20.15	16.40	-	3.86	14.03
Hy	9.13	19.06	15.11	24.64	15.43	15.82	22.14
Ol	13.60	-	-	-	10.28	-	-
Ilm	0.87	1.27	1.43	1.18	1.23	1.19	0.47
Ap	0.15	0.14	0.22	0.29	0.12	0.12	0.06
Rb	22	19	21	12	38	19	12
Sr	110	56	148	278	50	57	109
Ba	76	222	107	52	323	159	43
Zr	24	38	47	85	46	26	14
Cu	47	-	68	14	22	13	11
Zn	74	85	97	119	99	72	45
Cr	267	30	30	24	30	29	38
Ni	154	22	29	2	12	16	27

BV-140A Diabase dike
BV-141E to BV-144B From cores of pillow lavas.
BV-141 to BV-146 From isolated pillow breccia.

TABLE 6

Major and Trace Element Analyses

Eastern Block

	PR-32C1	PR-32C2	PR-32C3	PR-32D1	PR-32D2	PR-35
SiO_2	43.70	37.70	43.00	41.00	46.40	45.70
TiO_2	-	-	-	-	-	-
Al_2O_3	3.43	2.74	3.91	4.50	3.43	17.43
Fe_2O_3	6.78	10.19	8.01	5.71	7.06	3.98
MnO	0.10	0.15	0.11	0.09	0.09	0.08
MgO	32.34	33.88	32.63	27.47	26.52	12.08
CaO	4.36	3.07	2.82	10.83	10.15	17.45
Na_2O	-	-	-	-	-	0.80
K_2O	-	-	-	-	-	-
P_2O_5	0.03	0.07	0.04	0.08	0.01	0.01
L.I.	8.01	12.75	9.36	9.72	6.94	2.78
Total	98.75	100.55	99.88	99.40	100.60	100.31
Q	-	-	-	-	-	-
Or	-	-	-	-	-	-
Ab	-	-	-	-	-	1.89
An	10.39	8.62	11.89	13.78	10.07	45.27
Ne	-	-	-	-	-	2.75
Aug	10.58	6.67	2.70	35.36	34.88	34.81
Hy	34.62	11.89	38.65	-	24.77	-
Ol	44.33	72.64	46.65	50.30	30.26	15.25
Ilm	-	-	-	-	-	-
Ap	0.08	0.19	0.10	0.21	0.03	0.02
Rb	18	16	11	14	14	12
Sr	-	5	-	19	4	65
Ba	15	28	20	13	9	-
Zr	-	3	-	6	4	14
Cu	47	66	92	93	136	109
Zn	46	53	50	50	45	45
Cr	715	487	1093	2780	937	563
Ni	2199	2413	2249	1131	1829	324

PR-32C1 Serpentinised peridotite.
PR-32C2 Serpentinised peridotite.
PR-32C3 Serpentinised peridotite.
PR-32D1 Serpentinised peridotite.
PR-32D2 Pyroxenite
PR-35 Gabbro near peridotite.

TABLE 6 (Cont'd.)

	PR-36	PR-37A	PR-40	PR-42	PR-59	PR-59B
SiO_2	45.70	48.10	43.30	44.80	51.40	45.00
TiO_2	-	-	-	-	-	0.15
Al_2O_3	19.40	13.91	9.27	5.70	14.67	16.73
Fe_2O_3	3.95	5.03	8.61	7.50	3.75	4.69
MnO	0.07	0.10	0.12	0.12	0.09	0.09
MgO	10.36	15.00	22.20	24.69	10.88	11.86
CaO	18.53	15.43	10.17	10.08	15.33	18.26
Na_2O	0.58	0.51	0.39	0.10	2.20	0.46
K_2O	-	-	-	-	0.03	0.17
P_2O_5	0.04	0.05	-	0.02	-	0.01
L.I.	2.47	2.80	6.06	5.90	1.86	2.63
Total	101.10	100.93	100.12	98.91	100.21	100.05
Q	-	-	-	-	-	-
Or	-	-	-	-	0.18	-
Ab	0.46	4.42	3.54	0.92	19.00	-
An	51.24	36.53	25.26	16.37	30.69	44.44
Ne	2.46	-	-	-	-	2.18
Aug	33.54	33.03	23.02	29.92	37.35	35.62
Hy	-	12.45	8.72	19.47	3.74	-
Ol	12.21	13.45	39.46	33.27	9.05	15.32
Ilm	-	-	-	-	-	0.29
Ap	0.09	0.12	-	0.05	-	0.02
Rb	12	10	11	11	12	13
Sr	179	68	-	-	112	247
Ba	1	13	19	7	12	1
Zr	23	13	10	6	12	28
Cu	20	35	167	9	49	133
Zn	43	48	60	56	40	47
Cr	498	731	1199	1227	962	570
Ni	226	404	882	972	241	403

PR-36 Gabbro
PR-37A Gabbro
PR-40 Pyroxenite
PR-42 Pyroxenite
PR-59 Gabbro
PR-59B Gabbro

TABLE 6 (Cont'd.)

	PR-66	PR-71	PR-71A	PR-73	PR-74B	PR-74F
SiO_2	49.20	48.00	48.20	51.60	52.80	57.80
TiO_2	0.21	0.22	0.60	0.32	0.48	0.75
Al_2O_3	8.28	17.87	15.91	16.26	15.00	13.62
Fe_2O_3	6.32	6.07	11.25	9.07	10.01	10.84
MnO	0.14	0.09	0.09	0.09	0.09	0.08
MgO	15.47	10.25	10.12	7.07	8.87	5.38
CaO	14.34	10.68	6.49	8.06	6.49	8.05
Na_2O	1.15	1.67	2.57	4.62	2.80	0.65
K_2O	0.23	1.88	-	-	0.17	-
P_2O_5	0.01	-	0.03	0.04	-	0.07
L.I.	4.62	3.39	4.45	2.43	3.81	3.53
Q	-	-	-	-	2.53	23.31
Or	1.48	11.57	-	-	1.05	-
Ab	10.61	14.70	23.10	40.62	24.75	5.72
An	18.27	37.15	33.87	24.56	29.11	35.62
Ne	-	-	-	-	-	-
Aug	34.30	14.45	0.11	13.75	3.71	4.54
Hy	29.67	0.69	30.95	2.76	37.89	29.16
Ol	5.21	21.01	10.70	17.57	-	-
Ilm	0.44	0.44	1.21	0.63	0.95	1.48
Ap	0.03	-	0.07	.10	-	0.17
Rb	13	20	14	13	14	13
Sr	75	314	250	187	106	216
Ba	57	84	87	75	84	91
Zr	16	34	48	39	40	64
Cu	24	15	15	15	13	23
Zn	54	43	47	42	45	47
Cr	1316	346	36	54	57	33
Ni	270	243	33	56	60	8

PR-66 Gabbro
PR-71 Gabbro
PR-71A Diabase dike
PR-73 Diabase dike
PR-74B Diabase dike
PR-74F Silicified diabase dike
) Sheeted zone.

TABLE 6 (Cont'd.)

	PR-74H	PR-75A	PR-76C	PR-79	PR-77D	PR-77E
SiO_2	59.00	54.00	51.20	41.00	48.80	50.40
TiO_2	0.65	0.35	0.54	0.30	0.42	0.42
Al_2O_3	13.32	15.20	15.13	12.73	15.20	14.40
Fe_2O_3	9.28	8.35	8.30	10.85	9.35	8.25
MnO	0.07	0.12	0.13	0.20	0.12	0.10
MgO	5.24	7.41	9.28	12.80	10.31	4.91
CaO	8.53	6.66	6.68	8.68	5.42	13.23
Na_2O	1.01	3.35	1.96	0.48	3.00	0.88
K_2O	0.03	1.97	3.72	0.32	1.43	0.18
P_2O_5	-	-	0.05	0.03	0.01	0.01
L.I.	3.44	2.77	2.92	12.54	5.40	6.93
Total	100.57	100.18	99.91	99.93	99.46	99.71
Q	34.08	-	-	-	-	10.46
Or	0.20	12.07	22.88	2.17	9.08	1.16
Ab	9.37	29.35	17.25	4.65	27.26	8.10
An	19.20	21.35	22.35	36.24	25.54	37.86
Ne	-	-	-	-	-	-
Aug	-	10.54	9.57	10.45	2.66	27.74
Hy	30.09	20.99	10.29	29.67	13.85	13.79
Ol	-	5.02	16.48	16.10	20.73	-
Ilm	1.35	0.69	1.07	0.65	0.86	0.87
Ap	-	-	0.12	0.08	0.03	0.03
C	5.71	-	-	-	-	-
Rb	14	22	300	12	18	14
Sr	276	143	710	34	79	110
Ba	84	110	2200	113	107	64
Zr	62	40	380	33	28	40
Cu	29	19	190	10	14	18
Zn	46	47	530	86	51	48
Cr	39	31	168	810	81	55
Ni	23	52	102	478	69	53

PR-74H to PR-77E Dikes from sheeted diabase unit. Those with high normative quartz are silicified.

TABLE 6 (Cont'd.)

	PR-77G	PR-81B	PR-88	PR-89	PR-89A	PR-89B
SiO_2	54.00	58.60	40.80	44.80	48.00	48.80
TiO_2	0.35	0.32	0.39	0.39	0.43	0.39
Al_2O_3	14.45	16.29	13.91	14.35	16.19	14.05
Fe_2O_3	9.80	6.67	9.80	9.10	8.35	8.08
MnO	0.12	0.08	0.20	0.17	0.15	0.16
MgO	5.65	7.19	10.79	10.12	8.81	9.96
CaO	6.90	2.67	9.62	15.19	9.26	13.00
Na_2O	2.87	4.05	0.70	0.78	3.51	0.87
K_2O	0.03	0.65	0.65	0.15	0.36	1.13
P_2O_5	-	-	0.01	-	0.01	-
L.I.	4.14	3.77	12.35	4.60	5.27	3.88
Total	98.31	100.29	99.22	99.65	100.34	100.32
Q	9.07	11.76	-	-	-	-
Or	0.19	4.01	4.37	0.94	2.27	6.99
Ab	26.06	35.75	6.74	7.01	28.69	7.70
An	28.39	13.82	37.43	37.40	29.03	32.51
Ne	-	-	-	-	1.53	-
Aug	6.93	-	13.63	34.69	16.00	28.32
Hy	28.65	29.78	20.55	2.26	-	18.18
Ol	-	-	14.26	16.91	21.60	5.53
Ilm	0.71	0.63	3.00	0.79	0.87	0.78
Ap	-	-	0.03	-	0.03	-
C	-	4.25	-	-	-	-
Rb	12	13	24	14	13	28
Sr	122	22	49	96	52	88
Ba	75	122	101	81	103	65
Zr	37	-	18	31	5	38
Cu	14	97	50	56	74	67
Zn	49	58	84	75	70	87
Cr	48	220	315	253	290	144
Ni	33	105	212	196	222	99

PR-77G Diabase dike
PR-81B to PR-89B Amygdaloidal pillow lavas.

TABLE 7

Major and Trace Element Analyses
Deer Cove Block

	BV-13A	BV-13C	BV-14	BV-18	BV-21	BV-24
SiO_2	42.40	47.60	51.30	48.10	46.00	50.20
TiO_2	-	-	0.24	0.43	0.17	0.23
Al_2O_3	0.20	14.95	15.00	16.33	17.79	15.20
Fe_2O_3	5.33	4.77	6.60	8.10	5.90	5.24
MnO	0.10	0.10	0.12	0.13	0.11	0.10
MgO	37.98	12.29	10.92	7.61	10.59	10.50
CaO	0.15	15.00	6.48	8.29	13.76	13.85
Na_2O	0.05	1.54	3.53	3.99	0.88	2.01
K_2O	-	-	1.32	-	-	0.32
P_2O_5	-	-	-	0.02	0.01	-
L.I.	11.81	2.75	2.82	4.12	3.44	2.32
Total	98.02	99.00	98.33	97.19	98.65	
Q	-	-	-	-	-	-
Or	-	-	8.23	-	-	1.95
Ab	0.51	13.33	31.49	36.62	7.87	17.51
An	0.36	35.38	22.34	28.91	47.13	32.44
Ne	-	0.15	-	-	-	-
Aug	0.38	33.75	9.30	12.72	20.04	30.68
Hy	45.71	-	9.17	0.49	14.63	6.83
Ol	53.04	17.40	18.99	20.33	9.97	10.15
Ilm	-	-	0.48	0.89	0.34	0.45
Ap	-	-	-	0.05	0.03	-
Rb	11	12	22	14	12	13
Sr	-	205	204	206	206	171
Ba	24	40	130	43	-	45
Zr	-	19	24	34	20	24
Cu	-	104	79	90	123	32
Zn	41	46	58	71	54	48
Cr	2018	333	414	302	601	283
Ni	4586	338	129	167	251	234

BV-13A Serpentinised Peridotite Devil's Cove.
BV-13C Gabbro.
BV-14 Gabbro
BV-18 Gabbro
BV-21 Gabbro
BV-24 Pegmatitic Gabbro

TABLE 7 (Cont'd.)

	BV-27A	BV-30	BV-32-1	BV-32-2	BV-33	BV-34
SiO_2	51.20	49.00	48.20	47.10	47.40	50.20
TiO_2	1.24	0.15	0.16	0.13	0.05	0.15
Al_2O_3	15.00	16.78	12.94	17.20	6.57	11.20
Fe_2O_3	8.00	5.40	8.00	7.00	10.30	7.40
MnO	0.13	0.10	0.14	0.12	0.14	0.16
MgO	8.56	9.41	13.05	11.13	23.56	12.82
CaO	7.40	14.00	11.64	12.00	8.38	12.63
Na_2O	4.22	1.50	1.36	1.39	-	1.44
K_2O	-	0.52	0.36	0.51	-	-
P_2O_5	0.43	0.01	0.07	0.02	0.03	0.13
L.I.	4.34	2.42	3.78	1.39	5.16	3.96
Total	100.52	99.29	99.70	101.05	101.59	100.09
Q	-	-	-	-	-	-
Or	-	3.19	2.24	3.15	-	-
Ab	37.43	13.18	12.10	12.26	-	12.77
An	23.06	38.95	29.59	40.86	18.79	25.26
Ne	-	-	-	-	-	-
Aug	10.13	26.60	24.68	16.99	19.64	31.79
Hy	16.52	10.11	17.28	9.96	39.21	25.70
Ol	9.35	7.67	13.64	16.48	22.18	3.86
Ilm	2.47	0.30	0.32	0.26	0.10	0.30
Ap	1.05	.02	0.17	.05	0.07	0.32
Rb	12	17	15	18	13	11
Sr	524	175	157	267	-	189
Ba	108	62	68	80	22	22
Zr	188	21	20	23	8	24
Cu	43	65	28	9	22	132
Zn	78	48	61	58	76	64
Cr	262	239	124	109	573	297
Ni	264	126	186	174	683	212

BV-27A Diabase dike
BV-30 Gabbro
BV-32-1 Gabbro
BV-32-2 Gabbro
BV-33 Pyroxenite
BV-34 Gabbro

TABLE 7 (Cont'd.)

	BV-35	BV-40	BV-41A	BV-43A	BV-45
SiO_2	54.70	49.20	48.10	49.60	55.10
TiO_2	0.26	0.09	0.53	0.12	0.57
Al_2O_3	13.77	19.17	14.89	16.08	15.00
Fe_2O_3	7.50	3.00	6.90	4.20	10.90
MnO	0.13	0.07	0.12	0.10	0.26
MgO	10.53	8.06	6.41	10.86	6.47
CaO	7.67	18.36	8.46	16.66	2.76
Na_2O	3.70	1.32	4.41	1.09	4.88
K_2O	-	0.23	0.42	0.49	0.46
P_2O_5	0.06	0.01	0.03	0.01	0.01
L.I.	2.83	1.91	9.69	2.42	3.07
Total	101.15	101.42	99.96	101.63	99.54
Q	-	-	-	-	1.68
Or	-	1.37	2.77	2.93	2.85
Ab	32.08	9.25	36.70	9.34	43.29
An	21.49	46.07	21.88	38.00	13.88
Ne	-	1.09	2.68	-	-
Aug	13.82	36.37	20.23	36.34	-
Hy	29.99	-	-	3.21	35.30
Ol	1.97	5.65	14.54	9.93	-
Ilm	0.51	0.17	1.12	0.23	1.14
Ap	0.14	0.02	0.08	0.02	0.17
C	-	-	-	-	1.70
Rb	13	9	15	15	14
Sr	154	240	209	353	141
Ba	36	20	57	74	144
Zr	24	24	33	30	48
Cu	72	19	59	36	666
Zn	70	40	47	49	94
Cr	327	648	45	757	50
Ni	144	125	40	206	37

BV-35 Diabase dike
BV-40 Gabbro
BV-41A Gabbro
BV-43A Gabbro
BV-45 Chlorite schist

TABLE VI (Cont'd.)

	BV-52	BV-56A	BV-64	BV-64C	BV-64D
SiO_2	52.20	53.00	58.30	53.40	53.30
TiO_2	0.51	0.60	0.58	0.56	0.50
Al_2O_3	14.72	15.45	13.34	13.26	14.84
Fe_2O_3	12.10	11.50	7.80	9.90	7.90
MnO	0.40	0.17	0.11	0.14	0.14
MgO	7.00	6.64	2.20	2.67	2.61
CaO	2.02	5.59	7.23	8.57	8.82
Na_2O	3.39	3.58	3.22	2.13	3.77
K_2O	0.45	0.18	0.62	0.78	0.84
P_2O_5	0.06	0.02	0.19	0.09	0.06
L.I.	4.39	3.64	6.77	8.00	8.34
Total	97.24	100.37	100.36	99.50	101.12
Q	7.76	1.85	17.85	13.91	5.06
Or	2.90	1.11	3.95	5.10	5.40
Ab	31.30	31.69	29.35	19.91	34.67
An	10.51	26.74	21.67	26.87	22.93
Ne	-	-	-	-	-
Aug	-	1.78	13.28	16.56	20.49
Hy	40.73	35.59	12.22	16.25	10.27
Ol	-	-	-	-	-
Ilm	1.06	1.19	1.19	1.18	1.03
Ap	0.15	0.05	0.48	0.23	0.15
C	5.60	-	-	-	-
Rb	16	12	19	21	21
Sr	115	151	106	100	95
Ba	115	83	51	62	54
Zr	49	41	48	52	37
Cu	471	61	67	54	65
Zn	126	91	75	92	72
Cr	45	80	35	34	87
Ni	37	62	18	42	50

BV-52 to BV-64D Pillow Lavas

TABLE 8

Major and Trace Element Analyses

Point Rousse Block

	BV-2	BV-3B	BV-3E	BV-3F	BV-4	BV-7
SiO_2	49.00	49.90	49.10	49.40	47.70	48.10
TiO_2	0.41	0.51	0.60	0.60	0.15	0.15
Al_2O_3	17.86	14.70	16.47	14.44	11.71	15.98
Fe_2O_3	7.10	10.31	9.40	10.33	6.17	5.28
MnO	0.11	0.16	0.14	0.14	0.11	0.10
MgO	7.63	9.38	8.15	10.75	14.24	11.15
CaO	10.40	9.00	9.00	8.15	12.00	16.20
Na_2O	3.41	3.19	3.66	3.64	1.05	1.01
K_2O	0.24	-	0.17	-	-	-
P_2O_5	0.01	0.03	0.02	0.03	.02	-
L.I.	2.22	2.48	2.48	3.24	2.99	2.47
Total	98.39	99.66	99.19	100.72	96.14	100.44
Q	-	-	-	-	-	-
Or	1.49	-	1.05	-	-	-
Ab	29.70	28.07	32.33	31.93	9.60	8.77
An	34.28	26.83	29.25	23.92	29.44	40.10
Ne	0.29	-	-	-	-	-
Aug	16.03	15.88	14.12	14.50	27.76	33.92
Hy	-	13.17	1.05	3.70	24.73	6.14
Ol	17.38	14.98	20.97	24.70	8.11	10.79
Ilm	0.82	1.01	1.19	1.18	0.31	0.29
Ap	0.02	.07	0.05	0.07	0.05	-
Rb	12	11	12	11	11	11
Sr	334	212	311	188	130	421
Ba	46	67	81	74	210	14
Zr	38	40	49	37	16	38
Cu	17	39	22	5	121	115
Zn	50	52	62	44	55	49
Cr	60	153	142	96	933	418
Ni	95	113	97	86	487	241

BV-2 Gabbro
BV-3B to BV-3F Sheeted coarse diabase dikes.
BV-4 Gabbro
BV-7 Gabbro

TABLE 8 (Cont'd.)

	BV-8	BV-11	BV-11A	BV-11D	BV-12A	PR-15
SiO_2	48.20	51.60	51.40	49.40	46.20	50.80
TiO_2	0.26	0.46	0.60	0.75	-	0.39
Al_2O_3	7.34	14.52	15.00	15.14	6.20	14.37
Fe_2O_3	8.89	9.33	9.92	9.96	7.00	9.30
MnO	0.16	0.15	0.16	0.15	0.10	0.13
MgO	17.57	9.69	8.92	8.35	22.67	9.37
CaO	12.00	6.67	6.95	9.16	10.73	9.63
Na_2O	0.92	4.13	4.13	3.50	0.18	2.99
K_2O	-	0.42	0.16	-	-	0.84
P_2O_5	-	0.05	0.03	0.01	-	0.08
L.I.	3.12	2.67	2.68	2.54	5.97	2.47
Total	98.46	99.69	99.95	98.96	99.05	100.37
Q	-	-	-	-	-	-
Or	-	2.59	0.98	-	-	5.12
Ab	8.24	36.37	36.29	31.03	1.65	26.09
An	16.83	20.65	22.77	26.83	17.44	24.04
Ne	-	-	-	-	-	-
Aug	37.02	10.96	10.50	16.98	31.91	20.14
Hy	20.46	9.92	11.83	7.12	24.90	7.51
Ol	16.92	18.49	16.36	16.51	24.11	16.14
Ilm	0.52	0.91	1.18	1.49	-	0.76
Ap	-	0.12	0.07	0.02	-	0.19
Rb	14	13	7	14	0	14
Sr	28	182	147	217	-	155
Ba	34	108	108	102	13	71
Zr	18	26	10	41	-	30
Cu	127	9	16	22	117	9
Zn	66	47	39	49	55	49
Cr	890	253	109	131	1633	130
Ni	325	138	79	77	1786	97

BV-8 Pyroxenite
BV-11 Gabbro screen
BV-11A Coarse diabase dike
BV-11D Coarse diabase dike
BV-12A Pyroxenite
PR-15 High level gabbro

TABLE 8 (Cont'd.)

	PR-16	PR-16A	PR-16C	PR-16D	PR-23A	PR-23E
SiO_2	47.90	50.80	50.00	50.40	50.00	52.90
TiO_2	0.60	0.65	0.51	0.60	0.62	0.83
Al_2O_3	15.86	15.90	14.37	15.07	15.40	15.77
Fe_2O_3	9.23	9.38	7.80	8.66	9.19	9.38
MnO	0.18	0.15	0.14	0.15	0.13	0.09
MgO	9.37	7.31	9.81	10.25	10.25	6.47
CaO	6.82	8.21	8.32	7.36	5.80	6.76
Na_2O	3.69	4.00	3.37	2.93	4.37	5.40
K_2O	1.58	0.61	1.40	2.03	0.76	0.36
P_2O_5	0.02	0.07	0.04	0.08	0.07	0.12
L.I.	2.84	2.31	2.77	3.25	3.48	1.66
Total	98.09	99.39	98.53	100.78	100.07	99.74
Q	-	-	-	-	-	-
Or	9.91	3.75	8.72	12.42	4.70	2.19
Ab	25.32	35.20	28.83	25.65	37.29	45.94
An	23.38	24.58	21.00	22.73	21.07	18.25
Ne	4.22	-	0.65	-	0.74	0.59
Aug	10.08	14.22	17.96	11.77	6.93	12.74
Hy	-	3.13	-	3.07	-	-
Ol	25.83	17.66	21.73	23.00	27.88	18.37
Ilm	1.21	1.28	1.02	1.18	1.23	1.62
Ap	0.05	0.17	0.10	0.19	0.17	0.29
Rb	18	17	17	25	21	14
Sr	144	212	104	111	201	191
Ba	74	55	61	70	71	96
Zr	29	46	29	36	41	60
Cu	73	33	13	10	79	8
Zn	62	58	50	55	76	41
Cr	166	89	286	302	253	54
Ni	82	62	184	199	124	35

PR-16 to PR-23E Diabase dikes from sheeted unit.

TABLE 8 (Cont'd.)

	PR-23F	PR-23G	PR-23L	PR-23M
SiO_2	51.40	50.30	51.90	49.80
TiO_2	0.48	0.86	0.92	0.82
Al_2O_3	15.70	14.40	13.88	14.37
Fe_2O_3	8.85	10.46	10.47	10.54
MnO	0.11	0.14	0.13	0.16
MgO	10.39	8.98	7.29	8.79
CaO	5.58	7.22	7.10	7.50
Na_2O	4.56	4.16	4.90	4.15
K_2O	0.75	0.71	0.30	0.73
P_2O_5	0.04	0.08	0.05	0.05
L.I.	3.80	2.83	2.15	3.94
Total	101.66	100.14	99.09	100.85
Q	-	-	-	-
Or	4.58	4.36	1.85	4.51
Ab	39.79	35.63	43.23	33.56
An	20.79	19.24	15.64	19.22
Ne	-	0.51	-	1.66
Aug	6.08	14.26	17.01	15.78
Hy	0.02	-	0.97	-
Ol	27.72	24.11	19.27	23.52
Ilm	0.94	1.70	1.82	1.63
Ap	0.10	0.19	0.12	0.12
Rb	16	20	14	16
Sr	180	185	172	212
Ba	69	70	80	79
Zr	34	45	46	41
Cu	88	65	10	52
Zn	75	84	49	85
Cr	194	90	35	72
Ni	118	54	30	50

PR-23F to PR-23M Diabase dikes from sheeted unit.

Before calculation of norms and plotting of diagrams, totals were recalculated to 100%, adjusting for hydration and oxidation (calculate Fe^{3+} with Fe^{2+} following the procedure outlined by Irving and Baragar (1971).

4.2.2. Chemistry

4.2.2.1. General Features:

The total alkalis vs. silica diagram, Fig. 5, shows that all rock types of the Baie Verte Group are tholeiitic except for the transitional nature of several samples from the sheeted diabase unit of the Point Rousse Block; this appears to be an alteration effect as they are otherwise chemically similar to sheeted dikes from other Blocks.

An ocean ridge affinity for the Baie Verte Group is first indicated in the Ti-Zr plot of Fig. 6. This figure is based on observations by Cann (1970) that Ti and Zr contents remain unchanged throughout metamorphic and weathering processes, and thus the concentration of these elements could be reliable indicators of the origin of various rock suites. Pearce and Cann (1971), using discriminant analysis, outlined the fields shown on Fig. 6 corresponding to different volcanic environments. Four well-known ophiolites of Troodos, Oman, Greece and Austria, selected by Pearce and Cann, plotted in the ocean-floor basalt field. The basalts and diabases of the Baie Verte Group ophiolitic rocks also plot in and near the ocean floor basalt field and agrees more specifically with the data given by Pearce and Cann for the Othrys ophiolite of Greece. The more mafic gabbro and ultramafic rocks of the Baie Verte Group ophiolites plot outside the ocean floor basalt field but on a line reflecting a differentiation trend with the dikes and pillow lavas.

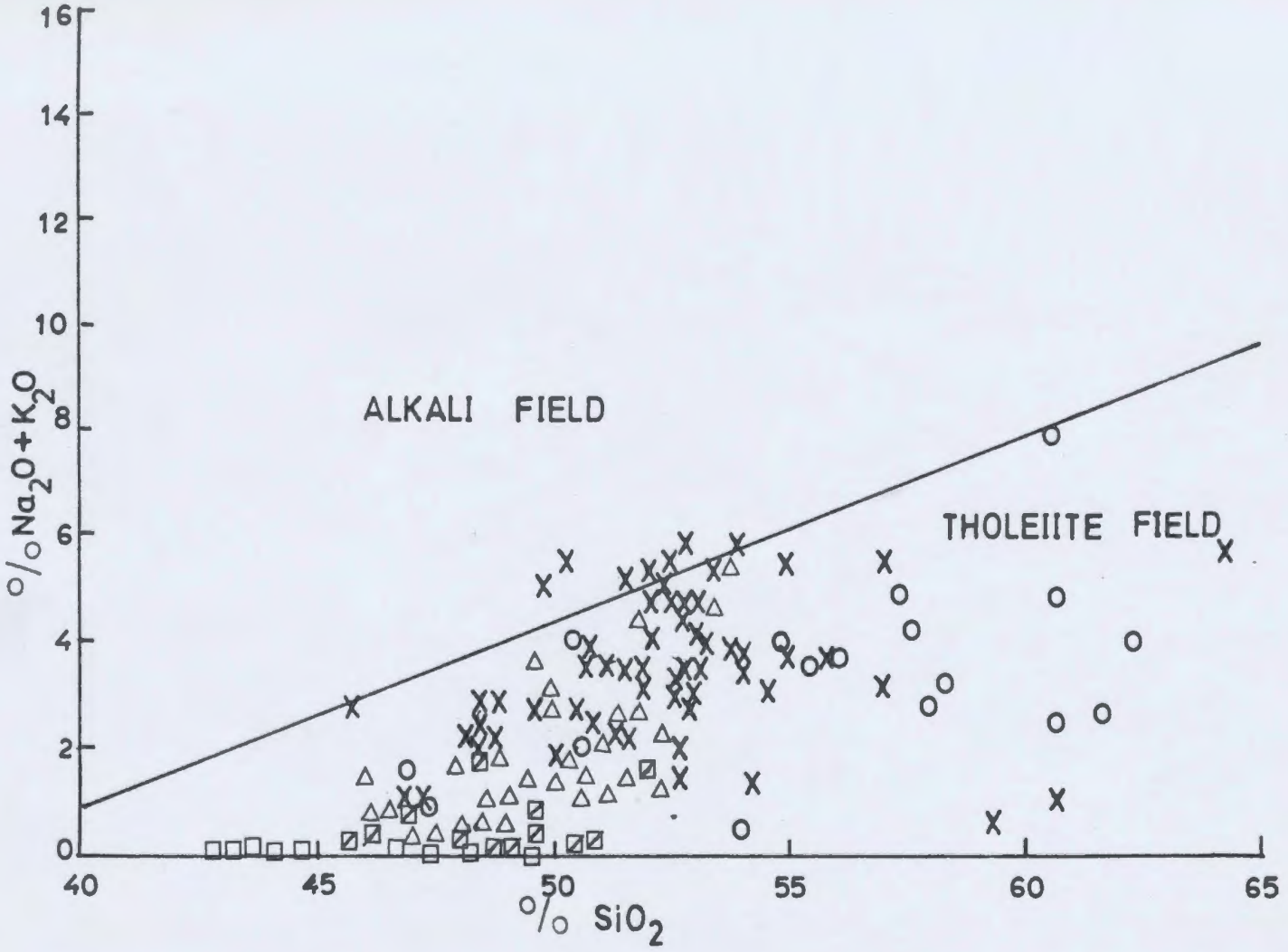

FIGURE 5: Total alkalies vs. SiO_2 variation diagram. Line separates the alkaline and tholeiitic series of the Hawaiian volcanic rocks (Macdonald and Katsura, 1964). o - pillow lavas; x - sheeted dikes; △ - gabbro; ▨ - pyroxenite; □ - peridotite.

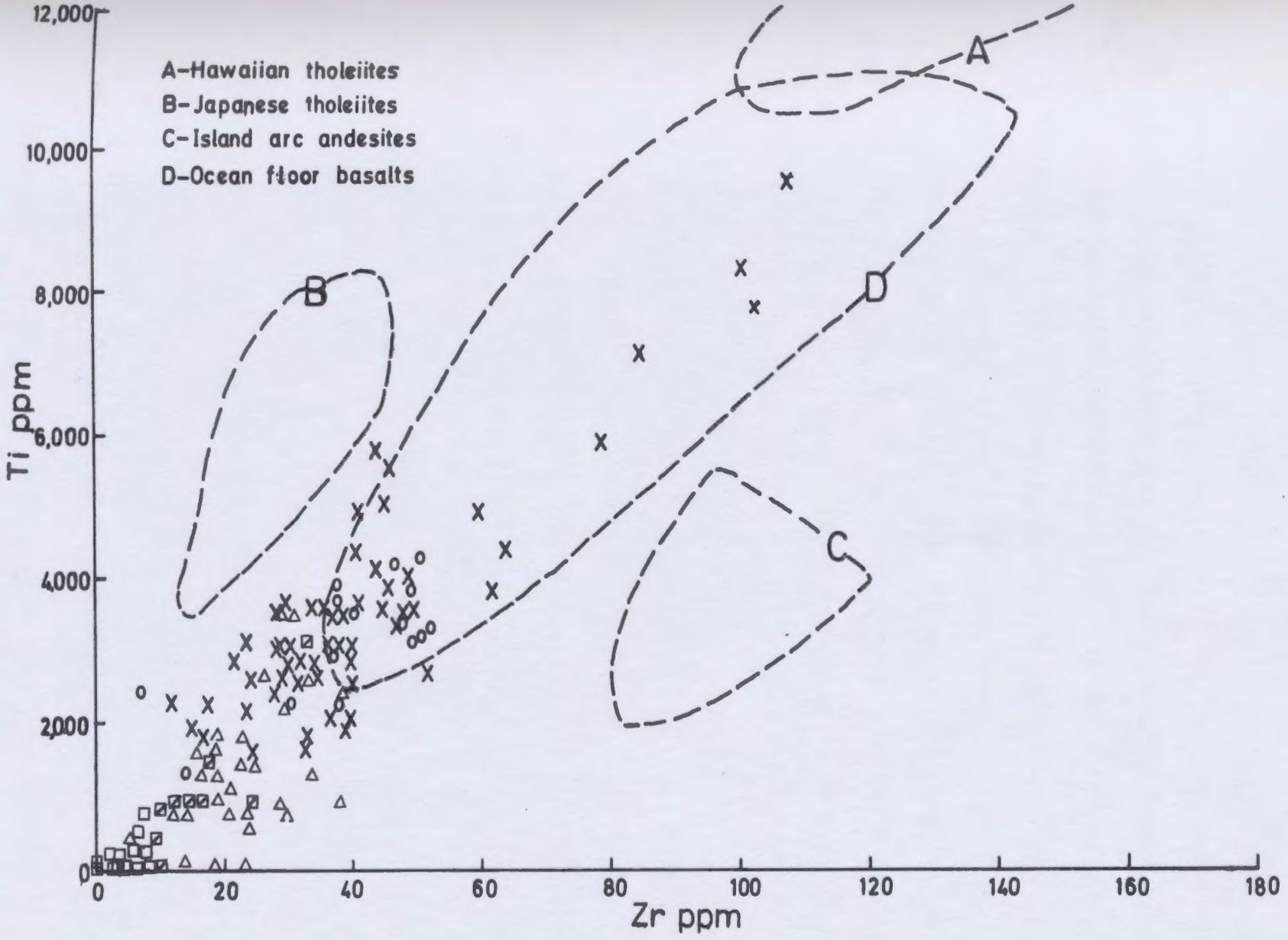

FIGURE 6: Ti-Zr plots comparing the Baie Verte rocks with the fields defined by Pearce and Cann (1971).

The cumulate peridotites of the Baie Verte ophiolites have low CaO (averaging 2%), Al_2O_3 (averaging 3%) and low TiO_2 concentrations comparable to the cumulus ultramafics of the Papuan Complex (Davies, 1971) and the so called "Alpine-type" peridotite of the Bay of Islands Complex (Irving and Findlay, 1972), reinterpreted as residual upper mantle material by Malpas (1973). Figure 7, after Irvine and Findlay (1972, Fig. 2), shows normative percentages of olivine, clinopyroxene and orthopyroxene in feldspar-free rocks of the Bay of Islands Complex; the Baie Verte peridotites plot near those of Bay of Islands, and associated clinopyroxenite and websterite plot in the appropriate classification fields outlined by Irvine and Findlay.

Irvine and Findlay noted that NiO-Cr_2O_3 relations in the "Alpine-type" peridotite differed from those in the critical zone (the gradational contact between the ultramafic and gabbro) and in layered intrusions of the Muskox type, the Cr_2O_3 content being higher and NiO lower in the latter. Such differences prompted these workers to distinguish between cumulate and alpine-type peridotite on the basis of the NiO-Cr_2O_3 relations (Fig. 8). However, the Baie Verte peridotites, interlayered with pyroxenite and gabbro typical of the Bay of Islands critical zone, plot in the field of the "Alpine-type", or mantle, Bay of Islands peridotite (Fig. 8) but generally have lower Cr_2O_3 content than the latter. The pyroxenite and gabbro compare favourably with those of the Bay of Islands critical zone.

It is, thus, apparent that the suggestion of Irvine and Findlay (1972) and Malpas (1973) that cumulate and alpine-type or mantle peridotite can be separated on the basis of NiO-Cr_2O_3 content should be taken

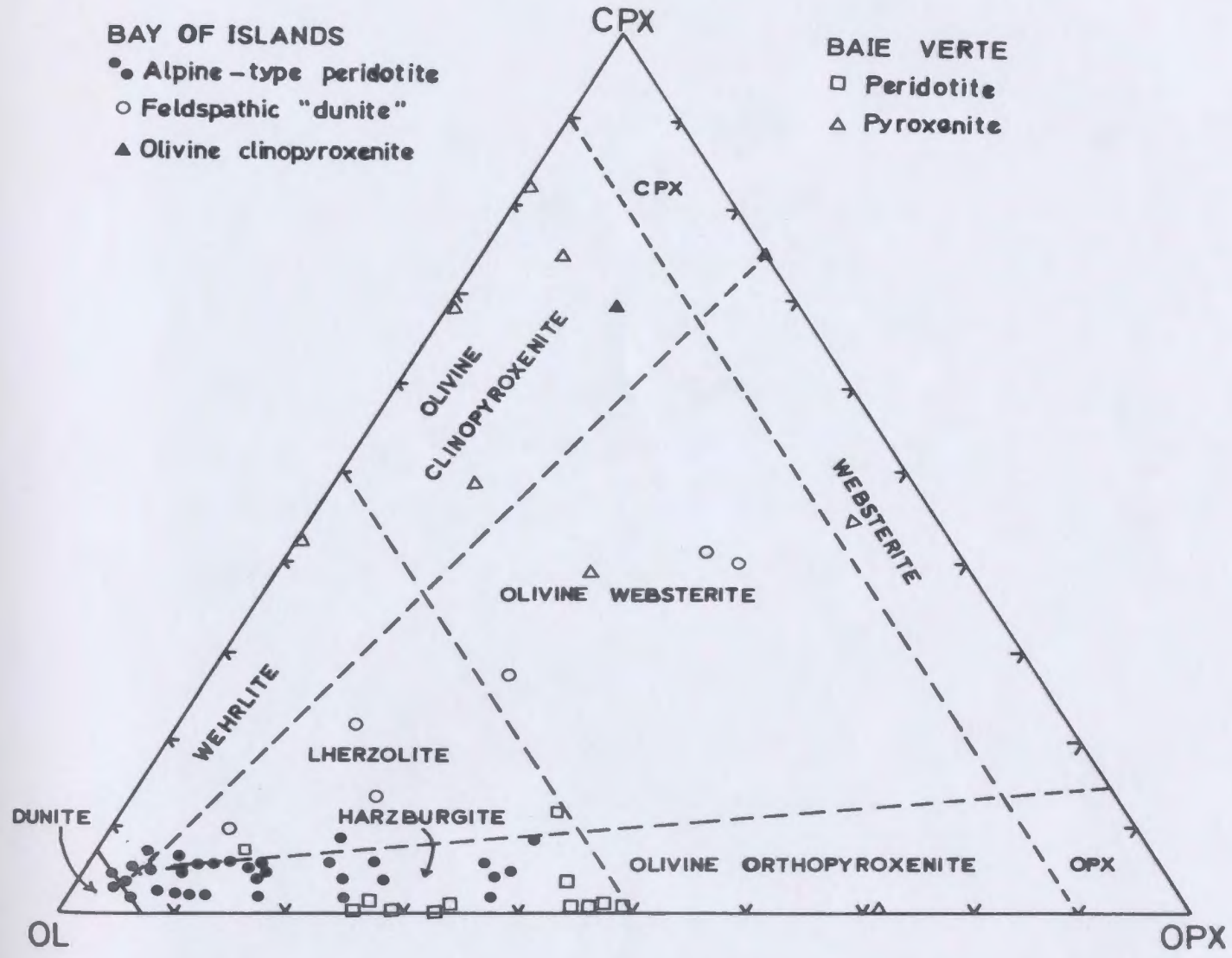

FIGURE 7: Ternary plots of Ol, Cpx and Opx comparing Baie Verte peridotites with alpine-type peridotite from Bay of Islands (after Irving et al., 1972).

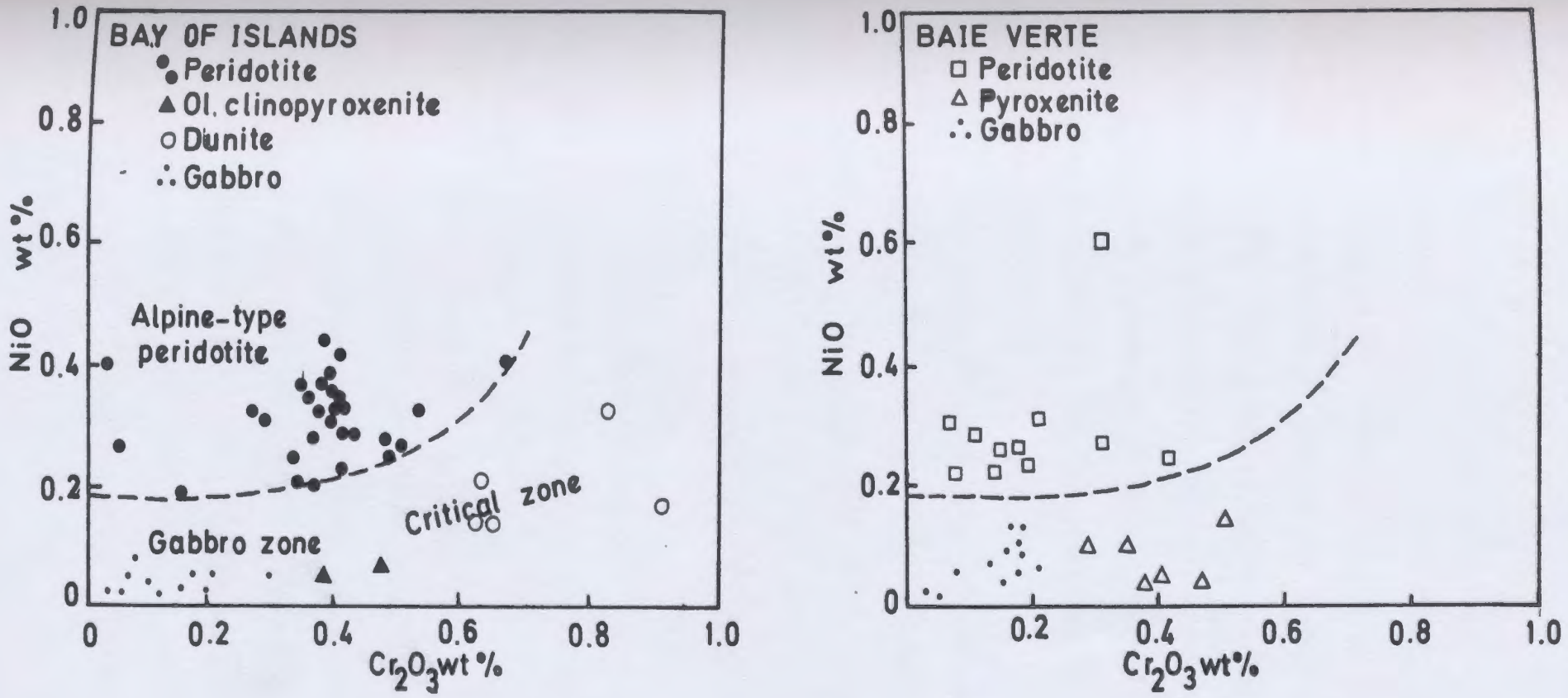

FIGURE 8: Plots showing the relative abundances of NiO and Cr_2O_3 in peridotites from Bay of Islands (alpine-type, after Irving et al., 1972) and Baie Verte. Dashed line is used by Irving et al. to separate alpine-type peridotite from rocks of the Critical and Gabbro Zones.

cautiously. It should also be emphasized that Irvine and Findlay did not compare 'peridotite' from the critical zone, but instead compared 'olivine-clinopyroxenite' (which can differ drastically in chemistry and mineralogy from typical peridotite depending on olivine-clinopyroxene ratio) with Alpine-type peridotite; their interpretations are invalid when considering that a comparison of true peridotite from the critical zone with the Alpine-type peridotite gives quite different results, as shown by the present work.

The gabbro of the Baie Verte ophiolites is also chemically comparable to those of the Alpine-type complexes of Papua (Davies, 1971), Bay of Islands (Irvine et al., 1972) and the Canyon Mountain Complex, Northeastern Oregon (Thayer and Himmelberg, 1968). They have high CaO (averaging 19.2%) and MgO (averaging 12.0%) and low alkalis (especially K_2O) and TiO_2.

The sheeted diabases and pillow lavas also have low K_2O and TiO_2 typical of oceanic tholeiite rocks (Engel et al., 1972; Cann, 1970; Hart et al., 1970).

The petrographic differences between the pillow lavas of the Western Block and those of the Eastern Block, described in section 4.1.4., are also reflected in the chemistry as follows (Table 9). The more mafic pillow lavas of the Eastern Block are comparable to mid-oceanic ridge basalts (MORB) in having similar Al_2O_3 and Cr concentrations but they tend to be higher in MgO and Ni, and lower in TiO_2 and Zr. They also tend to be lower in Sr and higher in Rb and Ba; this is not unusual as Sr depletion and Rb enrichment in MORB have been described by Cann (1970), and high Ba content from 50-94 ppm have been found in dredge hauls from the mid-Atlantic Ridge (Aumento, 1968).

TABLE 9

Composition	1	2	3	4
SiO_2	51.20	49.61	52.83	53.37
Al_2O_3	15.92	16.01	9.49	9.85
Fe_2O_3	8.98	12.63	10.71	12.04
MgO	10.02	7.84	14.21	10.22
CaO	10.61	11.32	10.22	10.11
Na_2O	2.08	2.76	2.00	2.68
K_2O	.63	0.22	0.12	.46
TiO_2	.40	1.43	0.16	.86
MnO	.16	0.18	0.17	.22
P_2O_5	.004	0.14	.07	.06
Ba	94	14	33	
Zr	18	95	14	
Sr	61	130	136	
Rb	18	10	3	
Zn	74	-	70	
Cu	68	77	14	
Ni	166	97	330	
Cr	244	297	1300	

1. Mean of 5 pillow lavas from Eastern Block of this study.
2. Mean of ocean-floor basalts (Cann, 1971). Trace elements from Engel et al., 1965.
3. Mean of 9 basaltic komatiites of Rambler Mines (Gale, 1972).
4. Mean of 3 basaltic komatiites of the Barberton type (Viljoen and Viljoen (1969).

The MgO, Ni, Ti and Zr contents of the Eastern Block pillow lavas are more comparable to that in basaltic komatiites which are characterized by high MgO, Ni and Cr, and low K, Ti, Ba, Zr, Sr and Y. Basaltic komatiites have been described by Viljoen and Viljoen (1969) in the Barberton Mountain Land of the Archean South Africa Shield. Gale (1972) reported similar rocks in supposed pre-Ordovician ophiolite in Rambler Mines area, south of the present map area. In both the Barberton Mountain and Rambler Mines occurrences, the basaltic komatiites are overlain by ocean-floor type basalts. The comparison is further enhanced in that the Rambler Mines area also contain pyroclastics and greywackes lithologically similar to those in the present area, although more deformed and metamorphosed.

These chemical features, comparable to both oceanic tholeiites and basaltic komatiites, suggest that the Eastern Block pillow lavas are transitional between the two.

From the Western Block, three specimens from pillow lava cores and three from isolated pillow breccias were analyzed (Table 5). Because of the wide chemical variations amongst the samples, further complicated by alteration, it is difficult to assign them to any one rock type without more analyses. However, they are significantly less basic than the Eastern Block pillow lavas in having lower MgO, CaO, Ni and Cr concentrations, all of which are taken as an indication of a more differentiated lava.

4.2.2.2. AFM Diagram:

On the AFM diagram (Fig. 9) the Baie-Verte ultramafic-mafic fractionation trend compares favourably with that for the Papuan Complex

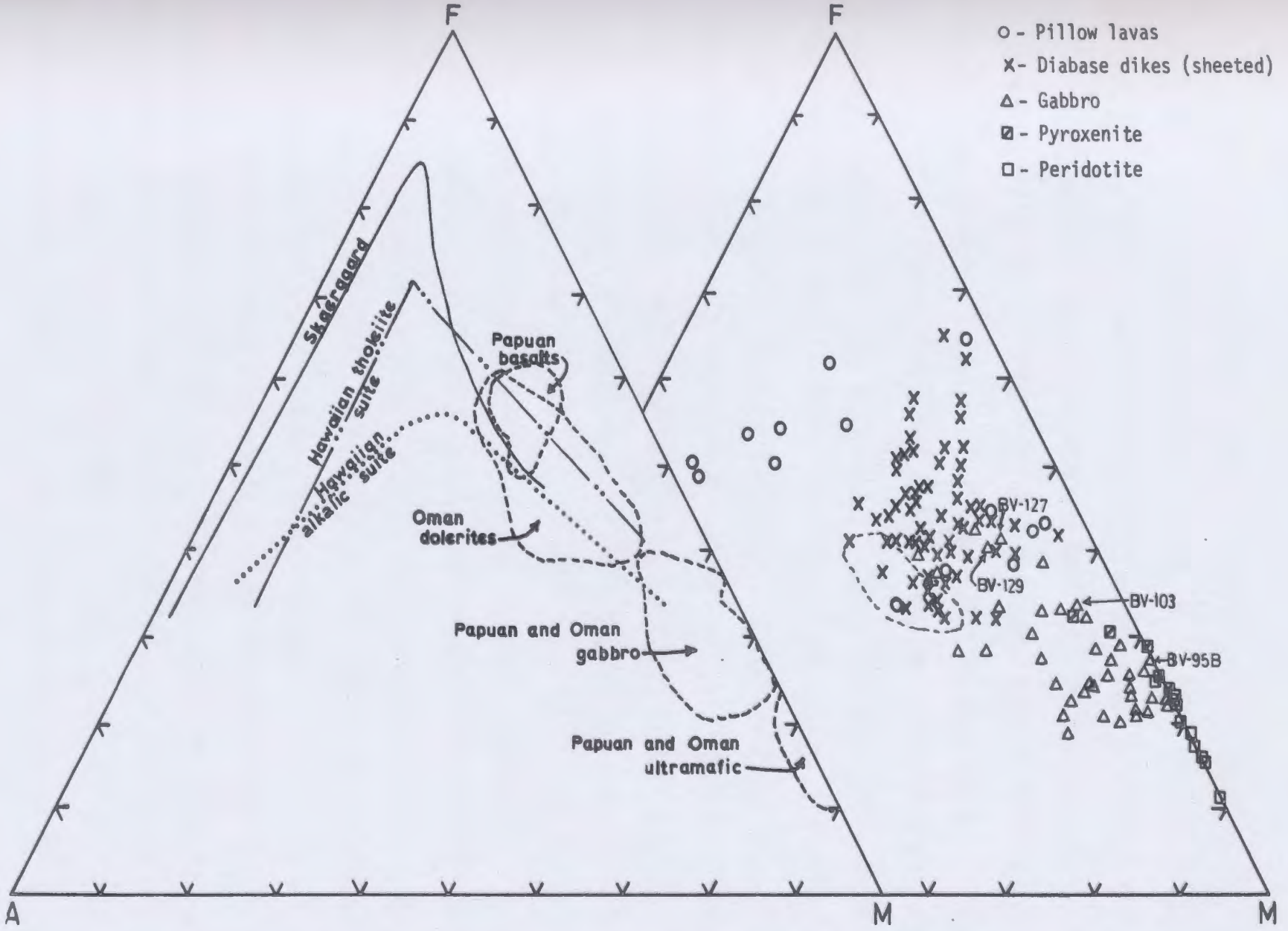

FIGURE 9: AFM diagram comparing the fractionation trend of the Baie Verte Group with other well-known suites. A = total alkalies, F = total iron as FeO; M = MgO in weight per cent.

and Oman, and is similar to the general ophiolite trend given by Thayer (1967). However, the ultramafic-mafic trend of the Baie Verte rocks is more complicated than it appears. Fractionation has been such that there is a gradual decrease in iron from ultramafic rocks to the lower level gabbros and a sudden enrichment in the higher level gabbros, dikes and pillow lavas (see MgO-Fe_2O_3 diagram, Fig. 10 and discussion in section 4.2.2.3.). This accounts for the tendency of lower gabbros to plot slightly across the diagram, i.e. away from the FeO apex. A similar trend could be produced by increased Na_2O or K_2O, but these rocks do not show any appreciable enrichment in alkalies (Figs. 10 and 12). Differentiation trends within the gabbro zones are still reflected in the diagram, however, lower level gabbros (e.g. BV-95B, Table 5) plot near the ultramafics, gabbros higher in the sequence (e.g. BV-103, Table 5) plot midway and upper gabbros, or high-level gabbros (e.g. BV-127, 129, Table 5) plot near the sheeted diabase dikes, i.e. there is a general fractionation trend upwards.

The sheeted diabase dikes plot within the field of the Oman dolerites. Dikes from the Point Rousse Block deviate slightly towards the alkali apex as a result of alteration; this alteration effect was noted above in the alkali-silica diagram, Figure 5.

The Mg-rich pillow lavas from the Eastern Block plot with the more mafic dikes and the higher level gabbros, i.e. are almost transitional between the gabbros and dikes. The more differentiated pillow lavas of the Western Block and Deer Cove Block cross the diagram along a differentiation path from sheeted diabases, following similar trends shown by Thayer (1967).

4.2.2.3. Linear Variation Diagrams:

Figures 10 to 13 show plots of the major element oxides and trace elements against MgO. Fractionation trends displayed on these diagrams show clearly the effects of removal of olivine, orthopyroxene, clinopyroxene, and in the gabbroic rocks, plagioclase. Figures 10 and 11 are plots of the Western and Eastern Blocks, and Figure 11 and 12 are of the Point Rousse and Deer Cove Blocks.

The CaO trend is distinctive, increasing with decreasing MgO until a maximum concentration in lower gabbro is reached, beyond which there is a sharp decrease to a minimum in the more differentiated lavas. This is obviously due to fractionation of olivine and orthopyroxene followed by Ca-rich clinopyroxenes. Al_2O_3 also increases until plagioclase starts to crystallize in the gabbro.

Fe_2O_3 decreases with MgO in the ultramafics and lower gabbro, but sharply increases in the high level gabbro, dikes and pillow lavas. The high Mg and Fe in the peridotites reflect accumulation of Mg- and Fe-bearing olivine. Fractionation of olivine was followed by crystallization of clinopyroxene, as described above. Plagioclase crystallization enriched the later liquids in iron, as evidenced by the sudden rise in Fe_2O_3 at the same MgO content as the slight decrease of Al_2O_3. The result of this iron enrichment was crystallization of magnetite and/or titaniferous magnetite in the final stages; TiO_2 also increases at the same MgO content as Fe_2O_3. The crystallization of the opaques caused the increase in SiO_2 in the late liquids. These interpretations are all in agreement with the relatively high normative ilmenite present in the dikes and pillow lavas, low in the gabbro and absent in the peridotites.

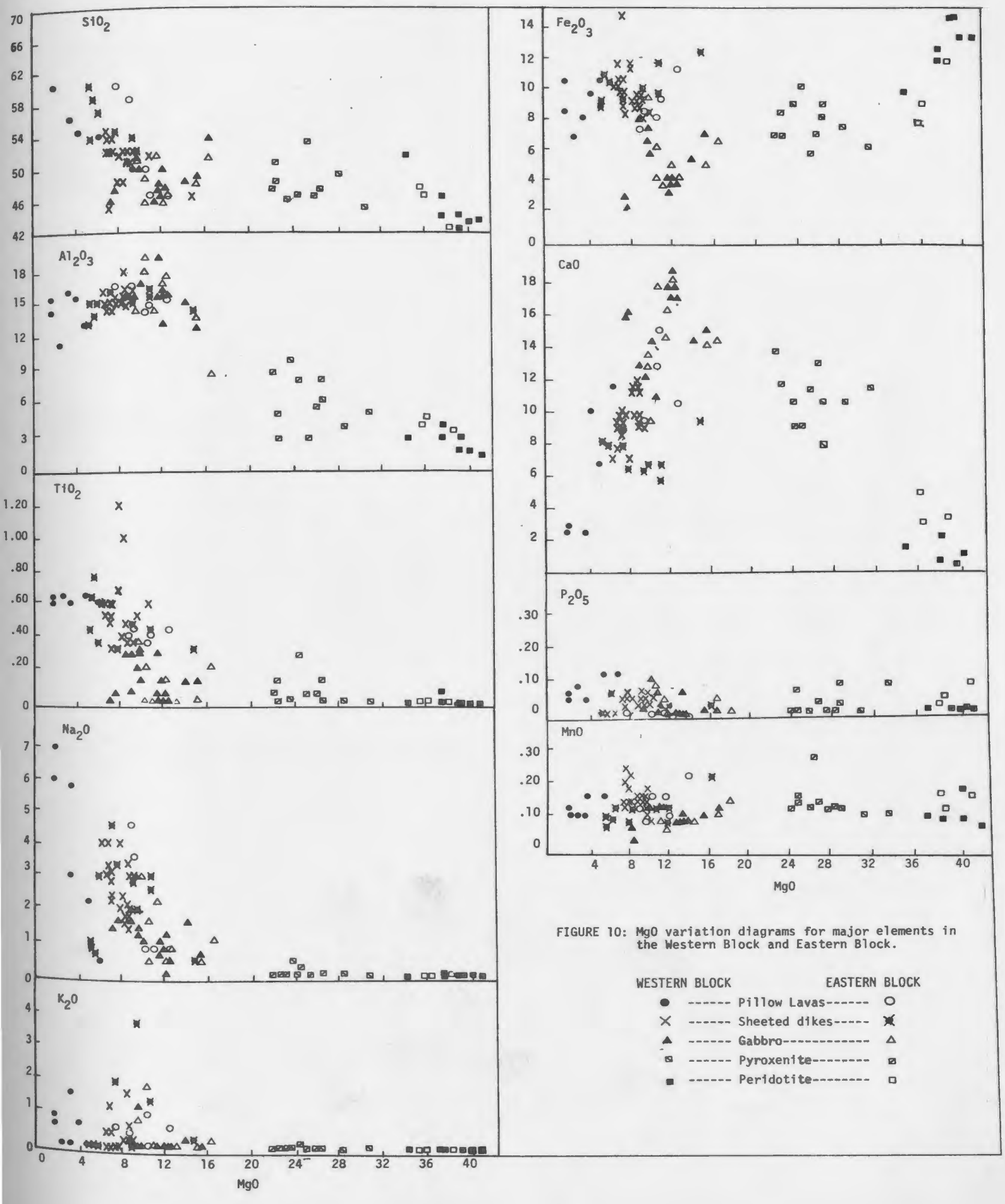

FIGURE 10: MgO variation diagrams for major elements in the Western Block and Eastern Block.

WESTERN BLOCK		EASTERN BLOCK
●	------ Pillow Lavas------	○
×	------ Sheeted dikes-----	⊠
▲	------ Gabbro----------	△
▨	------ Pyroxenite-------	▨
■	------ Peridotite-------	□

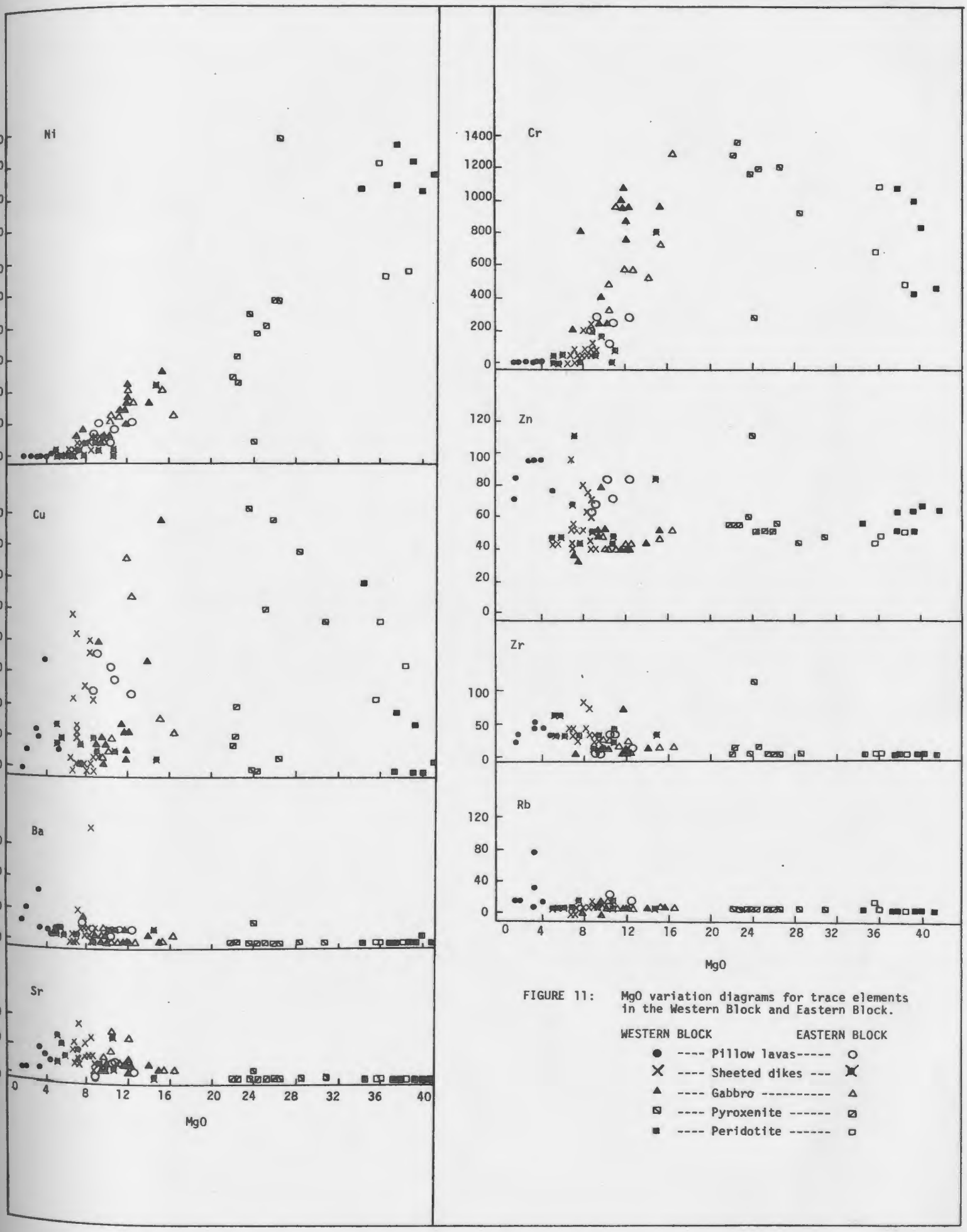

FIGURE 11: MgO variation diagrams for trace elements in the Western Block and Eastern Block.

WESTERN BLOCK EASTERN BLOCK

● ---- Pillow lavas----- ○

✕ ---- Sheeted dikes --- ✕

▲ ---- Gabbro ---------- △

▨ ---- Pyroxenite ------ ▨

■ ---- Peridotite ------ □

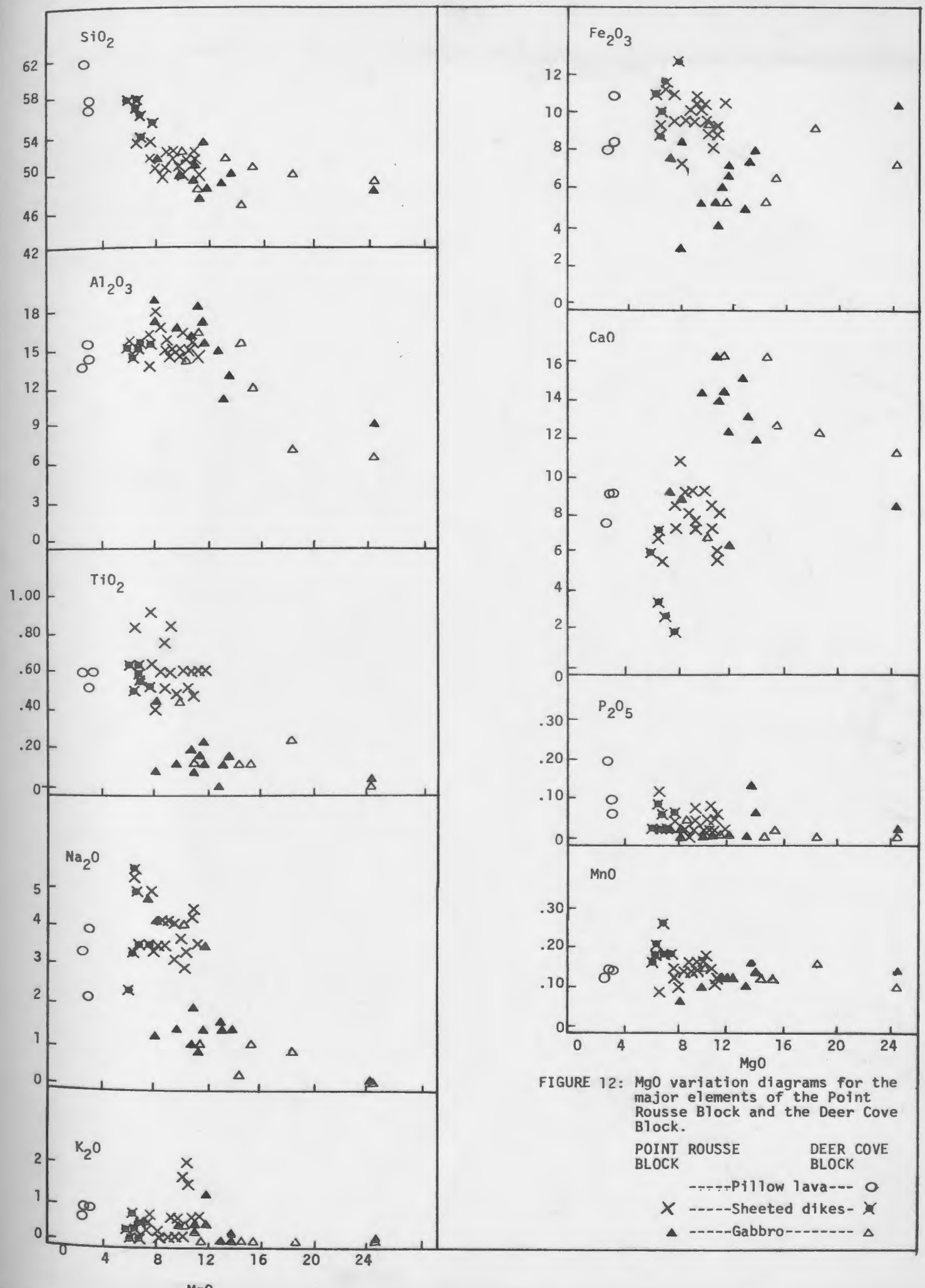

FIGURE 12: MgO variation diagrams for the major elements of the Point Rousse Block and the Deer Cove Block.

POINT ROUSSE BLOCK — DEER COVE BLOCK

-----Pillow lava--- O

X -----Sheeted dikes- X

▲ -----Gabbro-------- △

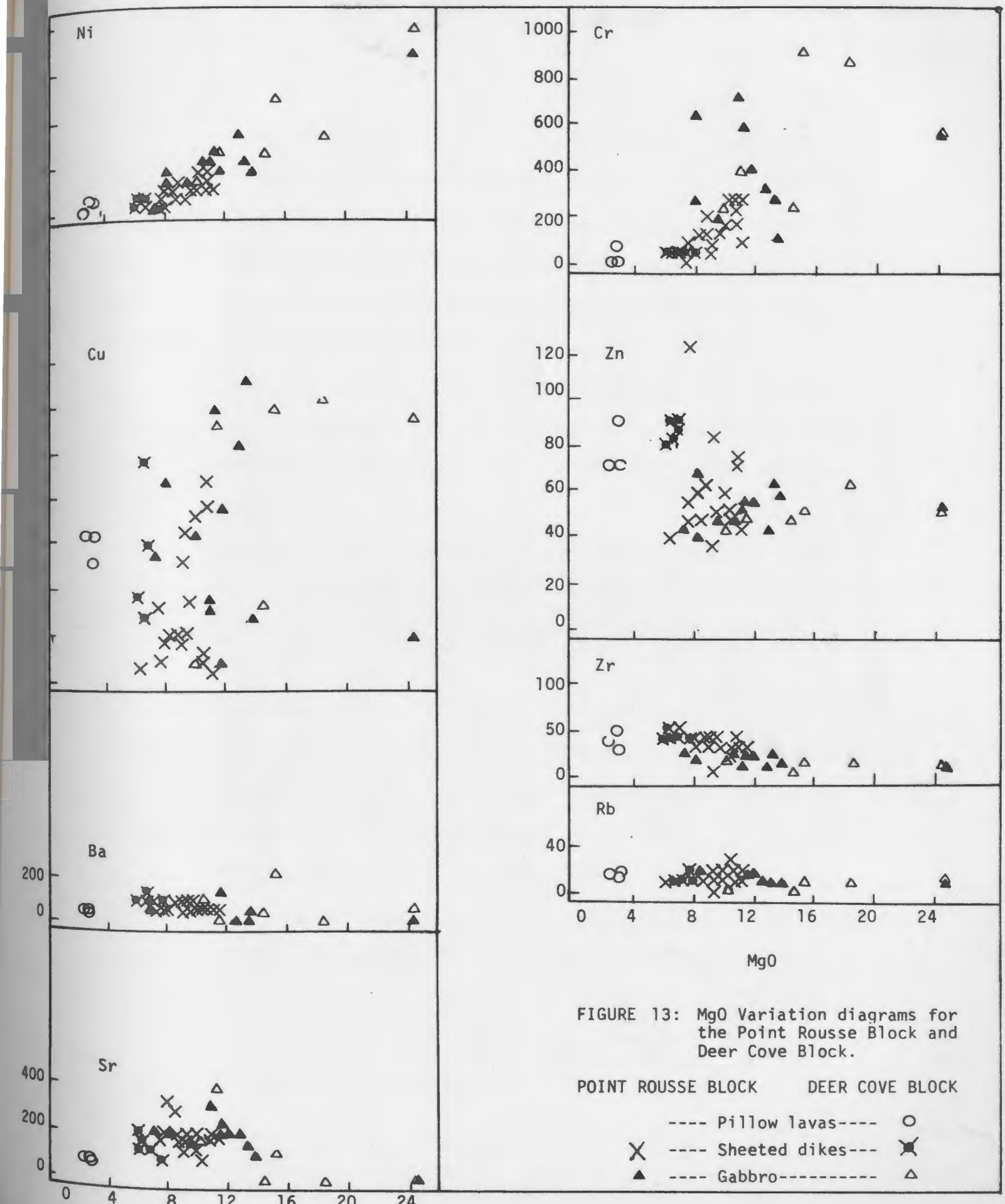

FIGURE 13: MgO Variation diagrams for the Point Rousse Block and Deer Cove Block.

POINT ROUSSE BLOCK DEER COVE BLOCK

---- Pillow lavas---- ○

× ---- Sheeted dikes--- ✱

▲ ---- Gabbro---------- △

Zn substitutes for iron (Taylor, 1965) and is noted to concentrate in magnetite (Wager and Brown, 1967). This also agrees strongly with the present interpretations, as Zn follows closely the Fe_2O_3 trend (Figs. 11 & 13). Zr is also concentrated in the later dikes and pillow lavas, possibly reflecting crystallization of $ZrSiO_4$ in the late liquids and also probable substitution for Ti in ilmenite.

The P_2O_5, Na_2O and K_2O trends are typical of fractional crystallization processes, concentrating in late liquids. MnO remains constant throughout reflecting the ability of Mn to enter a variety of crystal lattices.

Ba and Sr follow each other and readily substitute for Ca in plagioclases. The gabbros, dikes and pillow lavas are the only rocks containing appreciable amounts of Sr, with Ba following closely the Sr trend.

Cr enters Fe^{3+} positions in pyroxenes (Taylor, 1965) and becomes depleted early during fractional crystallization; this explains the maximum concentration of this element in the pyroxenites and the gradual depletion in the later dikes and pillows.

The behaviour of Cu is little known; Taylor, 1965, states that it will enter Na^{+} and Ca^{2+} positions in plagioclases, and Fe^{2+} positions in most minerals. The Cu trend, Figs. 11 & 13, is similar only to Cr and CaO, both elements which are concentrated in the pyroxenites. The maximum concentration of Cu is also in the pyroxenites, which may be explained by Cu substitution for Fe^{++} positions in clinopyroxenes.

4.2.3. Conclusion

Evidence has been given that the ultramafic-gabbro-diabase dikes-pillow lava sequence of the Baie Verte Group are genetically related, having been the result of fractional crystallization of a single parent magma. This is indicated by the field relationships, petrography and by the chemistry.

The cumulate peridotites interlayered with pyroxenite and gabbro in the map area are typical of the 'critical zone' of Alpine-type ophiolites. The trend of the rocks on the AFM diagram is similar to that of other ophiolites which have been referred to as Alpine-type ultramafic complexes, with a lower Fe/Mg and lower alkalies than that found in typical basalt fractionation trends of layered continental intrusions such as the Skaergaard. MgO variation diagrams further reveal the chemical relationships between the various rock types. The trends observed in the Baie Verte Group, summarized schematically in Figure 14, are due mainly to the fractionation in various proportions of olivine-orthopyroxene-clinopyroxene-plagioclase. The behaviour of the iron, having low Fe/Mg ratios in the earlier and later rocks and higher Fe/Mg ratio in the intermediate products, can be explained by fractional crystallization of a magma under conditions of low oxygen fugacity, i.e. low H_2O content, typical of abyssal tholeiitic series (Cann, 1971). The parental magma for the Baie Verte Group appears also to have been a low Ti and K basaltic magma that crystallized under conditions of low oxygen fugacity, probably in the upper crustal zones beneath a mid-oceanic ridge.

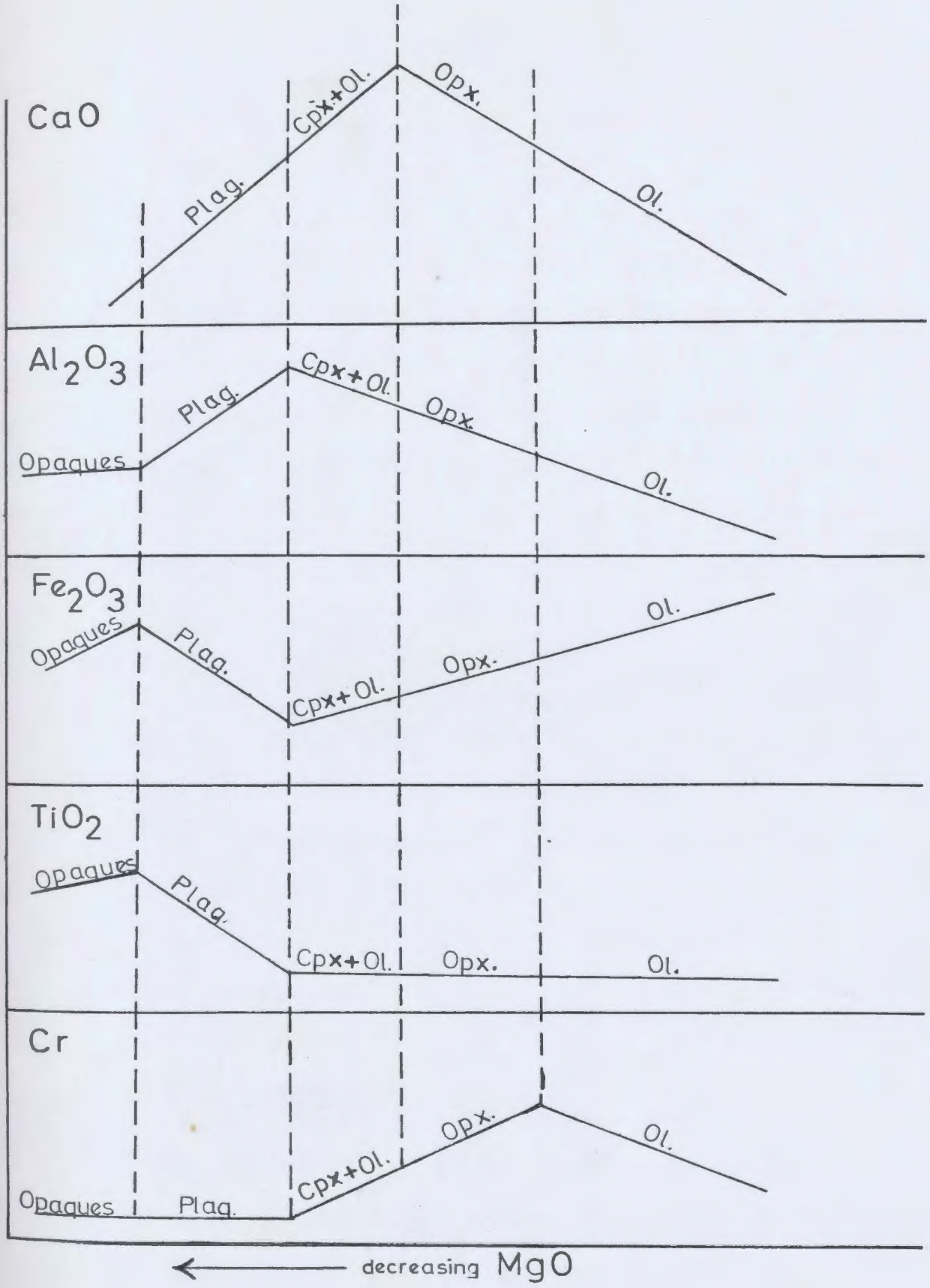

FIGURE 14: Schematic representation of the trends observed in the Baie Verte ophiolite.

CHAPTER 5

ECONOMIC GEOLOGY

5.1. Introduction

Many of the mineral occurrences in the Baie Verte area have been described by Snelgrove (1935) and Watson (1947). Two mines are presently in operation - Advocate Mines Ltd., producing asbestos, and Consolidated Ramber Mines, producing mainly copper. Past producers include Terra Nova Mine (copper) and Goldenville Mine (gold). Several other mineral occurrences were observed throughout the area.

5.2. Advocate Mines Ltd.

Advocate Mines Ltd. began production of asbestos in 1964. The deposit is located in the serpentinised peridotite belt near the Baie Verte-Fleur de Lys thrust contact. Only cross-fibre veinlets of chrysotile asbestos were observed in the serpentinised ultramafic rocks in the map area and veinlets of tremolite asbestos were noted in ultramafics and gabbro in a few places.

5.3. Consolidated Rambler Mines Ltd.

The property of Consolidated Rambler Mines Ltd. is situated approximately 6 miles south of the community of Ming's Bight. It was discovered in 1905 and after several periods of investigation by various workers was put into production in 1964. A new ore body has recently been

discovered, and is currently being mined, along the Ming's Bight road between the earlier deposits and the present map area.

Mineralisation is mainly pyrite and chalcopyrite with minor amounts of pyrrhotite and sphalerite, with some gold also being recovered. Most of the sulphide mineralisation occurs with quartz as bands within chloritic schist. The rocks in the area are intensely deformed and include ultramafics, tholeiitic pillow lavas and pyroclasties, thought to be representative of a pre-Ordovician ocean floor complex (Gale, 1971), and except for the differences in deformation is similar to those described in the present map area.

5.4. Terra Nova Mine

The Terra Nova Mine is located approximately 1 mile south of Baie Verte, and was last operated in 1915. The orebody is a massive sulphide deposit containing pyrite, chalcopyrite and pyrrhotite with minor sphalerite. The deposit occurs in greenschist of the Baie Verte Group near the contact with the Fleur de Lys Supergroup.

5.5. Goldenville Mine

The Goldenville Mine is located near Ming's Pond within the map area (Fig. 4). The last exploration activity was carried out in 1937 by Newfoundland Prospecting Syndicate, but the last production was in 1904 and 1906, totalling $1700 worth of gold (Watson, 1947, p. 27). Gold, along with pyrite, chalcopyrite and sphalerite occurs in quartz-carbonate veins

that cut a thin band of ferruginous chert. The ferruginous chert is interbanded with chlorite schist (pillow lavas?) pyroclastics and sedimentary rocks similar to that exposed at the coast in the vicinity of Big Head. Visible gold was observed in the loose quartz blocks near the old shaft by D.F. Strong and A.M. Frew in 1970, who also observed visible gold in quartz veins on the coast along strike from the Goldenville area (pers. comm., 1973).

Several other sulphide occurrences in the map area consist of pyrite-chalcopyrite with small amounts of pyrrhotite and sphalerite. They are all found in chlorite schist and pillow lavas, usually overlain by pyroclastics and sedimentary rocks. These occur on the west side of Ming's Bight (Barry and Cunningham adit), near Mud Pond, and north of Deer Cove. Chalcopyrite was also observed in quartz veins in the gabbro of the Deer Cove Block, and in sheeted dikes near the contact with pillow lavas at Green Cove.

5.6. Discussion

The concept of plate tectonics has been used to explain generation and distribution of sulphide deposits and other types of mineralization (Sawkins, 1972; Mitchell and Garson, 1972; Sillitoe, 1972). The environment and volcanic setting of various ore deposits have been related to the interaction of plate boundaries at various regimes. The cupreous pyrite deposits associated with ophiolites, e.g. in Cyprus, are examples of massive sulphides formed at divergent plate boundaries, or

spreading centres (Hutchinson and Searle, 1971; Sillitoe, 1972; Searle, 1972; Upadhyay and Strong, 1973). These deposits are of simple mineralogy (pyrite-pyrrhotite-chalcopyrite) and occur in mafic submarine flows.

The plate tectonic concept has recently been applied to sulphide deposits in Newfoundland (Strong and Peters, 1972; Upadhyay and Strong, 1973; Strong, 1973a, b). Upadhyay and Strong have compared sulphide deposits associated with the Bett's Cove and Bay of Islands ophiolites to those associated with other ophiolites such as Troodos. The mineralization in those areas (pyrite-chalcopyrite-pyrrhotite-sphalerite) occupy similar stratigraphic positions at the contact between the sheeted dikes and pillow lavas. The mineralogy of the sulphide deposits in the Baie Verte area is similar to that in other ophiolite areas and is found in pillow lava horizons. Thus, such stratigraphic controls may be an aid to exploration for sulphide deposits in this region. This approach may be especially promising considering the close geological similarities between the present map area and that containing the Rambler deposits just 6 miles to the south, and the numerous Au and Cu showings noted in the area.

CHAPTER 6

CONCLUSIONS

The following conclusions have been made from the present study:

1. The part of the Baie Verte Group underlying the map area represents a dismembered and incomplete ophiolite suite - exposed only from the cumulus rocks upwards, the residual ultramafic members being poorly represented.

2. The interlayered peridotite-pyroxenite-gabbro in the map area is representative of the critical zone that separates underlying ultramafics and overlying gabbro in a complete ophiolite suite.

3. The sequence has been disrupted into at least five structural blocks that are separated by fault zones containing serpentinised peridotite, serpentinite and talc-carbonate rocks.

4. Units within each block are also separated by faults.

5. The map area can be described as a 'schuppen zone' similar to that described in north-east Shetland, by Flinn (1958).

6. The deformational structures are related to early Ordovician emplacement and later Acadian deformation; the more deformed rocks of the Baie Verte Group are found near the contact with the Fleur de Lys Group.

7. The Baie Verte Group is chemically similar to other ophiolites and modern-day oceanic crust.

8. Fractionation trends are due to crystallization in various proportions of olivine-orthopyroxene-clinopyroxene-plagioclase and opaque oxides.

9. The parental magma for the Baie Verte Group was a low Ti and K basaltic magma.

10. This magma crystallized under conditions of low oxygen fugacity probably in the upper crustal zones beneath a mid-oceanic ridge.

11. These features, plus the presence of numerous sulphide and gold occurrences make the area closely comparable to the area around Rambler Mines, 6 miles to the south, and it may thus be considered a region of some economic potential.

BIBLIOGRAPHY

Allemann, F. and Peters, T.
1972: The ophiolite-radiolarite belt of the North-Oman Mountains. Eclogae Geologicae Helvetiae, vol. 65, no. 3, pp. 657-697.

Aumento, F.
1968: The Mid-Atlantic Ridge near 45° N II. Basalts from the area of Confederation Peak. Can. Jour. Earth Sci., 5, pp. 1-21.

Baird, D.M.
1951: The geology of Burlington Peninsula, Newfoundland. Geol. Surv. Can., Paper 51-21.

Betz, F. Jr.
1948: Geology and Mineral Deposits of southern White Bay. Nfld. Geol. Surv., Bull. 24.

Bird, J.M. and Dewey, J.F.
1970: Lithosphere plate - continental margin tectonics and the evolution of the Appalachian orogen: Bull. Geol. Soc. Am., v. 81, p. 1031-1060.

Cann, J.R.
1970: Rb, Sr, Y, Zr and Nb in some ocean floor basaltic rocks. Earth Planet. Sci. Letters 10, pp. 7-11.

1971: Major element variations in ocean-floor basalts. Phil. Trans. Roy. Soc. Lond. A. 268, pp. 495-505.

Carlisle, D.
1963: Pillow breccias and their aquagene tuffs, Quadra Island, British Columbia. Jour. of Geol., vol. 71, no. 1, pp. 48-71.

Church, W.R.
1965a: Structural evolution of Northeast Newfoundland. Maritime Sediments, vol. 1, no. 3, pp. 10-14.

1965b: Structural evolution in Northeast Newfoundland - comparison with that of the British Caledonides. Bull. Can. Inst. Mining Met., vol. 58, no. 634, p. 219 (abst.).

1966: Geology of the Burlington Peninsula, Northeast Newfoundland; Geol. Assoc. Can. Technical Program 1966 Annual Meeting (Abst.), pp. 11-12.

1969: Metamorphic rock of Burlington Peninsula and adjoining areas of Newfoundland, and their bearing on continental drift in the North Atlantic. In North Atlantic - Geology and Continental Drift, M. Kay (ed.). Amer. Assoc. Petrol. Geol., Mem. 12, pp. 212-233.

1972: Ophiolite: its definition, origin as oceanic crust and mode of emplacement in orogenic belts, with special reference to the Appalachians. Publications of the Earth Physics Branch, Dept. of Energy, Mines and Resources, Canada, vol. 42, no. 3, pp. 71-86.

Church, W.R. and Stevens, R.K.
1971: Early Paleozoic ophiolite complexes of the Newfoundland Appalachians as Mantle-Oceanic Crust sequences. Jour. of Geophys. Res., vol. 76, pp. 1460-1466.

Davies, H.L.
1971: Peridotite-gabbro-basalt complex in Eastern Papua: an overthrust plate of oceanic mantle and crust. Department of National Development, Australia, Bull. 128.

Dewey, J.F. and Bird, J.M.
1971: Origin and emplacement of the ophiolite suite: Appalachian ophiolites in Newfoundland. Jour. of Geophys. Res., vol. 76, no. 14, pp. 3179-3206.

Engel, A.E.J., Engel, C., and Havens, J.
1965: Chemical characteristics of oceanic basalts and the upper mantle. Bull. Geol. Soc. Amer., vol. 76, p. 719.

Flinn, D.
1958: On the nappe structure of north-east Shetland. Geol. Soc. of Lond. Quart. Jour., vol. 114, pp. 107-136.

1965: On the symmetry principle and the deformation ellipsoid; Geol. Mag., vol. 102, pp. 36-45.

G.S.A. Penrose Conference
1972: Penrose Field Conference - Ophiolites. Geotimes, vol. 17, no. 12, p. 25.

Gale, G.H.
1971: An investigation of some sulphide deposits of the Rambler area, Newfoundland. Ph.D. thesis, Univ. of Durham, England.

1972: Paleozoic basaltic komatiite and ocean-floor basalts from northeastern Newfoundland. Earth and Planetary Sci. Letters 18, pp. 22-28.

Hutchinson, R.W. and Searle, D.L.
1971: Stratabound pyrite deposits in Cyprus and relations to other sulphide ores; In Proc. IMA-IAGOD meetings '70, IAGOD Volume (Tokyo: Society of Mining Geologists of Japan, 1971), pp. 198-205.

Irvine, T.N. and Findlay, T.C.
1972: Alpine-type peridotite with particular reference to the Bay of Islands igneous complex. Publications of the Earth Physics Branch, Dept. of Energy, Mines and Resources, Canada, vol. 42, no. 3, pp. 97-128.

Irvine, T.N. and Baragar, W.R.A.
1971: A guide to the chemical classification of the common volcanic rocks. Can. Jour. Earth Sci., vol. 8, pp. 523-548.

Kay, M.
1966: Newfoundland structures and continental drift. Bull. Can. Petrol. Geol., vol. 14, pp. 613-620.

Kennedy, M.J.
1971: Structure and stratigraphy of the Fleur de Lys supergroup in the Fleur de Lys area, Burlington Peninsula, Nfld. Geol. Assoc. of Can. Proc., vol. 24, no. 1, pp. 59-71.

1973: Pre-Ordovician polyphase structure in the Burlington Peninsula of the Newfoundland Appalachians. Nature, Physical Science, vol. 241, no. 110, pp. 114-116. (Also unpub. manuscript 1972).

Kennedy, M.J. and Phillips, W.E.A.
1971: Ultramafic rocks of Burlington Peninsula, Newfoundland. Geol. Assoc. of Can., Proc., vol. 24, no. 1, pp. 35-46.

Macdonald, G.A. and Katsura, T.
1964: Composition and origin of Hawaiian lavas, in Coats, R.R., Hay, R.L., and Anderson, C.A. (eds.), Studies in Volcanology: Geol. Soc. America, Mem. 116, pp. 477-522.

Malpas, J.
1973: A restored section of oceanic crust and mantle in western Newfoundland. Geol. Soc. Amer., Northeastern Sec. 8th Ann. Mtg., Abs. 5, p. 191.

Mitchell, A.H.G. and Garson, M.S.
1972: Relationships of porphyry copper and circum-Pacific tin deposits to paleo-Benioff zones. Trans./Sec. B, Inst. Min. and Metall., vol. 81, pp. B10-B25.

Murray, A.
1864: Report upon the Geological Survey of Newfoundland.

Neale, E.R.W.
1957: Ambiguous intrusive relationships of the Bett's Cove-Tilt Cove Serpentine Belt, Nfld., Proc. Geol. Assoc. Can., vol. 9, pp. 95-106.

Neale, E.R.W. and Nash, W.A.
1963: Sandy Lake (east half), Nfld. Geol. Surv. Can., Paper 62-28.

Neale, E.R.W. and Kennedy, M.J.
1967: Relationships of the Fleur de Lys Group to younger groups of the Burlington Peninsula, Nfld. Geol. Assoc. Can., Spec. Paper No. 4, pp. 139-169.

Pearce, T.H. and Cann, J.R.
1971: Ophiolite origin investigated by discriminant analyses using Ti, Zr, and Y. Earth Planet. Sci. Letters 12, pp. 339-349.

Phillips, W.E.A., Kennedy, M.J. and Dunlop, G.A.
1969: A geologic comparison of western Ireland and northeastern Newfoundland; Am. Assoc. Petrol. Geol., Mem. 12, pp. 194-211.

Sawkins, F.J.
1972: Sulfide ore deposits in relation to plate tectonics, Jour. of Geol., vol. 80, no. 4, pp. 377-397.

Snelgrove, A.K.
1935: Geology of Gold Deposits of Newfoundland. Nfld. Dept. Nat. Res., Geol. Sect., Bull. no. 2.

Searle, D.L.
1972: Mode of occurrence of the cupriferous pyrite deposits of Cyprus. Trans. of the Inst. of Min. and Met., vol. 81.

Sillitoe, R.H.
1972: Formation of certain massive sulfide deposits at sites of seafloor spreading. Trans. I.M.M., vol. 81, pp. B141-B148.

Strong, D.F. and Peters, H.R.
1972: The importance of volcanic setting for base metal exploration in central Newfoundland. Proc. C.I.M.M., Ottawa, April, 1972.

Strong, D.F.
1973a: Plate tectonic setting of Newfoundland mineral deposits (in prep.).

1973b: Plate tectonic setting of Appalachian-Caledonian mineral deposits as indicated by Newfoundland examples. Soc. of Mining Engineers of A.I.M.E., Sept. 1973, Reprint no. 73-I-320.

Strong, D.F., Dickson, W.L., O'Driscoll, C.F., Kean, B.F., and Stevens, R.K.
1973: Geochemical evidence for eastward Appalachian subduction in Newfoundland. Nature (in press).

Taylor, S.R.
1965: The application of trace element data to problems in petrology. Physics and Chemistry of the Earth, vol. 6, pp. 133-213.

Thayer, T.P.
1967: Chemical and structural relations of ultramafic and feldspathic rocks in alpine intrusive complexes. In Wyllie, P.J. (ed.), Ultramafic and Related Rocks. Wiley, N.Y., pp. 222-39.

Thayer, T.P. and Himmelberg, G.R.
1968: Rock succession in the alpine-type mafic complex at Canyon Mountain, Oregon. 23rd Int. Geol. Cong., Prague, pp. 175-186.

Upadhyay, H.D., Dewey, J.F. and Neale, E.R.W.
1971: The Betts Cove ophiolite complex, Newfoundland: Appalachian oceanic crust and mantle: Proc. Geol. Assoc. Can., v. 24, p. 27-34.

Upadhyay, H.D. and Strong, D.F.
1972: Geological setting of the Betts Cove copper deposits, Nfld: an example of ophiolite mineralization. Econ. Geol. 68, pp. 161-167.

Viljoen, M.J. and Viljoen, R.P.
1969: The geology and geochemistry of the lower ultramafic unit of the Onverwacht Group and a proposed new class of igneous rocks, in Geol. Soc. South Africa, Spec. Pub. No. 2: "Upper Mantle Project", p. 55.

Wager, L.R. and Brown, G.M.
1967: The Skaergaard intrusion, East Greenland. In Layered Igneous Rocks, W.H. Freeman and Company, pp. 11-242.

Watson, K. de P.
1947: Geology and mineral deposits of the Baie Verte-Ming's Bight Area. Geol. Surv. Nfld. Bull. 21.

Williams, H.
1964: The Appalachians in northeastern Newfoundland - A two-sided symmetrical system: Am. Jour. Sci., vol. 262, pp. 1137-1158.

Williams, H., Kennedy, M.J. and Neale, E.R.W.
1972: The Appalachian Structural Province. In Tectonic Styles in Canada. Geol. Assoc. Can. Spec. Paper 11, Price, R.A. and Douglas, R.J.W. (eds.), pp. 181-261.

PLATE 1

Fig. a: Subrounded blocks of serpentinized peridotite in sheared serpentinite matrix at Devil's Cove.

Fig. b: Indistinctly layered peridotite from Grassy Island.

PLATE 2

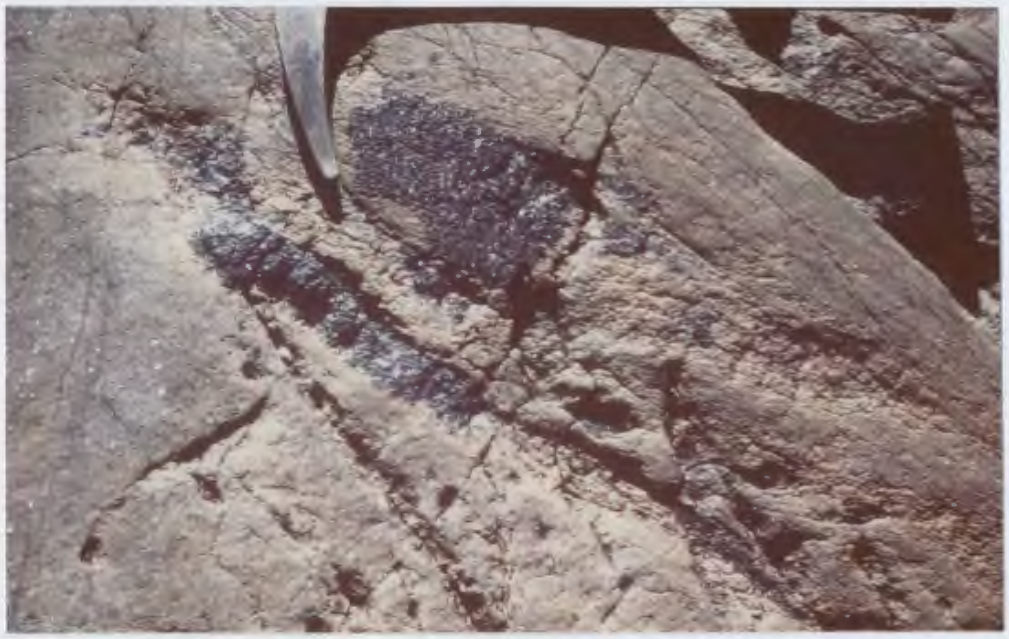

Fig. a: Lenses and patches of chromite associated with peridotite on Grassy Island.

Fig. b: Layering in carbonate-talc body south of Point Rousse.

PLATE 3

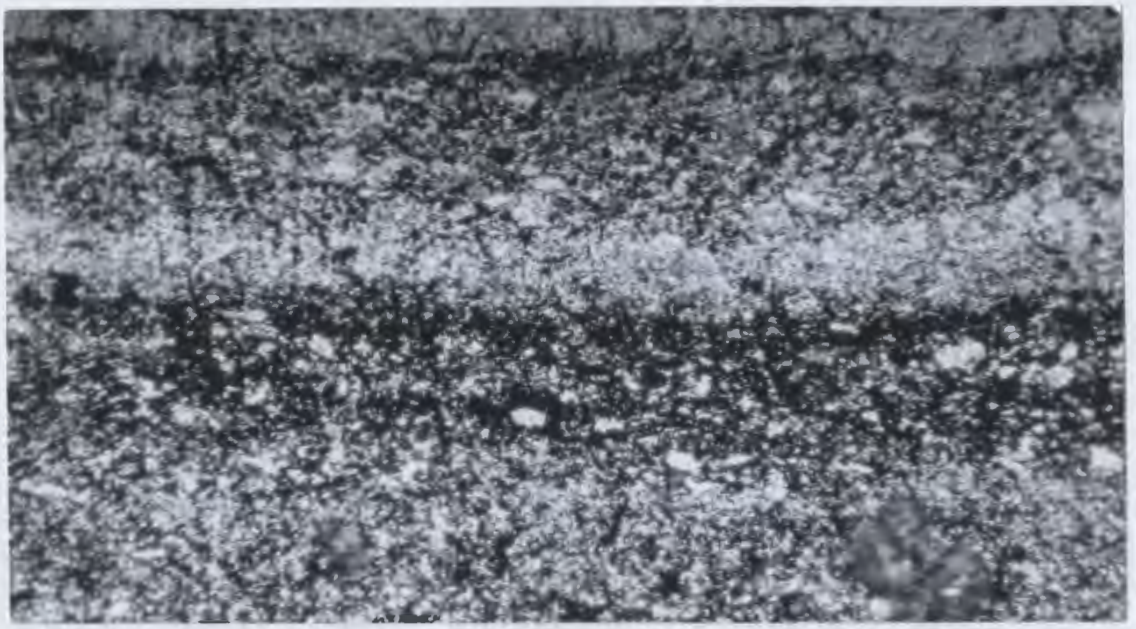

Fig. a: Photomicrograph. Interlayered talc-carbonate-magnetite. Plane light. 120x

Fig. b: Photomicrograph. Secondary, dust particles of magnetite concentrated in centres of carbonate grains. X-nicols. 120x.

PLATE 4

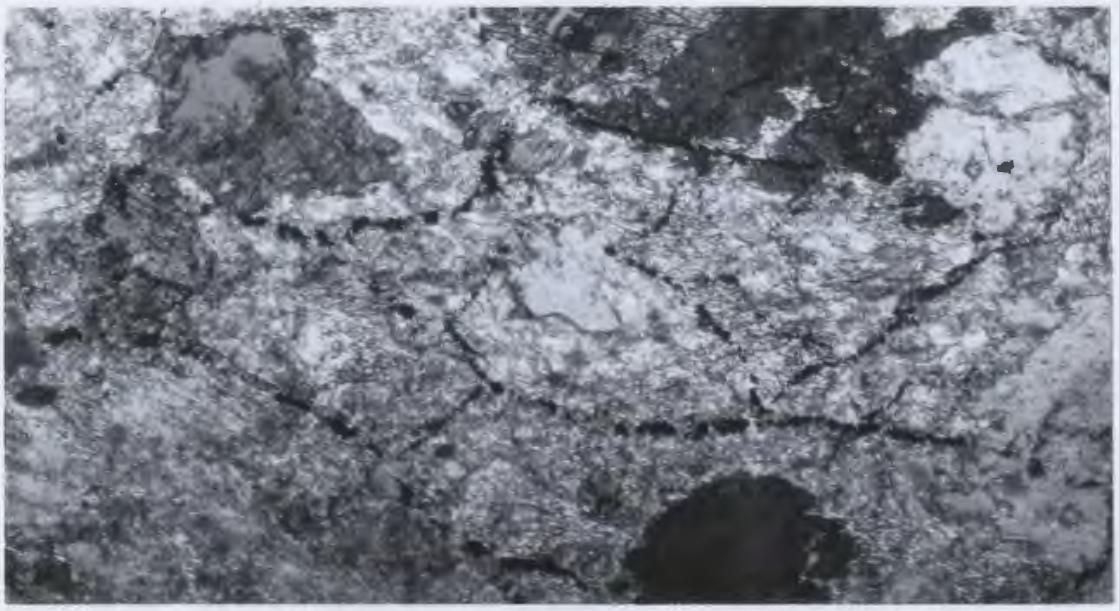

Fig. a: Photomicrograph. Magnetite grains forming rings around talc pseudomorphs of olivine. Plate light. 120x

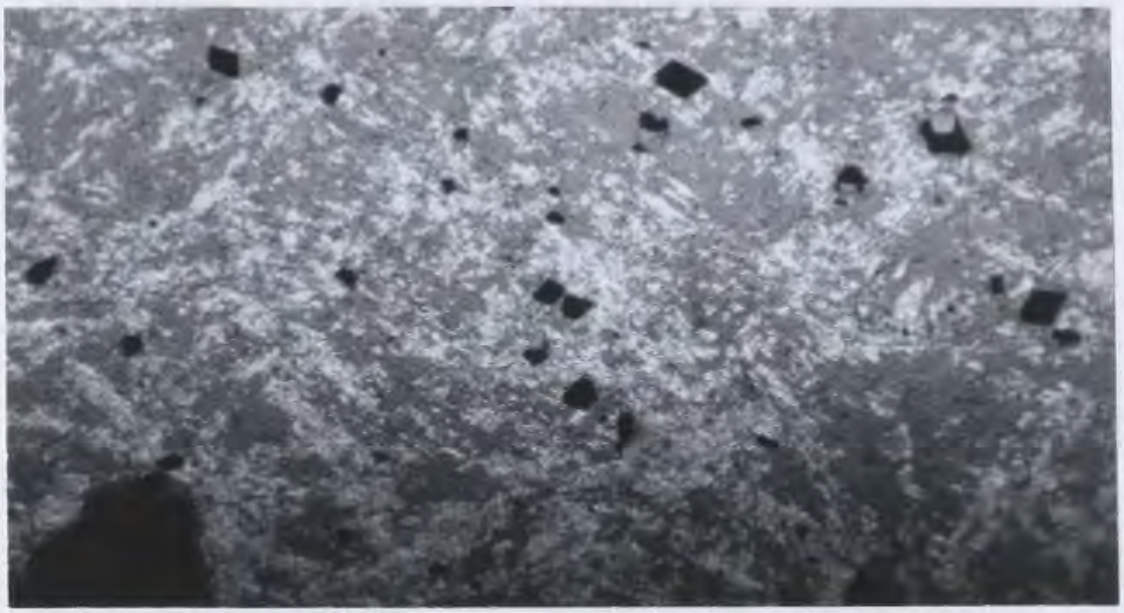

Fig. b: Grains of magnetite disseminated throughout talc and carbonate. Plane light. 100x

PLATE 5

Fig. a: Typical section showing transitional layering from peridotite to pyroxenite (websterite) overlain by layered gabbro.

Fig. b: Patches of lherzolite (dark areas) in harzburgite (light areas).

PLATE 6

Fig. a: Poikilitic actinolite crystals in peridotite.

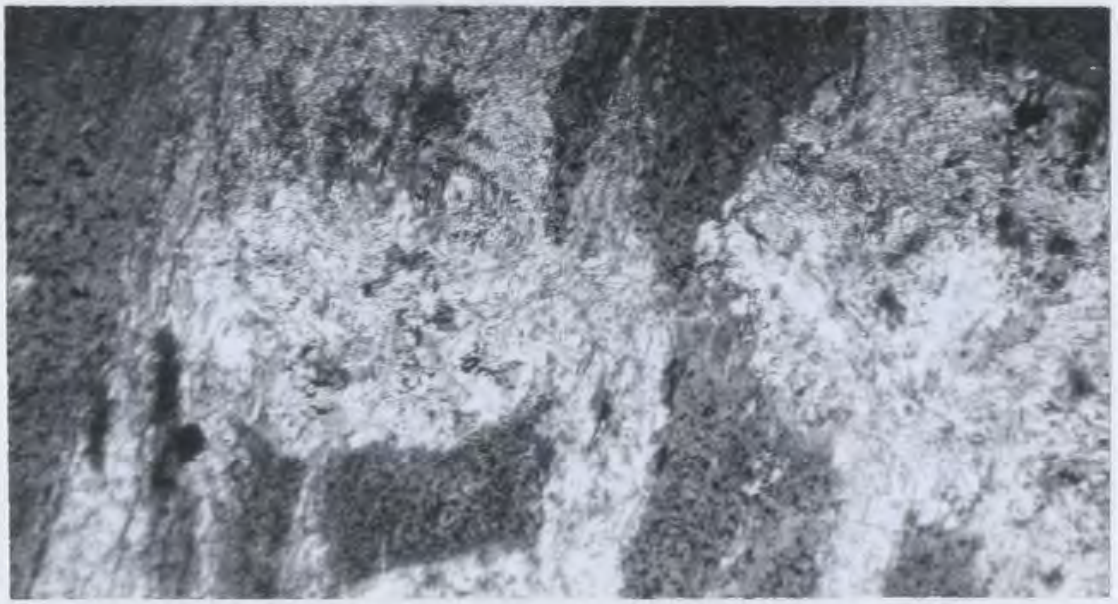

Fig. b: Poikilitic actinolite crystal (as seen in Fig. a) containing round steatitised olivine grains. x-nicols 200x

PLATE 7

Fig. a: Slump features in sharp contact between pyroxenite and gabbro layers.

Fig. b: Pegmatitic pyroxenite layers grading into finer grain pyroxenite.

PLATE 8

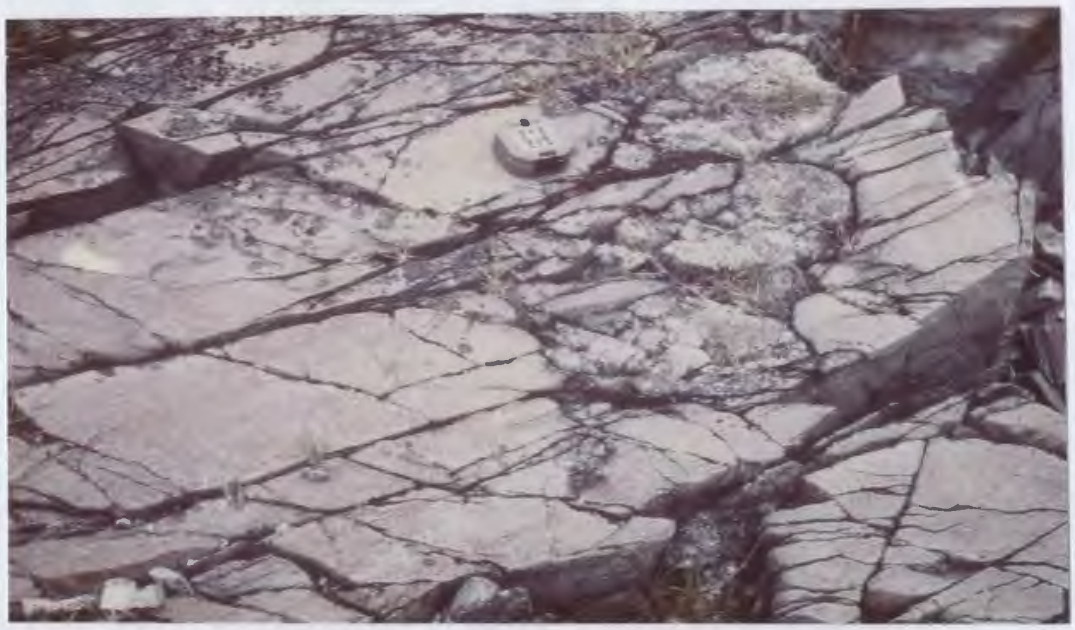

Fig. a: Gabbro inclusions in coarse diabase dike.

Fig. b: Close packed pillow lava from the Western Block, south of Green Cove.

PLATE 9

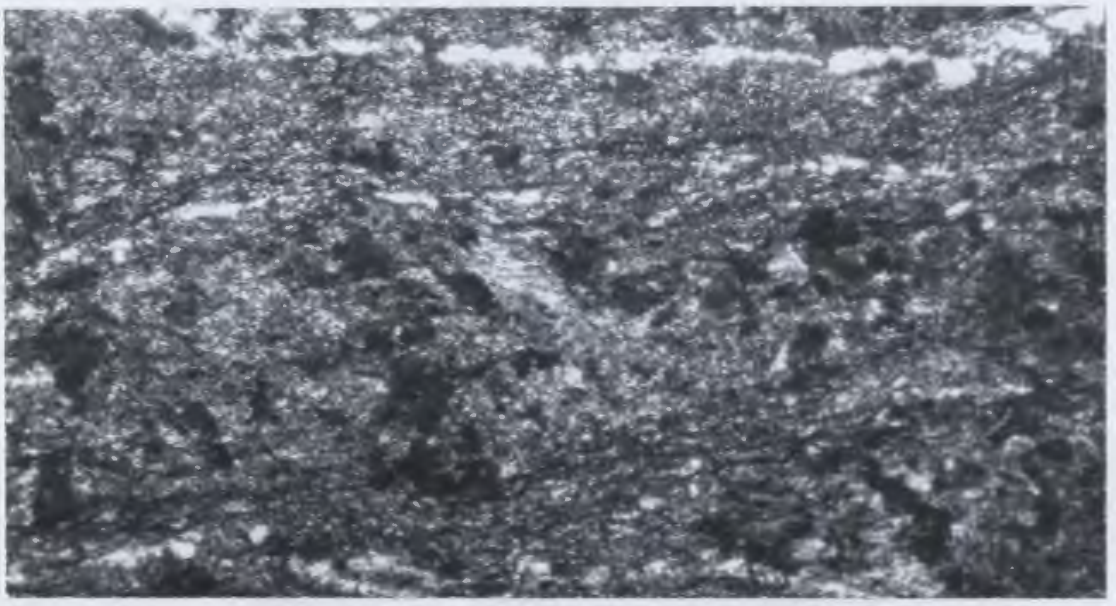

Fig. a: Photomicrograph. Alternating bands of quartz (light) and chlorite (dark) due to metamorphic differentiation. X-nicols. 150x

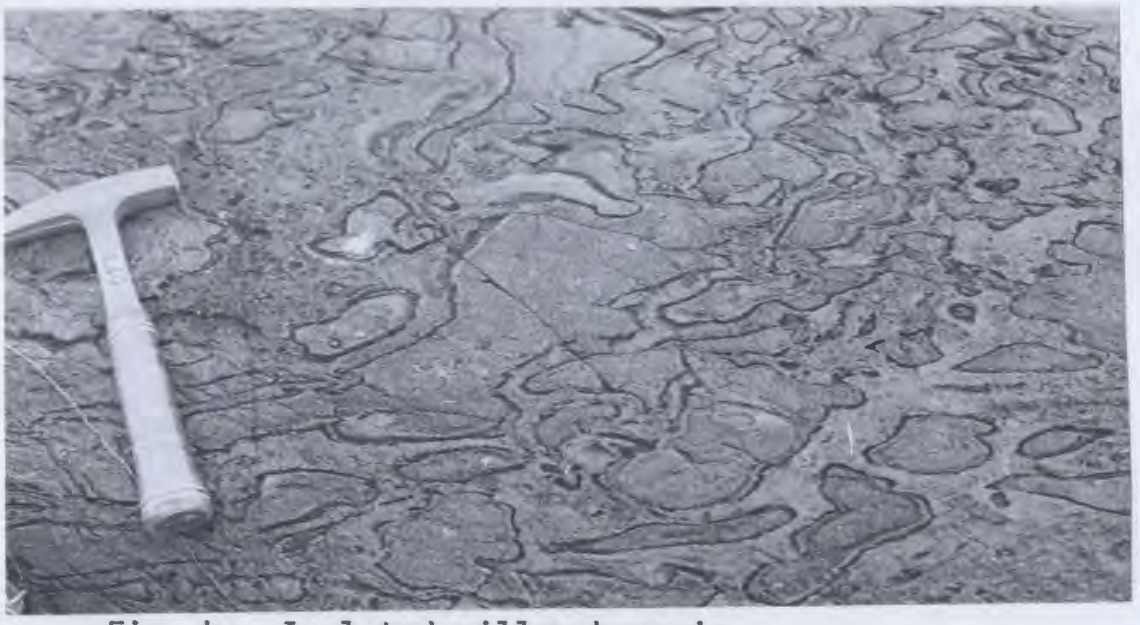

Fig. b: Isolated pillow breccia.

PLATE 10

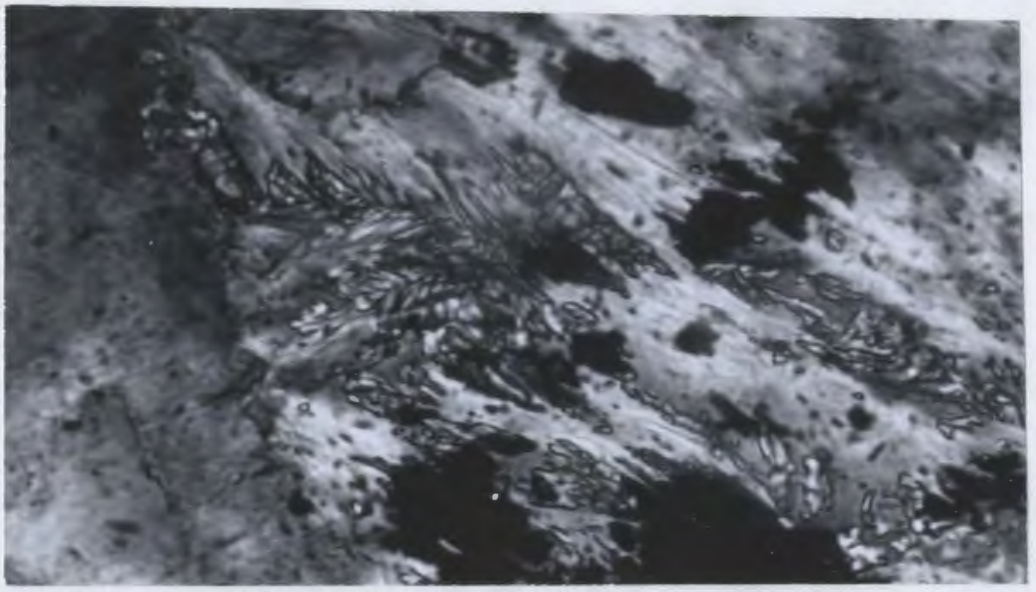

Fig. a: Photomicrograph. Talc replacing serpentine in serpentinized peridotite layers of the Eastern Block near the talc-carbonate body.

Fig. b: Layering in peridotite of the Eastern Block.

PLATE 11

Fig. a: Pegmatitic gabbro zones within normal gabbro.

Fig. b: Pillow lavas set in a brecciated matrix; from Eastern Block, south of Big Head.

PLATE 12

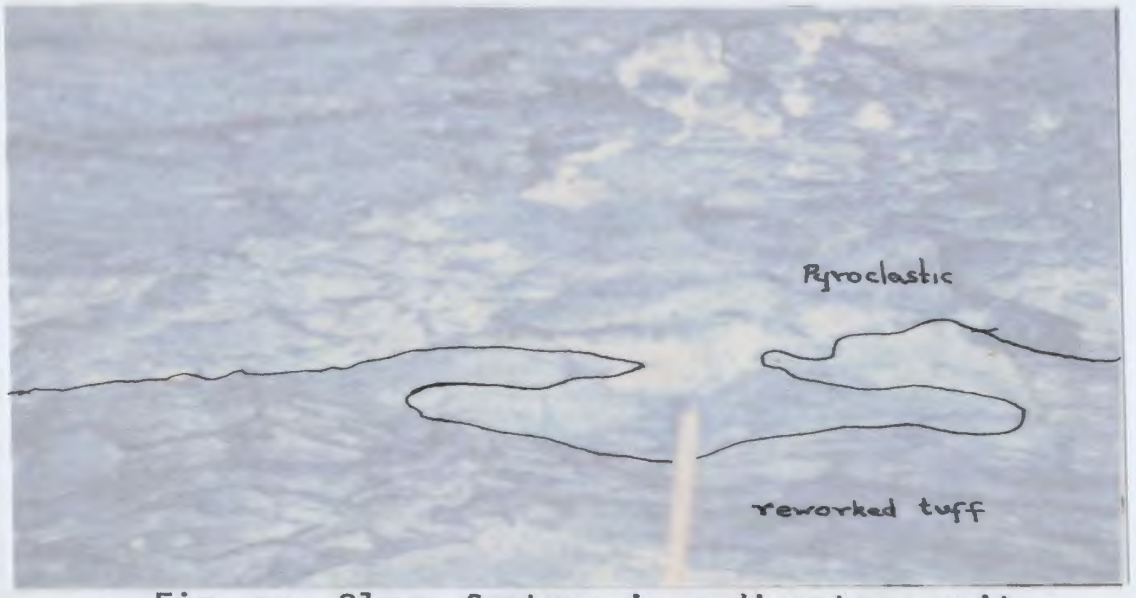

Fig. a: Slump feature in sedimentary unit of the Eastern Block.

Fig. b: Layered gabbro of the Deer Cove Block.

PLATE 13

Fig. a: Intensely sheared dikes and pillow lavas of the Deer Cove Block. Noted folded quartz vein (F_1) about 2 feet thick, with axial planes parallel to schistosity (S_1).

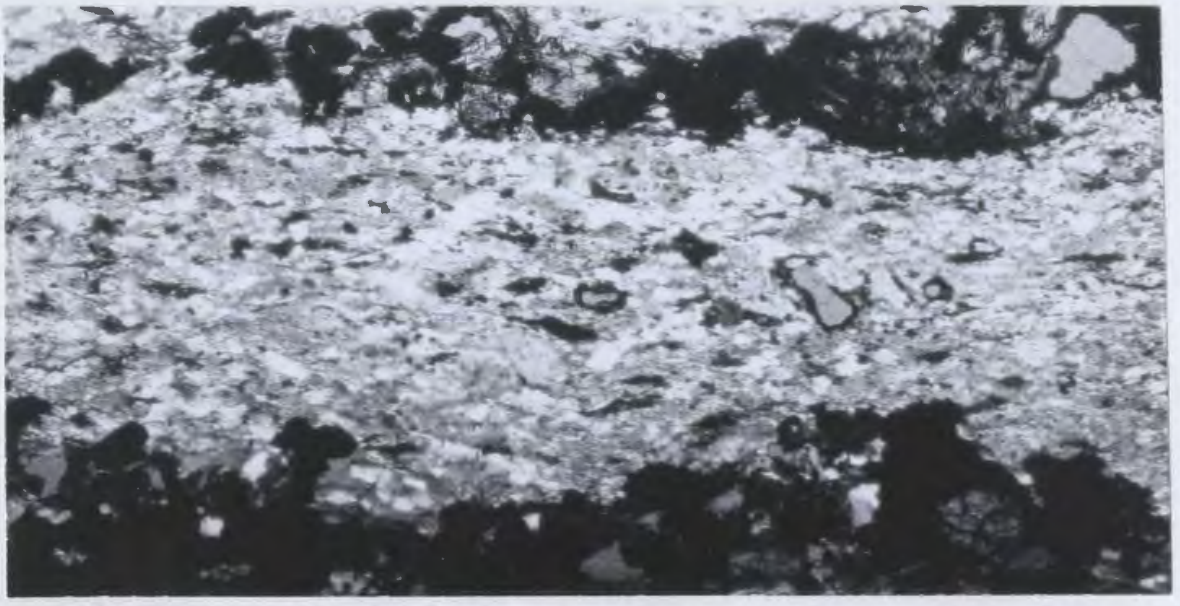

Fig. b: Photomicrograph. Layers of pyrite and epidote (dark) interbanded with quartz. X-nicols. 120x.

PLATE 14

Fig. a: Intrusive breccia, resulting from intrusion of trondhjemitic material (light coloured) into dikes.

Fig. b: Boudinaged dikes formed in plane of the S_1 schistosity.

PLATE 15

Fig. a: Intensely deformed zones (left) of reworked tuff in close proximity to undeformed reworked tuff to the right.

PLATE 16

Fig. a: Photomicrograph. Cross-hatched fibers of serpentine in serpentinized peridotite. X-nicols. 120x.

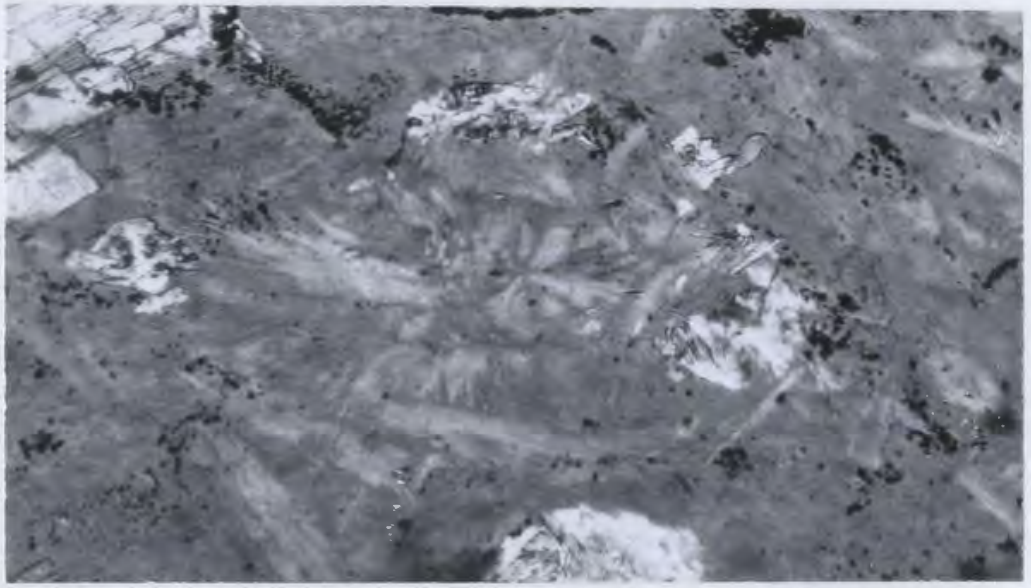

Fig. b: Photomicrograph. Radiating sheaves of serpentine in serpentinized peridotite. X-nicols. 120x.

PLATE 17

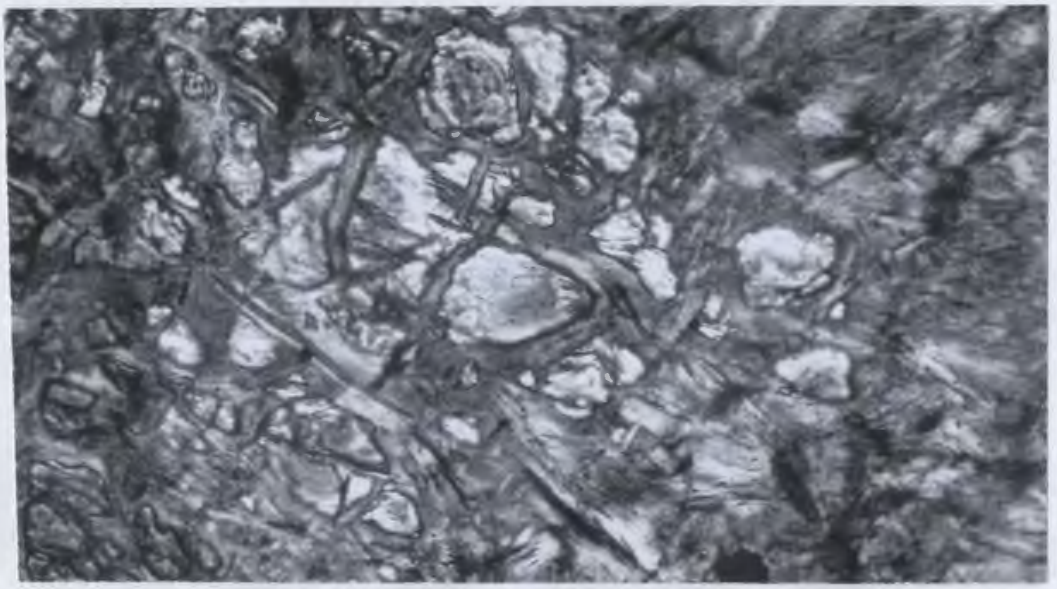

Fig. a: Photomicrograph. Olivine cores surrounded by mesh-network of serpentine in dunite underlying the Sisters. X-nicols. 120x.

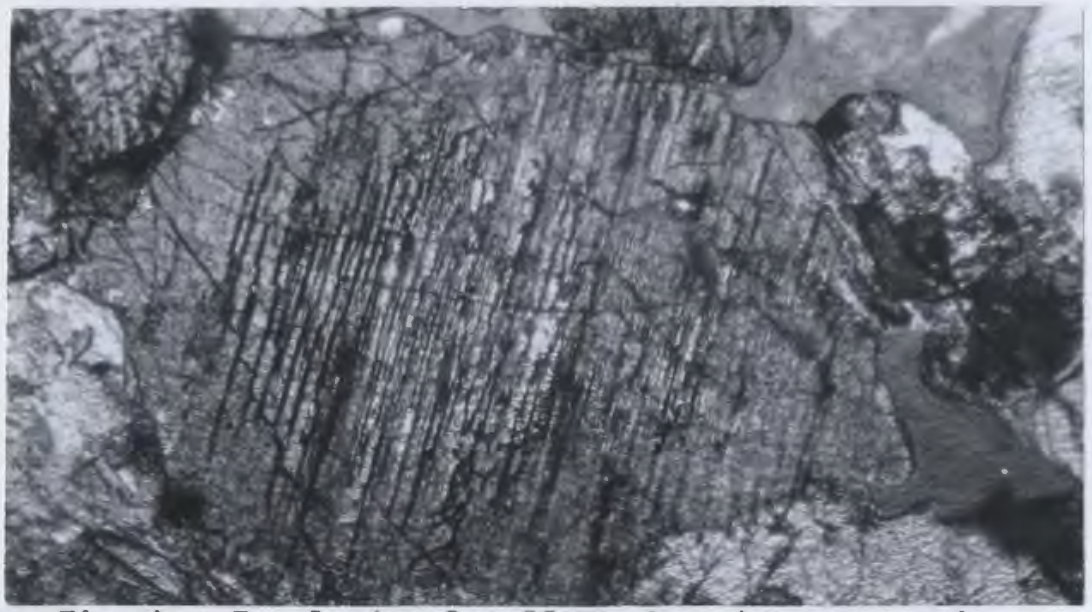

Fig. b: Exsolution lamellae of orthopyroxene in clinopyroxene. X-nicols. 100x.

PLATE 18

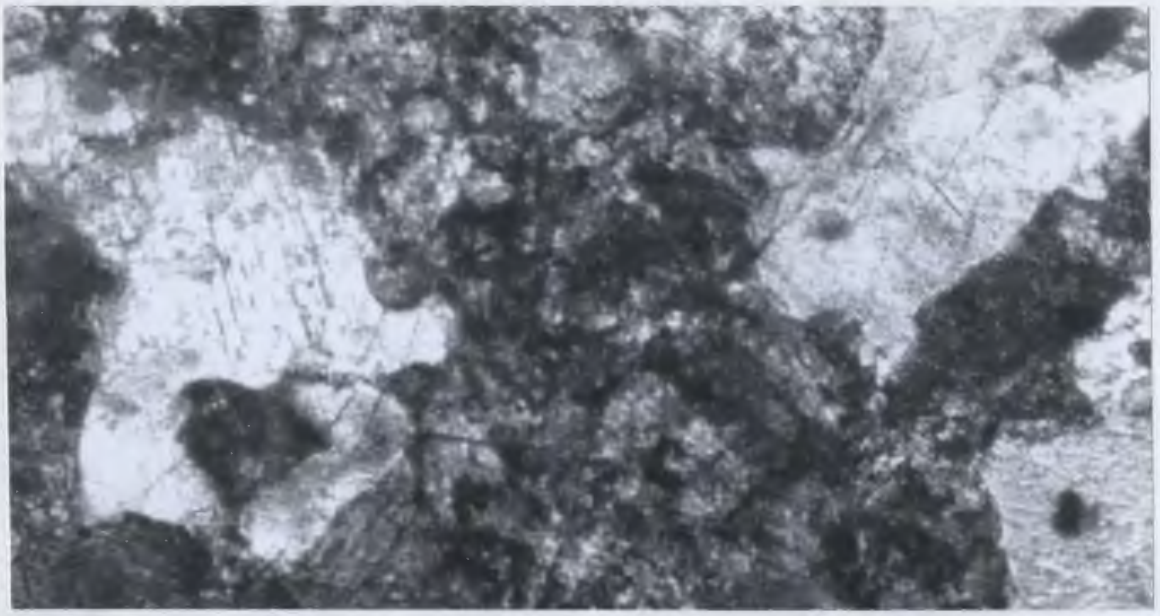

Fig. a: Pyroxene crystals having embayed margins in a matrix now consisting of epidote. X-nicols. 100x.

Fig. b: Diopside crystals rimmed by tremolite (light). X-nicols. 100x.

PLATE 19

Fig. a: Photomicrograph. Irregular pathces of cross-hatched serpentine (grey areas) in a matrix of the sheave variety. X-nicols. 120x.

Fig. b: Serpentinized pyroxene crystals exhibiting the "rib" texture. The lighter areas in the crystal are pyroxene remnants and the darker serpentine. X-nicols. 120x.

PLATE 20

Fig. a: Photomicrograph. Magnetite (black) outlining serpentinized olivine crystals in layered peridotite. X-nicols. 100x.

Fig. b: Amygdules, containing radiating crystals of acicular actinolite, in pillow lavas. X-nicols. 100x.

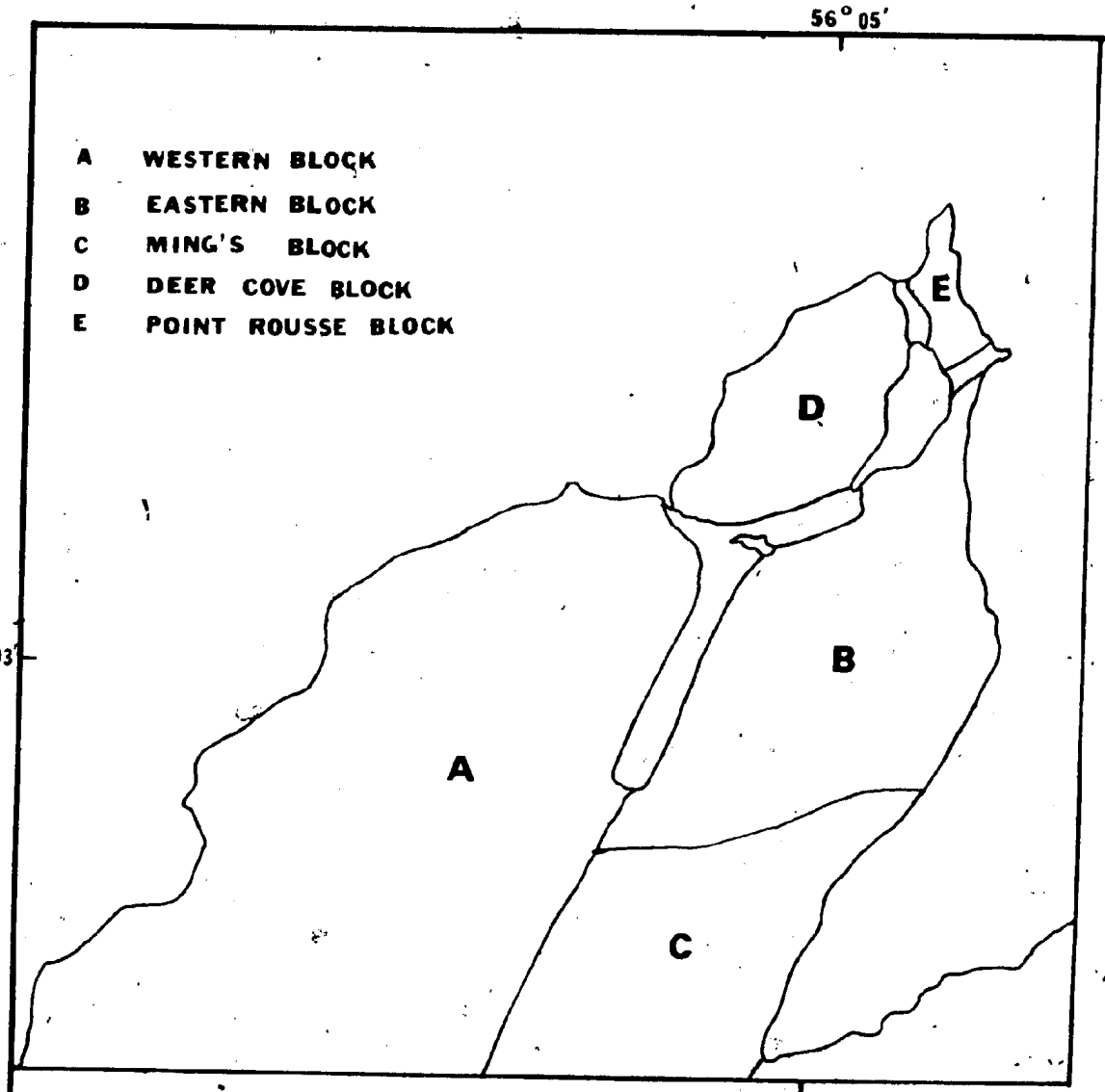
56° 05'
A WESTERN BLOCK
B EASTERN BLOCK
C MING'S BLOCK
D DEER COVE BLOCK
E POINT ROUSSE BLOCK
56° 03'
A
B
C
D
E

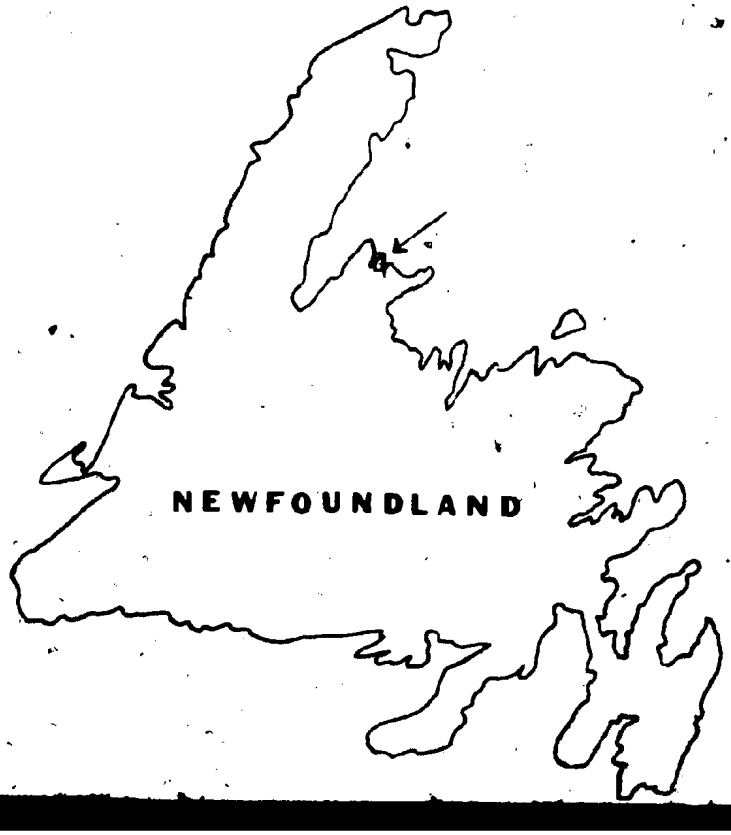
NEWFOUNDLAND

1 of

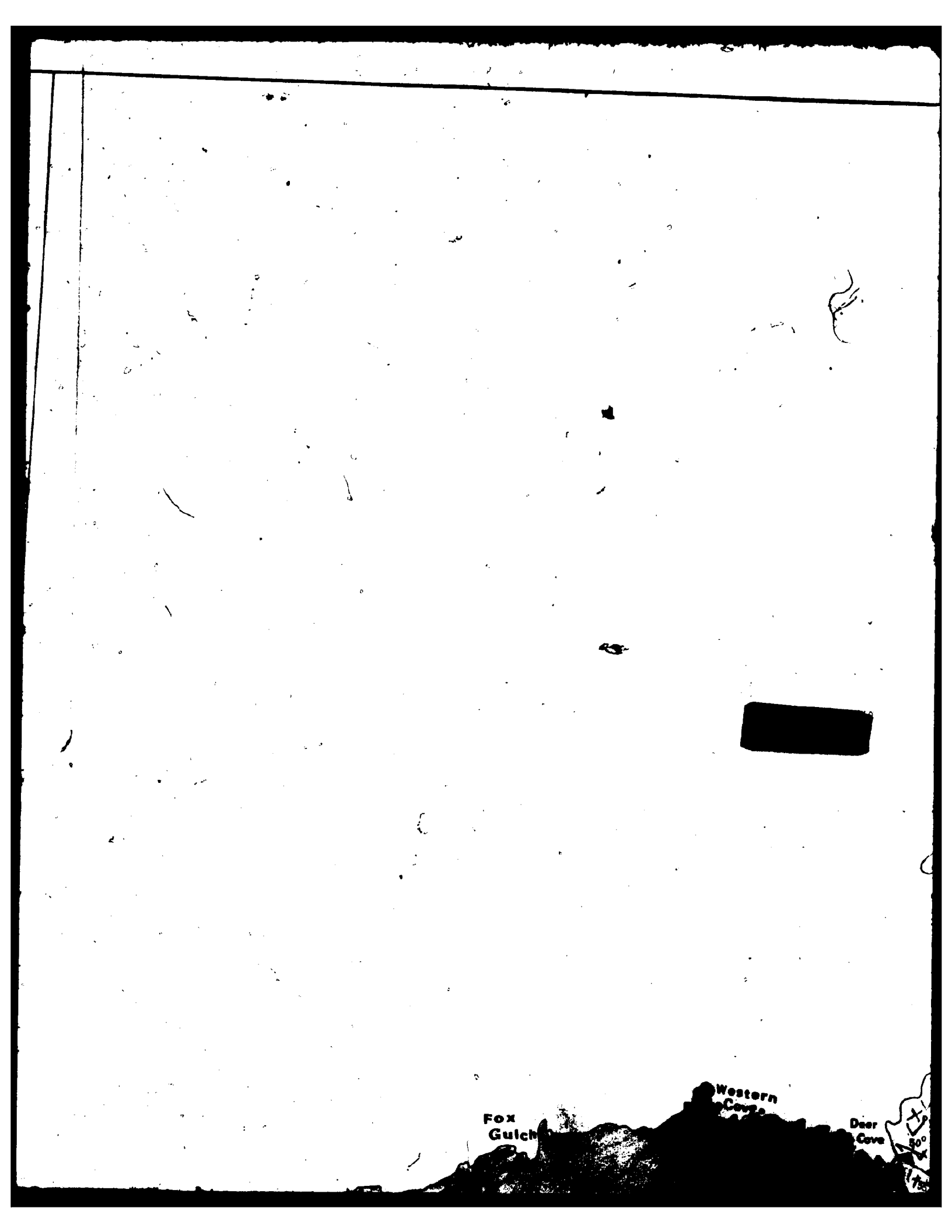
Western
Cove
Fox
Gulch
Deer
Cove
80°

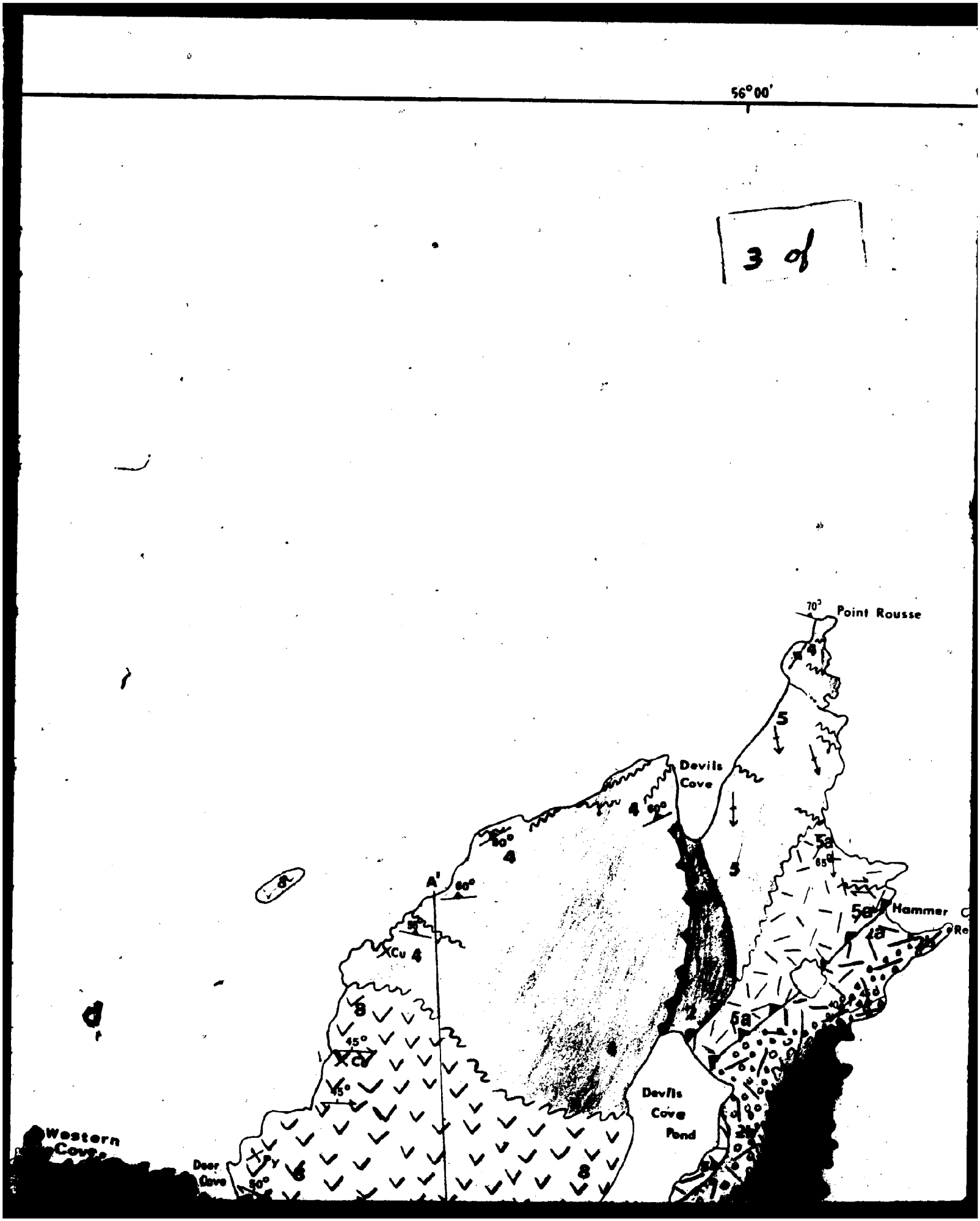
56°00'
3 of
70°
Point Rousse
Devils Cove
Devils Cove Pond
Western Cove
Deer Cove
Hammer
A'
Cu
4
5
5a
6
8
2
45°
60°
65°
50°

21

4 of

50° 03'

N

ORDOVICIAN

BAIE VERTE GROUP

8 — Undifferentiated diabase dikes, pillow lava and volcanic sediment.

7 — Agglomerate, crystal tuff, crystal-lithic tuff, red to green, thinly bedded reworked tuff, and tuffaceous breccia.

6 — Pillow lava and isolated pillow breccia.

5 — 5. Sheeted, wide, coarse grained diabase dikes with gabbro screens. 5a. Sheeted, fine grained diabase dikes.

4 — Layered, fine to coarse grained, gabbro.

3 — Interlayered peridotite - pyroxenite - gabbro.

2a 2b — 2. Serpentinised peridotite and sepentinite. 2a. Talc - carbonate. 2b. Carbonate-talc.

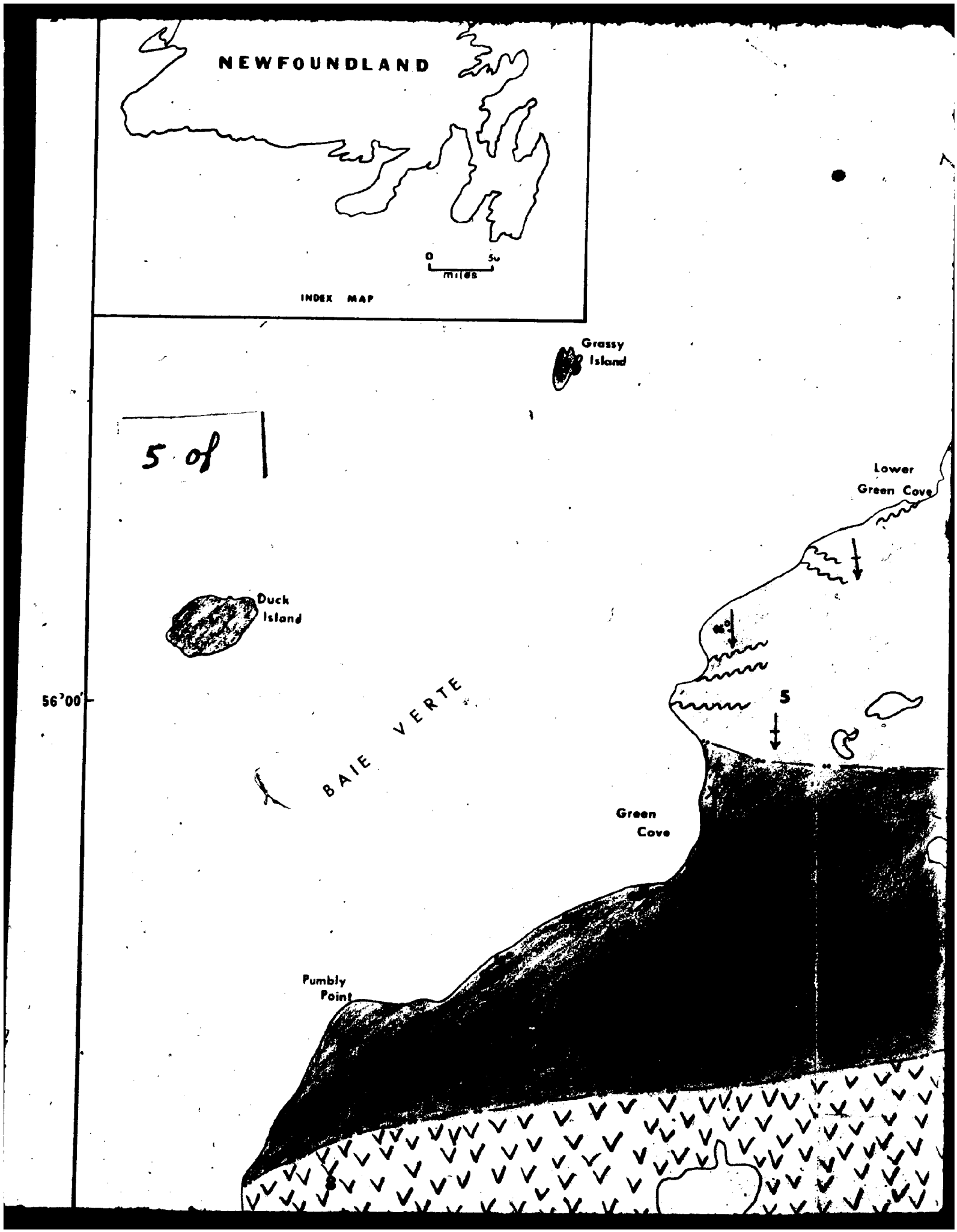
NEWFOUNDLAND
0
5w
miles
INDEX MAP
Grassy Island
5 of
Lower Green Cove
Duck Island
56°00'
BAIE VERTE
5
Green Cove
Pumbly Point

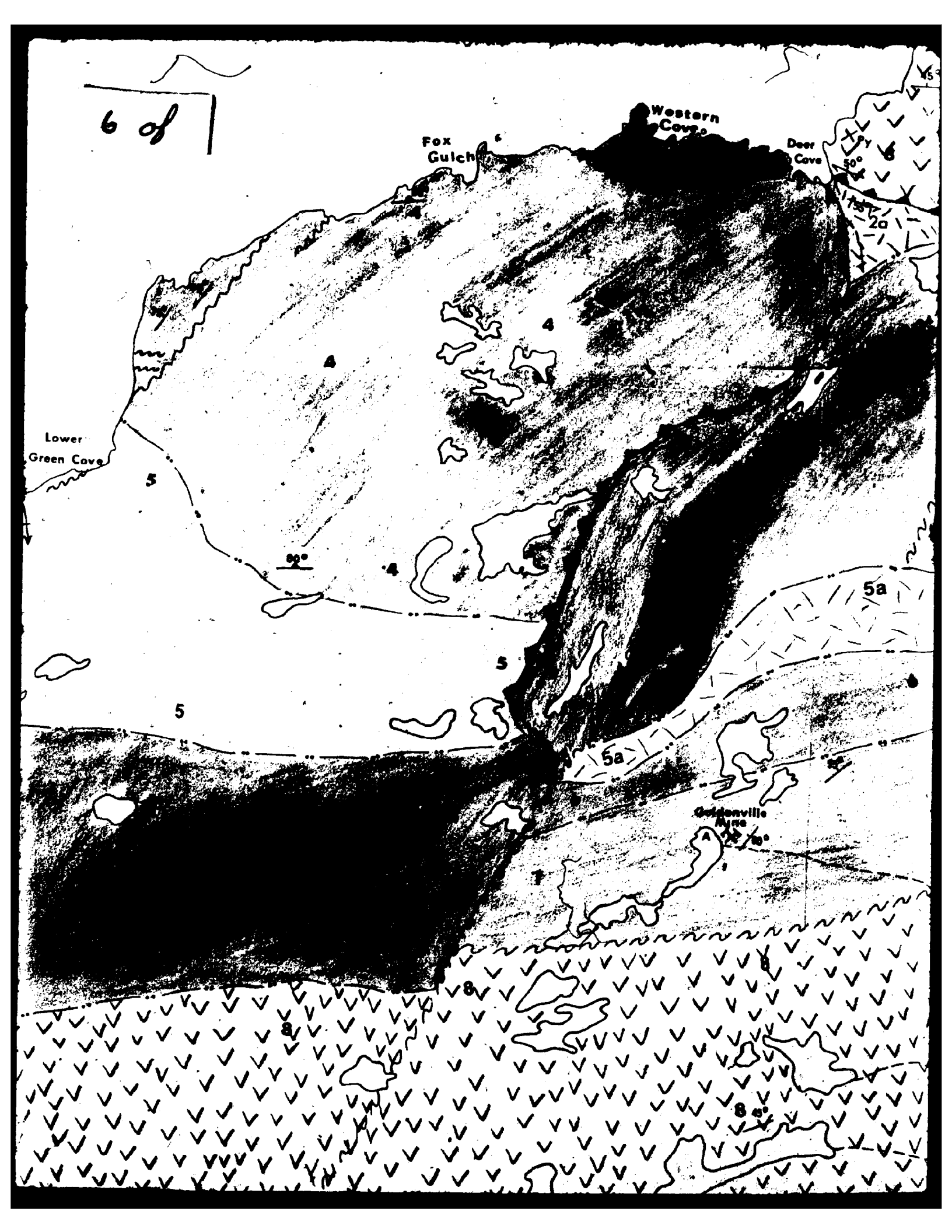
6 of
Western Cove
Fox Gulch
Deer Cove
Lower Green Cove
4
5
5a
8
Goldenville

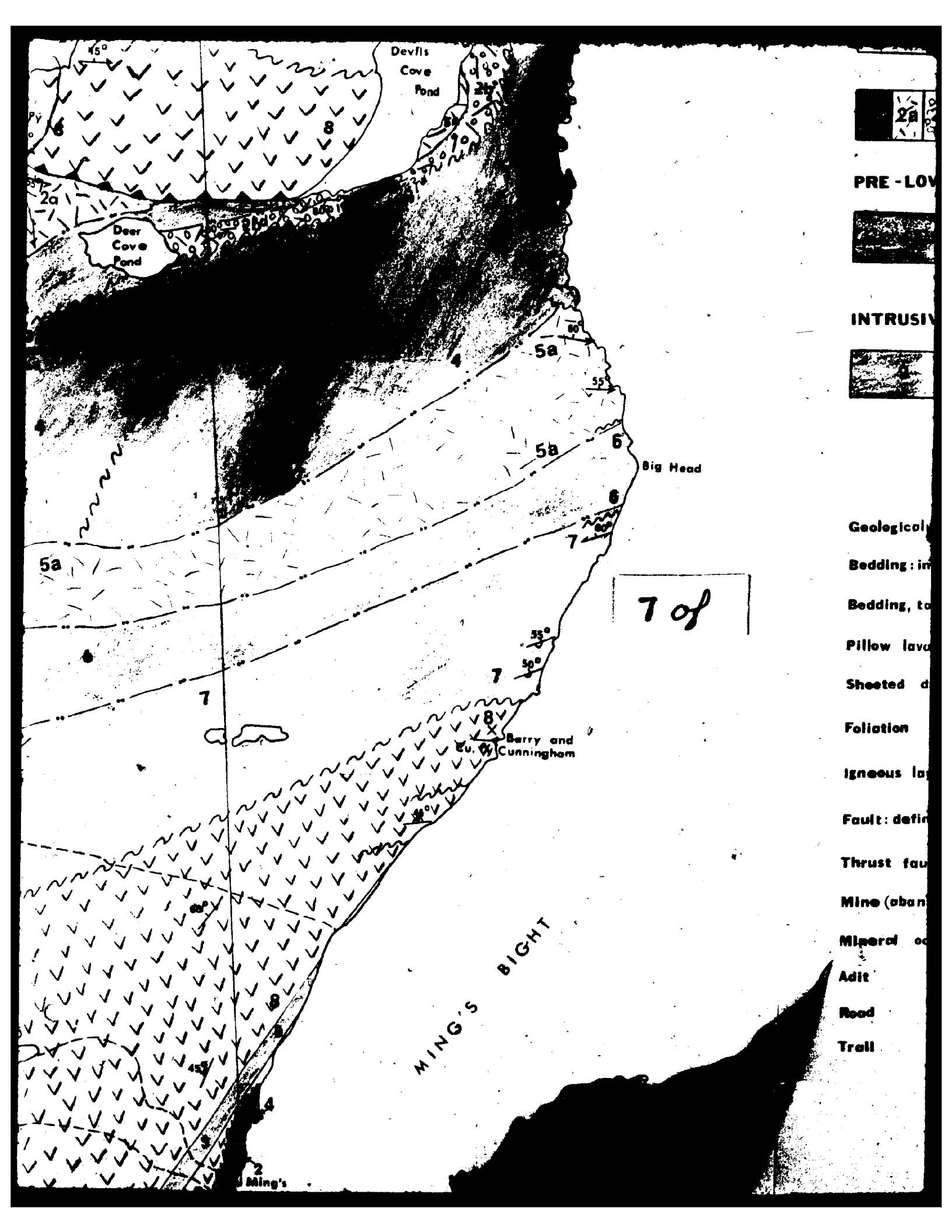
Devils
Cove
Pond
Deer
Cove
Pond
Big Head
Berry and
Cunningham
MING'S BIGHT
Ming's
5a
7 of
PRE - LOW
INTRUSIV
Geological
Bedding : in
Bedding, to
Pillow lava
Sheeted d
Foliation
Igneous la
Fault : defi
Thrust fau
Mine (aban
Mineral oc
Adit
Road
Trail

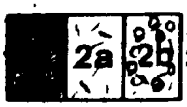

2. Serpentinised peridotite and sepentinite.
2a. Talc - carbonate. 2b. Carbonate - talc.

PRE - LOWER ORDOVICIAN

MING'S BIGHT GROUP

Dominantly semi-pelitic and psammitic metasediment.

INTRUSIVE ROCKS

Porphyritic diabase.

Geological boundary: gradational

Bedding : inclined

Bedding, tops known: overturned

Pillow lava, tops known : inclined, overturned

Sheeted dikes: inclined, vertical

Foliation

Igneous layering: inclined, vertical

Fault: defined, approximate, assumed

Thrust fault

Mine (abandoned)

Mineral occurrence

Adit

Road

Trail

50°00'

8 of

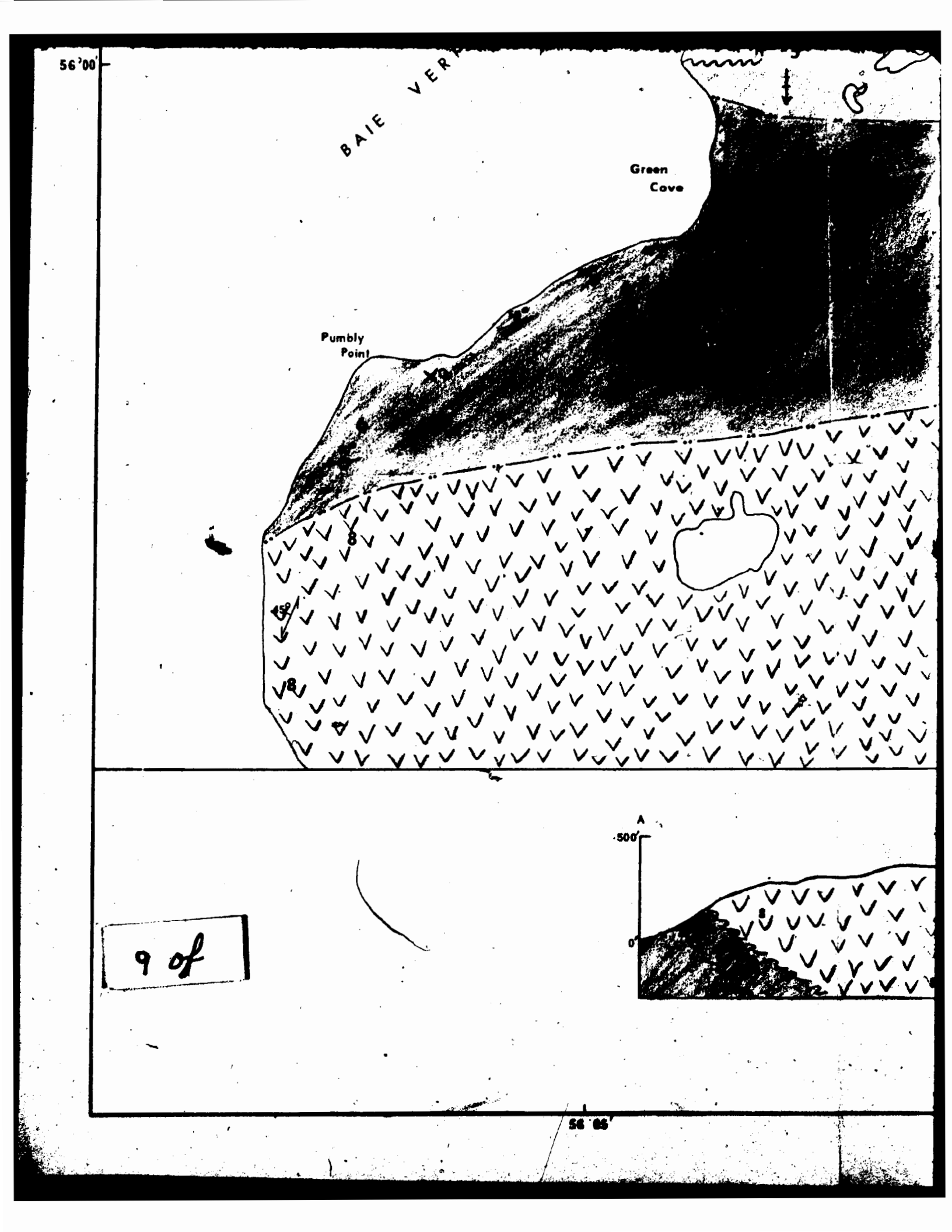

9 of

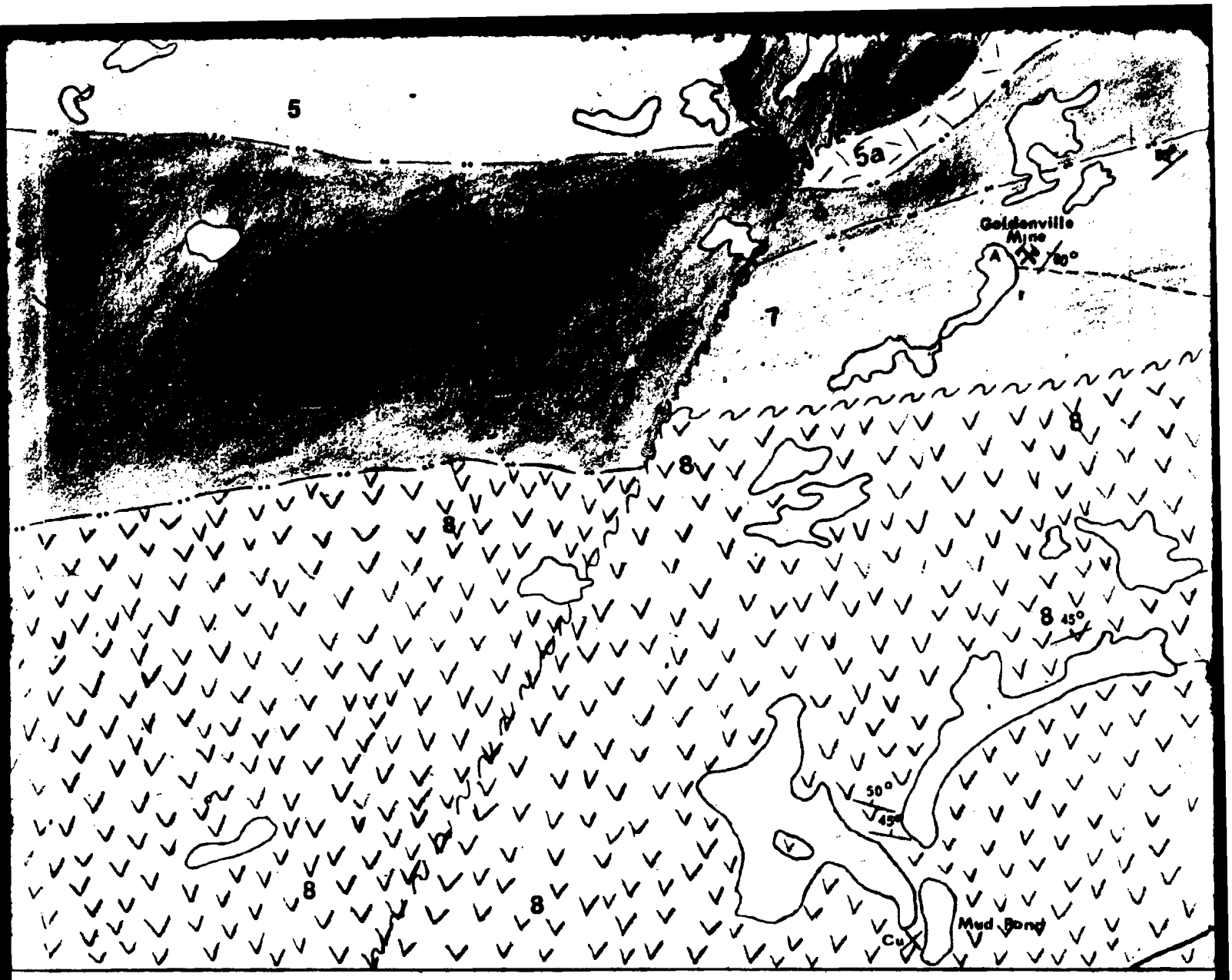

CROSS SECTION

10 of

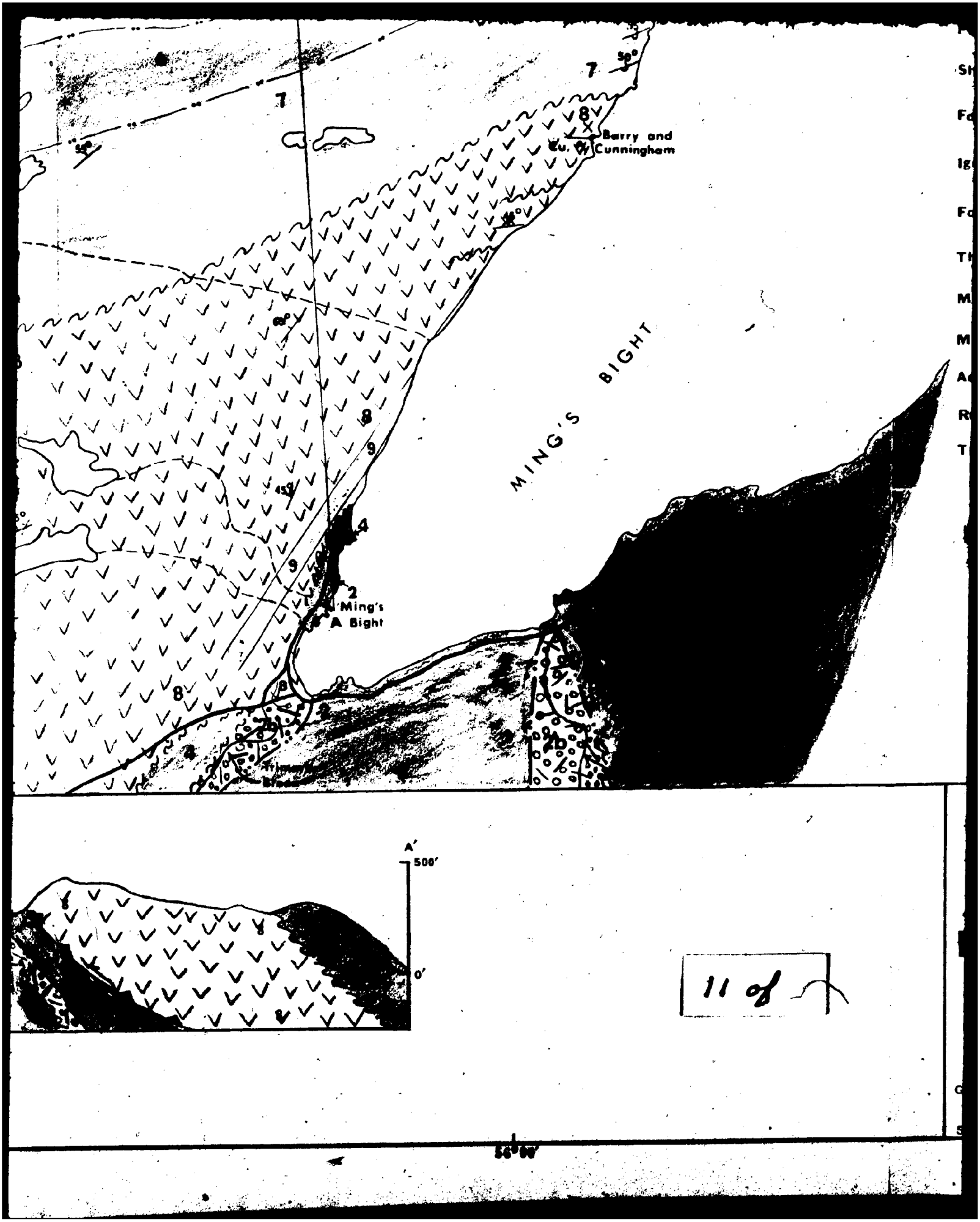
MING'S BIGHT
Ming's Bight
Barry and Cunningham
A
A'
500'
0'
11 of

-50°00'

Sheeted dikes: inclined, vertical

Foliation

Igneous layering: inclined, vertical

Fault: defined, approximate, assumed

Thrust fault

Mine (abandoned)

Mineral occurrence

Adit

Road

Trail

0 .25 .5 1

SCALE 1 INCH TO 1/4 MILE

12 & 12

GEOLOGY OF BAIE VERTE – MING'S BIGHT PENINSULA

GEOLOGY BY: R. NORMAN

DRAWN BY: R.N.

SEPT. 1973

FIGURE 4